CHALMERS

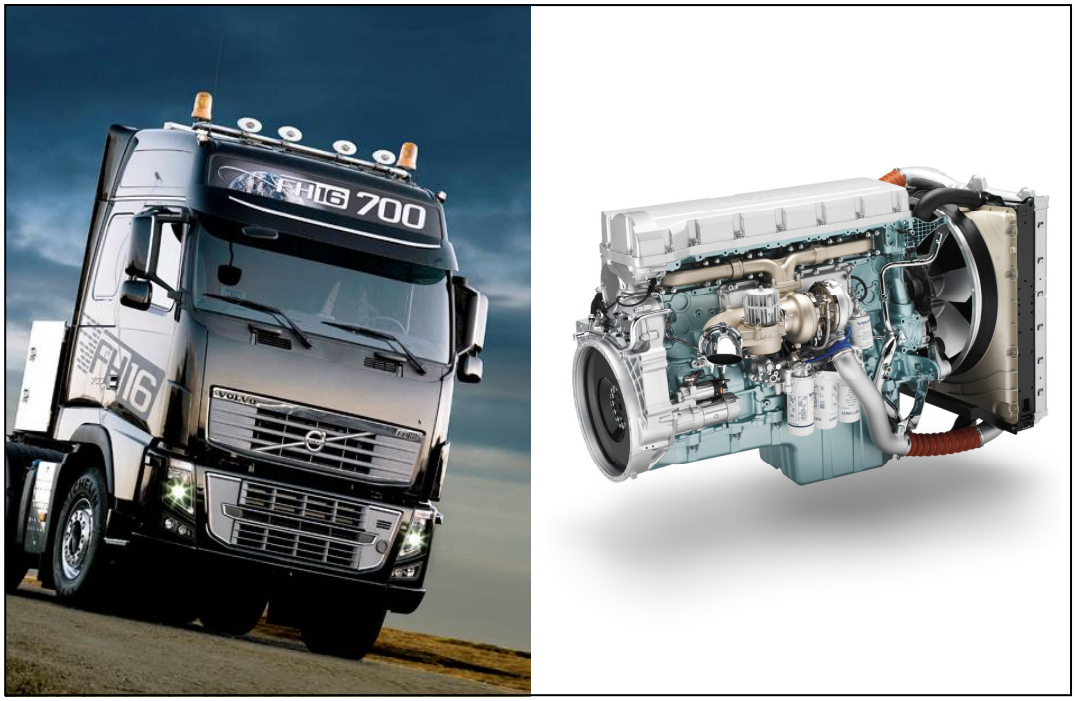

Modeling and Calculating Electric Power Consumption of a Diesel Truck Engine

Master of Science Thesis

KAMBIZ SETHNA
KHALED EL SAYED

Department of Energy and Environment
Division of Electric Power Engineering
CHALMERS UNIVERSITY OF TECHNOLOGY
Göteborg, Sweden, 2011

Modeling and Calculating Electric Power Consumption of a Diesel Truck Engine

KAMBIZ SETHNA
KHALED EL SAYED

Department of Energy and Environment
Division of Electric Power Engineering
CHALMERS UNIVERSITY OF TECHNOLOGY
Göteborg, Sweden, 2011

Modeling and Calculating Electric Power Consumption of a Diesel Truck Engine

KAMBIZ SETHNA
KHALED EL SAYED

Department of Energy and Environment
Division of Electric Power Engineering
Chalmers University of Technology
SE–412 96 Göteborg
Sweden
Telephone +46 (0)31–772 1000

Cover:
Volvo truck model FH16, powered by a 16 litre diesel engine (D16E).

Chalmers Bibliotek, Reproservice
Göteborg, Sweden 2011

Modelling and Calculating Electric Power Consumption of a Diesel Truck Engine

KAMBIZ SETHNA
KHALED EL SAYED
Department of Energy and Environment
Division of Electric Power Engineering
Chalmers University of Technology

Abstract

In order to dimension alternators and batteries as well as power management control strategies, there is a need to analyse the electrical current consumption in various systems of a diesel truck engine for different modes of operation. The aim of this project is to develop a general way (method and tool support) to calculate and analyse current consumption of the powertrain system. In this work several models with different levels of accuracy have been designed in order to simulate the current consumption of the urea dosing system, which is one of the main systems of the exhaust after treatment system (EATS). The main reason for selecting such a system was its independent characteristics, having its own controller known as the ACM (After treatment Control Module) and as well it is of primary interest of the Volvo system engineering group due to its new developing technology, designed for future Euro VI heavy duty engines. All the models and simulations have been implemented in Matlab®/Simulink®. Moreover the models were compared and verified with measurements that were carried out at Volvo Powertrain test labs. A user friendly graphical interface was also designed as an interface between the user and the Simulink® model. The tool was designed via Matlab®GUI with convenient viewing and post processing capabilities.

The results show that the basic model, being a rather simple model with static simulation is sufficient for modeling the air valve, coolant valve and the hose heaters of the Urea dosing system. The accuracy of the implemented basic model structure is found to be 98% of the real measured values. However the urea pump requires a more advanced model due to its complexity, which was implemented in the detailed model. The detailed model, which is based on dynamic simulation and detailed mechanical characteristics in addition to the detailed magnetic characteristics of the pump, produces reasonably good results with an error of 23.8 % in the average coil current. The main contribution to this error is probably the unknown parameters of the electronic control circuit. Finally, the general model is the most suitable model for the urea pump according to the project's specifications and in comparison with the detailed model, it over predicts the current consumption by 4.3 %.

Keywords: Current consumption, Dynamic simulation, EATS, Electric design, GUI, Model, Power consumption, Powertrain, Static simulation, Urea dosing system

Acknowledgements

This master thesis has been carried out at the Department of Energy and Environment, division of Electric Power Engineering at Chalmers University of Technology. The work has been performed at Volvo Powertrain Corporation and within System Engineering Group who introduced the topic and provided unlimited support during the course of the project.

The team work was truly fun and challenging at the same time. We learned a lot and met many interesting engineers who shared their knowledge and experience which we are very grateful and would like to thank.

First we would like to thank our supervisors at Volvo Powertrain, Peter Härslätt and Mathias Malmgren. Their constant encouragement and support throughout the project made it possible for us to complete the work. We would also very much like to thank Stefan Lundberg, our supervisor at Chalmers, who always had the answer to all our questions and guided us to the right way.

A special thanks to our co-workers and manager Styrbjörn Törngren, in the System Engineering Group; it was a pleasure working by their side and truly enjoyed their company.

Finally we would like to thank everyone who was involved in this project and helped us accomplish the goal of this thesis work.

Last but certainly not least we would like to thank our families for their unconditional love and support. Thank you for always being there for us; you are the true reason of our achievements in life.

Thank you all,

Kambiz and Khaled
Göteborg, Sweden, 2011

Preface
Introduction to Volvo Powertrain

Volvo Group based on its three fundamental corporate values; quality, safety and environmental care, is one of the world's leading suppliers of transport solutions for commercial use. The Volvo group organization is currently structured by its seven core companies as follows:

- Volvo 3P
- Volvo Powertrain
- Volvo Parts
- Volvo Logistics
- Volvo Technology
- Volvo Information Technology
- Volvo Group Real Estate – Volvo Business Services

Volvo Powertrain, being one of the major companies within the Volvo Group, is responsible for the development and production of the driveline, which consists of the engine, gearbox and the driven axles. Moreover, the company's product offer includes conventional drivelines, hybrid drivelines and engine after treatment systems.

Volvo Powertrain, is the world´s largest manufacturer of heavy-duty diesel engines (over 10 liter engine capacity) and covers seven business areas within the Volvo Group including:

- Volvo Trucks
- Renault Trucks
- UD Trucks
- Mack Trucks
- Volvo Construction Equipment
- Volvo Buses
- Volvo Penta

Supporting around 8,500 employees globally and having business operations in Sweden, France, India, Japan, Brazil and United States Volvo powertrain has produced over 200,000 heavy duty engines, 125,000 transmissions and 45,000 Marine Drives (during 2010).

This Master thesis has been introduced and carried out in the System Engineering Department within Volvo Powertrain Corporation with the main focus on the after treatment system of the EU VI, HDE 13 TC engine model.

Table of Contents

Abbreviation list

ACM	Aftertreatment Control Module
AHI	Aftertreatment Hydrocarbon Injection
APV	Air Purge Valve
AVU	Air Valve Unit
BVU	Buffer air Valve Unit
CAC	Charge Air Cooler
CO	Carbon Monoxide
CO_2	Carbon Dioxide
CS	Control Systems
DC	Direct Current
DI	Direct Injection
DPCRS	Distributed Pump Common Rail System
EATS	Exhaust After Treatment System
ECE R-49	Steady-state Engine Test
ECU	Electronic Control Unit
EECU	Engine Electronic Control Unit
EEV	Enhanced Environmentally Vehicle
EGR	Exhaust Gas Recirculation
ELR	European Load Response
EMS	Engine Management System
EPG	Exhaust Pressure Governor
EPRV	Electrical Pressure Release Valve
ESC	European Stationary Cycle
ETC	European Transient Cycle
EU	European Union
FDV	Fuel Delivery Valve
FGT	Fixed Geometry Turbo
FSOV	Fuel Shut Off Valve
GUI	Graphical User Interface
HC	Hydrocarbons
HD	Heavy Duty
HDE	Heavy Duty Engine
HT	High Temperature
ITV	Intake Throttle Valve
LT	Low Temperature
LTC	Low Temperature Cooler
MG	Main Gallery
N_2	Nitrogen
N/C	Normally Closed
NCV	Nozzle Control Valve
N/O	Normally Open
NOx	Nitrogen Oxides
NRV	None Return Valve
O_2	Oxygen
OMV	Outlet Metering Valve
PCJ	Piston Cooling Jet
PM	Particulate Matter
PWM	Pulse Width Modulated
SCR	Selective Catalyst Reduction

Abbreviation list

TC	Turbo Compound
TECU	Transmission Electronic Control Unit
VEB	Volvo Engine Braking
VECU	Vehicle Electronic Control Unit
VPT	Volvo Powertrain
WG	Waste Gate

Symbol list

A	Cross sectional area of piston
a, $\dot{v}$, $\ddot{z}$	Acceleration of urea
B	Magnetic flux density
b_{Urea}	Urea damping coefficient
F_{damp}	Damping force
F_e	Electric force
F_s	Spring force
F_{stop}	Stop force
F_v	Velocity controller
F_z	Position controller
$freq$	Frequency
G_v	Velocity process function
G_z	Position process function
$I_{on,max}$	Maximum pump coil current at t_{on} time
i_{air}	Air gap current
i_c, $i_c(t)$	Pump coil current
$i_{c,avg}$	Average pump coil current
$i_{c,max,linear}$	Pump maximum linear coil current
$i_{c,meas}$	Measured pump coil current
$i_{c,rms}$	RMS pump coil current
$i_{c,sat}$	Saturated pump coil current
$i_{c,unsat}$	Unsaturated pump coil current
$i_c(t)_{decay}$	Pump coil current, decay component
$i_c(t)_{rise}$	Pump coil current, rising component
i_d	Pump current, battery perspective
$i_{d,avg}$	Average pump current, battery perspective
$i_{d,rms}$	RMS pump current, battery perspective
i_{iron}	Iron core current
$i_{iron,,sat}$	Saturated iron core current
$i_{iron,,unsat}$	Unsaturated iron core current
i_{off}	Current decay component
i_{on}	Current rising component
i_{pulse}	Pulse signal, coil current dependent
K_{psi}	Slope constant ($i_{iron} - \varphi$ curve)
L	Coil Inductance
L_{max}	Maximum coil inductance
L_{meas}	Measured coil inductance
L_{min}	Minimum coil inductance
l_{core}	Core coil length
l_g	Air gap length
m	Urea mass
N	Number of coil turns
P	Urea pressure
P_{copper}	Copper losses
$P_{core\ losses}$	Core losses
$P_{electric}$	Electric power
P_{mech}	Mechanical power
$P_{mech.\ losses}$	Mechanical losses
P_{si0sat}	Starting point constant ($i_{iron} - \varphi$ curve)

Symbol list

Q	Urea flow
R	Coil resistance
R_{don}	Diode resistance
R_{dson}	Switch resistance
$\mathfrak{R}_{air}$	Air reluctance
$\mathfrak{R}_{iron}$	Iron core reluctance
s	Laplace variable
T_{off}	Total off time
T_{on}	Total on time
T_amb	Ambient temperature
T_pump	Pump temperature
T_tank	Tank temperature
t_{off}	Off time
t_{on}	On time
V_c	Pump coil voltage
$V_{c,meas}$	Measured pump coil voltage
V_d	Battery voltage
V_{on}	Diode voltage drop
v	Piston velocity
v_{ref}	Reference piston velocity
W_ψ	Energy stored in the magnetic field
Z	Piston displacement
Z_{max}	Maximum piston displacement
Z_{min}	Minimum piston displacement
Z_{ref}	Reference position
α_v	Velocity controller bandwidth
α_z	Position controller bandwidth
$\mu_\circ$	Absolute permeability
μ_r	Relative permeability
φ	Magnetic flux
ψ_{meas}	Measured magnetic flux linkage
ψ_{sat}	Critical magnetic flux linkage at the saturation starting point
Δi_{linear}	Coil linear region current difference
Δt_{linear}	Coil linear region time difference

Chapter 1
Introduction

The thesis subject was introduced by the System Engineering Department within Volvo Powertrain. The project includes a combination of theoretical and practical work, which means that besides studying and analysing the components for modeling, measurements will be performed in Volvo's test labs for verifying and comparing the models with the measurements.

This chapter will explore the main reasons of introducing the project and shine light on the overview and purpose of the work. Moreover, principals, conditions and limitations of the work in addition to the solving approaches and methods will be thoroughly discussed.

1.1 Problem background

Due to the increasing number of electrically controlled components in modern heavy duty engines on one hand and sever legal, environmental and commercial requirements on the other, there is a need for a good estimation and overview method for the electrical current consumption and management. One trend is that actuators and auxiliaries are powered electrically, supplied from the battery and the alternator. The new generation of heavy duty engines are equipped with electronic control units (ECUs) controlling different systems in the engine. These engine ECUs are powered by the engine battery and depending on their control functionality they have a certain amount of input and output signals. The input signals are usually connected to different kinds of measuring instruments, such as sensors and transmitters, that are used in the control strategy. The outputs of the control strategy are mainly controlling some type of hardware equipment, such as a solenoid valve or a pump. Eventually adding all these control units to the engine, makes the engine even more complicated from the electrical perspective and increases the electrical power supply it needs.

From a different perspective electrical current consumption can also effect the fuel consumption and therefore can play an important role in fuel economy. In fact, it takes about 500 litres of diesel fuel in one million kilometres to produce around 100 W electrical power (equal to transporting 100 kg of weight); this means 0.5 millilitres extra fuel consumption per kilometre for producing 0.1 kW electrical power.

Therefore, to calculate the total electrical power supply required for energizing the electrical components in the engine and to design the corresponding protection circuits (for example determining the fuse ratings) and performing the load balance between the power consumers, it is required to have a good estimation of the amount of current consumed by each and every component inside the engine. In other words, in order to dimension alternators and batteries as well as power management control and protection strategies, there is a need to analyse the electrical current consumption in various systems of an engine for different modes of operation.

1.2 Thesis objective

The purpose of this work is to develop a method and a computer tool to simulate, document and analyse the electric current consumption of the components within the powertrain system. Since this thesis work is the start of such a project, the main focus is dedicated to design and formulate a convenient method suitable for the project, in order to achieve realistic results with acceptable accuracy.

To fulfil this principle, the project includes a combination of theoretical and practical work. This means that besides studying and analysing the components for modeling, measurements will be performed in the test labs for verifying and comparing the models with reality.

The expected results will be in the form of simulations, current calculations, and a graphical user interface display, which can be used as a software tool to check and predict the current consumption in the engine for different modes and operational states.

The main condition for the modeling is that it should be as general as possible. This means that the model should not be specifically designed for a particular component with exact ratings and specifications. Instead it should be possible to use the model for comparable components with similar characteristics and type of control. The objective of designing such kind of a general model is that it can be used for similar components that will be developed in the future and it should be able to have a good estimation of current consumption of the component in its primary stages of utilization as a component in the engine. An additional requirement on the model is that the model should also be as simple as possible. In other words, to be able to run the model, one should not have to gather extensive amount of information about the electrical and mechanical specifications of the component in order to set a lot of variables as inputs to the model.

As mentioned earlier, the project includes a user friendly graphical user interface, which should be designed in such a way that is easy to start and run the model, the input variables are easily definable and the current graphs can be easily analysed, saved and printed if required.

1.3 Thesis outline

The first stage of the project included studying and analysing various systems involved in a heavy duty truck engine, such as the after treatment system, fuel injection system, air management system, cooling system and the oil system. This primary study had two main purposes; first, to basically get familiar with the functionality of each system and its responsible ECU and second, which was actually the main focus, to identify the electrical power consuming components in each system.

As a result of the study, the urea dosing system was selected as the first case study. It was selected due to the fact that it is an independent system, with an own controller known as the ACM (After treatment Control Module). The system was also selected since it was of primary interest of the Volvo system engineering group due to its new developing technology, designed for future Euro VI heavy duty engines.

The general approach towards calculating the current consumption of the desired components was by modeling and simulating the components via simulation software tools. Hence, during the course of the project several models with different level of accuracy were designed and developed in order to simulate the current consumption of the urea dosing system.

1.4 Method

Prior to discussing in depth about the different methods of modeling and simulations implemented in this project, let's have a brief introduction to what is modeling? and what does simulation mean?

Anu Maria author of the journal titled 'Introduction to Modeling and Simulation' has a very clear description on modeling and simulation in which she states that "A model is similar to but simpler than the system it represents. A simulation of a system is the operation of a model of the system. In its broadest sense, simulation is a tool to evaluate

the performance of a system, existing or proposed, under different configurations of interest and over long periods of real time" [1].

One of the main reasons of creating a model is to analyse the effect of changes to the system. According to Maria, a well-designed model is a trade-off between realism and simplicity. She also adds that it is important that "On the one hand, a model should be a close approximation to the real system and incorporate most of its salient features. On the other hand, it should not be so complex that it is impossible to understand and experiment with it" [1].

Typically models can be classified into four main categories [1]:

- Deterministic (input and output variables are fixed values)
- Stochastic (at least one of the input or output variables are probabilistic)
- Static (time is not taken into account)
- Dynamic (time-varying interactions among variables are taken into account)

At the beginning stages of the project, choosing the right solving method (tool) was one of the most important issues that had to be taken into consideration. The two main candidates were Matlab®/Simulink® as modeling and simulating tool and Microsoft Excel® as a tool with a mathematical approach. Eventually Matlab®/Simulink® was selected as the solving tool since the work had to be carried out via modeling and simulation and simply using mathematical formulas were not sufficient to achieve the required level of accuracy in the results. Therefore all the modeling and simulations carried out in this project have been implemented via Matlab®/Simulink® due to its high performance as a simulation tool on one hand and its availability as a software tool on other. The models can be classified as stochastic and dynamic models, which were compared and verified by schematics provided by the supplier; in addition to measurements that were carried out at Volvo powertrain test labs.

1.5 Thesis boundaries

Regarding the limitations of the work, at the primary stages of the project, the scope of the work was planned to include the current consumption modeling and simulations for different systems within the engine. However, due to the in depth level of required details and lack of detailed information of the components specially detail electrical data sheets of equipment, it took allot of effort to develop a detail model so that the general model could be verified. Therefore, the project framework was limited to the Urea dosing system as one of the main power consumers in the exhaust after treatment system.

Chapter 2
Technical background

This chapter is a literature review of Volvo's internal documents, which mainly serves as an overview on the history of the diesel engine, its definition, an introduction to its different systems, the Engine Control Units (ECUs) and different engine modes. In addition there will be a brief overview of emission standards which will focus on the European emission regulations and limits.

2.1 Diesel engine

2.1.1 History

It all began in 1892 when Rudolf Diesel was granted a patent for a new type of engine. It was to be far more efficient than all previously known engine types (specially the steam engine which was the main power source for large industries) and it would be powered by a fuel which was cheaper than gasoline. Rudolf Diesel initially intended to power his new engine with coal dust, but soon his attention switched to a liquid fuel. Today, all diesel engines are driven by diesel oil. Diesel's first engine was completed in 1893. It suffered from many problems and did not produce enough power to keep itself running. It was not until 1897 that Diesel managed to produce an engine which performed anything like he had imagined. Since then, considerable efforts has been invested in research and development to bring the diesel engine to today's levels of efficiency and operational reliability.

The first diesel engines were large and clumsy and they were certainly not designed for installation in moving vehicles. Rather, they were intended as power plants for industries or as prime movers powering generators or pumps. As mentioned earlier, it took considerable time and effort before the diesel engine was ready for installation in moving vehicles. The first vehicle engines were introduced in the early 1920s and they were used in heavier vehicles such as trucks and tractors. One of the first vehicle engines is a Benz from 1922 and it is shown in *Figure 2.1*. It had two cylinders and produced 22 kW equal to 30 horsepower [2].

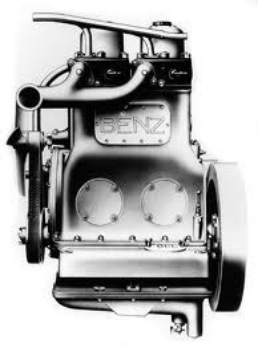

Figure 2.1 The two-cylinder Benz diesel engine from 1922, the world's first diesel engine installed in a vehicle [2]. **(Photo courtesy of DaimlerChrysler)**

Diesel engines were first fitted into Volvo trucks in 1946. The first engine was a six cylinder unit producing 71 kW (96 horsepower) and carried the VDA (Volvo Diesel engine type A) designation. More than a decade before, in 1933 Volvo's trucks were powered by an engine similar in concept to the diesel engine known as the

Hesselman[1]engine (also referred to as the "Semi-Diesel" engine) which ran on the same fuel as the diesel engine but featured an electrical ignition system.

2.1.2 Working principal

Similar to gasoline engine, a diesel engine is an internal combustion engine which basically converts the chemical energy stored in the fuel into mechanical power by means of the conventional piston-cylinder configuration. In principal the fuel and air mixture is ignited in the combustion chamber known as the cylinder, the released energy moves the piston connected to the crankshaft that converts the reciprocating motion of the piston into rotary motion and is routed through the transmission components to the driven wheels [3].

In general, diesel engines can be categorised in various ways depending on their different characteristics. The two main classifications of diesel engines (due to their crucial influence on the engine working principal) are the number of strokes completing a power stroke in the combustion cycle and the type of diesel injection. Diesel engines operate according to two or four stroke principal. The two stroke strategy is often smaller in size and is less fuel efficient due to the fuel charge escape during the exhaust part of the cycle. Hence they are quite common when it comes to small engines with one or two cylinders [4].

Therefore the focus will be on the four stroke strategy that includes inlet stroke, compression stroke, operating or power stroke and exhaust stroke. As illustrated in *Figure 2.2*, the operation begins with the inlet stroke where, clean air flows in through the inlet duct passing the inlet valve while the piston is moving away from the inlet valve. Next at the compression stroke the piston compresses the air to about one-twentieth of the volume it had at the start of the compression stroke which raises the pressure to 20-30 bars and the air temperature reaches to 700–900 °C. It is at this point that fuel injection occurs; an injector sprays in fuel under high pressure and the fuel is ignited by the hot air causing the temperature to reach around 2000-2500 °C and the pressure to 130 bars. This high pressure pushes down the piston and the force is transferred to the crankshaft. This stroke is known as the operating stroke or the power stroke. Finally in the exhaust stroke the combustion gases are expelled through the open exhaust duct and a new operating sequence begins.

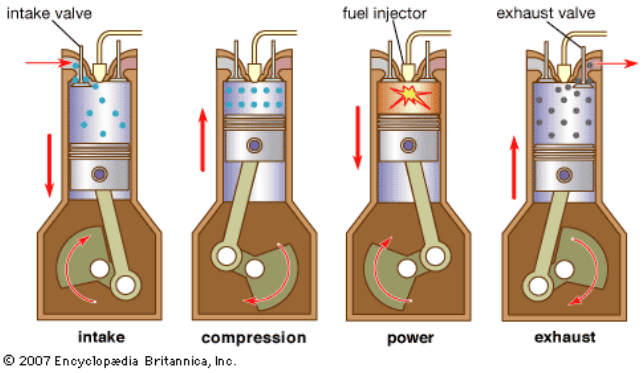

Figure 2.2 The Four Stroke Diesel Operation

[1] ***Hesselman engine:*** "The Hesselman engine is a hybrid between a petrol engine and a Diesel engine introduced by Swedish engineer Jonas Hesselman in 1925. It represented the first use of direct gasoline injection on a spark-ignition engine."

As mentioned earlier, diesel engines can also be classified into three categories depending on how the diesel fuel is being injected; the direct-injection (DI) engines, pre-chamber or indirect-injection engines and swirl-chamber engines. All these fuel injection methods have their own characteristics with different advantages and disadvantages. In brief, the direct injection has smaller losses, higher efficiency rating and lower fuel consumption in comparison to the other two methods. However, engines equipped with indirect-injection or swirl-chamber have quicker combustion and the engine can operate at high speeds up to about 6000 rpm; whereas its 4000 rpm in direct-injection engines [2].

2.1.3 Engine systems

A diesel engine like any other engine is comprised of various components and systems. Today's engines are much more complex in structure and have an advanced design due to their highly improved performance, efficiency and much lower emissions than their ancestors.

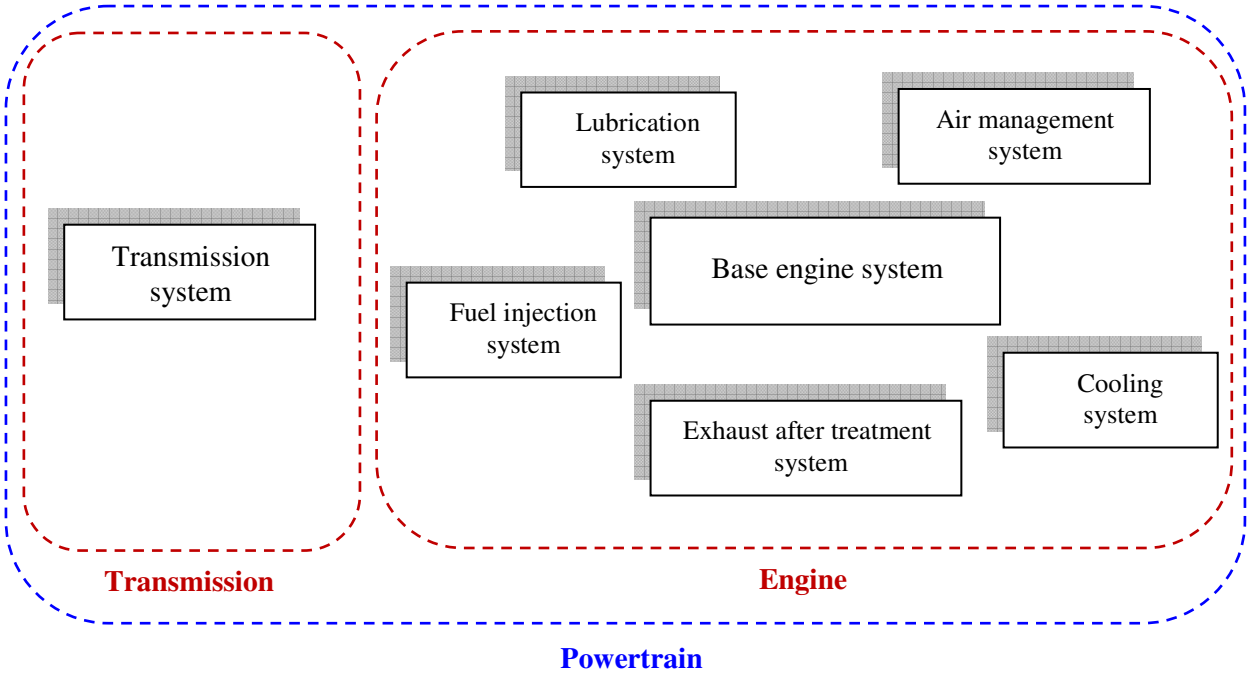

Figure 2.3 Basic powertrain block diagram

There are no definite rules as to what constitutes the main components in an engine as they all are essential and have a specific task for the engine to function safely and reliably. *Figure 2.3* illustrates a simple powertrain block diagram, including the transmission and different systems within the engine. The engine block is one of the main components in the engine which is also referred to as the base engine system and it basically includes the cylinder block with the valve mechanism, the crankshaft mechanism and the timing mechanism.

As mentioned earlier there are many different systems functioning in an engine, see *Figure 2.3*. These systems include the fuel injection system which is responsible for injecting the right amount of fuel at a specified pressure and at the right time, the lubrication (oil) system which is designed to lubricate and conduct the heat from all moving engine parts, the air management system which should control the intake and exhaust air, the cooling system that should basically cool down the engine to a temperature range of 75 to 105 °C depending on engine state and capacity. Finally the exhaust after

treatment system known as the EATS, which is designed to reduce the exhaust pollutants and to control the engine emission. The electrical and electromechanical components of the above introduced systems within the engine block (excluding the base engine system which is mainly a mechanical system) will be explained in more details in chapter 3.

2.2 Powertrain ECUs

There are various controllers involved in controlling the complete powertrain (the engine plus the transmission), which are often referred to as Electronic Control Units (ECUs). This section will introduce some of the main powertrain ECUs and the connections between them.

The most important ECU of the engine is the Engine Electronic Control Unit (EECU) also known as the Engine Management System (EMS) that basically manages everything that is in the engine, e.g. fuel injection, camshaft, crank shaft and a number of temperature and pressure sensors, see *Figure 2.4*. The transmission system has its own ECU, called the TECU (Transmission Electronic Control Unit) and it is responsible for controlling the gearbox. Moreover, the ACM (After treatment Control Module) controls the Exhaust After Treatment System (EATS), keeping the emissions always within the limits. Finally there are two sensor ECUs that are responsible for controlling the smart sensors, which are utilized for measurements taken from the exhaust gases.

All these ECUs need to communicate together in a functional and reliable manner. The following topology illustrated in *Figure 2.4*, is an example of a control system architecture utilized in a heavy duty engine.

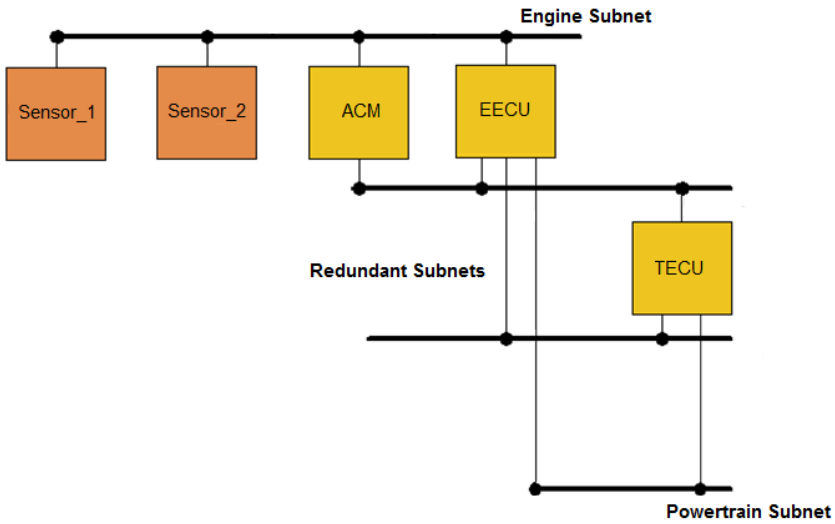

Figure 2.4 Control system architecture for Heavy Duty Engine (HDE) vehicles

In order to handle complexity and to achieve efficiency in the utilization of communication resources (buses[2]), the network topology will be segmented into subnets such as the engine and powertrain subnets, as is shown in *Figure 2.4*.

[2] ***Vehicle bus:*** "A vehicle bus is a specialized internal communications network that interconnects components inside a vehicle. Protocols include Controller Area Network (CAN), Local Interconnect Network (LIN) and others."

2.3 Engine operating modes

There is no standard definition for engine operating modes, since each engine has its own operating conditions depending on the engine type and characteristics. However, in general, one can categories the operating modes as:

- Cold start: Cranking at cold weather conditions (typical -20 ˚C)
- Normal start: Cranking at normal weather condition (+10 ˚C)
- Steady-state running: Condition that the engine is running and is coupled to the drivetrain and the throttle pedal is depressed maintaining a constant speed.
- Idle running: Condition that the engine is running but is uncoupled to the drivetrain and the acceleration pedal isn't depressed, engine idle speed differs depending on the engine, but a general truck idle speed is between 450 to 600 rpm.
- Acceleration: Condition that the engine is running and is coupled to the drivetrain and the throttle pedal is depressed, causing an increase in speed.
- Retardation by VEB+: It stands for Volvo Engine Braking, which provides an increase in braking power without the need of using the vehicle's service brakes (wheel brakes) that eventually prevents increasing thermal and mechanical loads.

2.4 Diesel emissions and standards

2.4.1 Diesel emissions

Diesel fuel is based on hydrocarbons, which means that in theory it should only produce carbon dioxide (CO_2) and water vapour (H_2O) in the time of combustion. In reality a part of the charged air (pressurized air input to the cylinder) is added and the following gases will be generated [5]:

- CO_2
- H_2O
- O_2
- N_2

Out of all the above, CO_2 is the only greenhouse gas that can be considered harmful for human health and the environment [5]. However the main threat which can have a sever adverse effect on human health and the environment are the diesel pollutants, which are basically by-products of the none-idealistic diesel combustion process that are present in a real engine. Diesel pollutants are generally divided into two categories, regulated and unregulated emissions. Regulated emissions are emissions that are regulated in US, Europe and Japan (plus some other countries) and are the main challenge of today's emission standards. Whereas unregulated emissions are diesel pollutants with much lower concentration levels. Hence the current focus of the exhaust after treatment systems are on eliminating the following compounds, known as the regulated emissions [5]:

- PM (Particulate Matter)
- NOx[3] (Nitrogen Oxides)
- HC (Hydrocarbons)
- CO (Carbon Monoxide)

[3] ***NO_x:*** is a generic term for the mono-nitrogen oxides NO and NO_2

2.4.2 Emission standards

In today's world there is a standard for almost everything that is being produced, and when it comes to the mankind's health and environmental issues, emission standard plays an essential role. Emission standards basically set the limit for different pollutants in different applications. There are various emission standards defined specifically for each industry such as in automobile industry, aviation industry, power plants and many more.
In the automobile industry itself, the emission standard can differ depending on the type of the vehicle (passenger cars, light commercial vehicles, Trucks, busses, and …) and also the country that the vehicle will be used in, such as the European emission standard, US emission standard, Japan emission standard etc.

The European emission standard is the standard responsible for setting the exhaust pollutants level in vehicles utilized in EU member states. Moreover, these standards are introduced through documentation known as the "European Union directives" that are defined in series of increasingly rigorous regulations addressed to the automobile manufacturers [6]. These standards are defined separately for light-duty (Euro1 … 6) and heavy-duty (Euro I … VI) vehicles. According to the European commission (division of transport and environment), for light-duty vehicles "Euro 5 has been entered into force in September 2009. The main effect of Euro 5 is to reduce the emission of particulate matter from diesel cars from 25 mg/km to 5 mg/km. Euro 6 is scheduled to enter into force in January 2014 and will mainly reduce the emissions of NOx from diesel cars further, from 180 mg/km to 80 mg/km" [6].
Table 2.1 shows the European emission standards for heavy-duty diesel engines, including the different standards, their implementation dates and emission limits.

Table 2.1 EU Emission Standards for HD Diesel Engines, g/kWh (smoke in m−1) [7]

Tier	*Date*	*Test cycle*	*CO*	*HC*	*Nox*	*PM*	*Smoke*
Euro I	1992, < 85 kW	ECE R-49	4.5	1.1	8.0	0.612	
	1992, > 85 kW		4.5	1.1	8.0	0.36	
Euro II	October 1996		4.0	1.1	7.0	0.25	
	October 1998		4.0	1.1	7.0	0.15	
Euro III	*October 1999 EEVs* only*	ESC & ELR	1.0	0.25	2.0	0.02	0.15
	October 2000	ESC & ELR	2.1	0.66	5.0	0.10 0.13*	0.8
Euro IV	October 2005		1.5	0.46	3.5	0.02	0.5
Euro V	October 2008		1.5	0.46	2.0	0.02	0.5
Euro VI	January 2013		1.5	0.13	0.4	0.01	
*For engines of less than 0.75 dm^3 swept volume per cylinder and a rate power speed of more than 3000 per minute. *EEV is "Enhanced Environmentally friendly Vehicle".							

It should be noted that the ECE R-49 was the earlier steady-state engine test and on the Euro III stage it has been replaced by two test cycles, the ESC which is the European Stationary Cycle and the European Transient Cycle known as the ETC test cycle. Furthermore the smoke opacity is measured via the ELR (European Load Response) test.

Chapter 3
System description

This chapter explains and describes the systems in the powertrain shown in *Figure 2.3* of the diesel truck with more focus on the electric loads which are controlled by the engine electronic control unit (EECU) and the after treatment control module (ACM). The description includes the used concepts, to provide any overview of the different subsystems, the purpose of the subsystem/component and the type of components (sensors, actuators) in each system. The flow charts in *Figure 3.1* and *3.2* explain only the electromechanical systems and electric components controlled by the EECU and the ACM. All components in the figures are briefly described in this chapter.

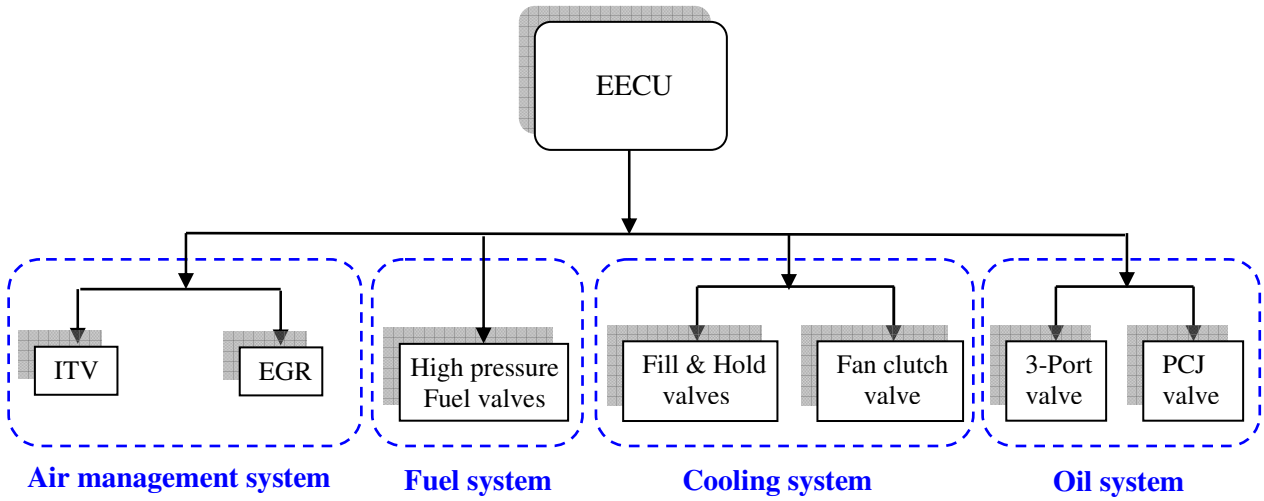

Figure 3.1 Electromechanical systems and components connected to the EECU

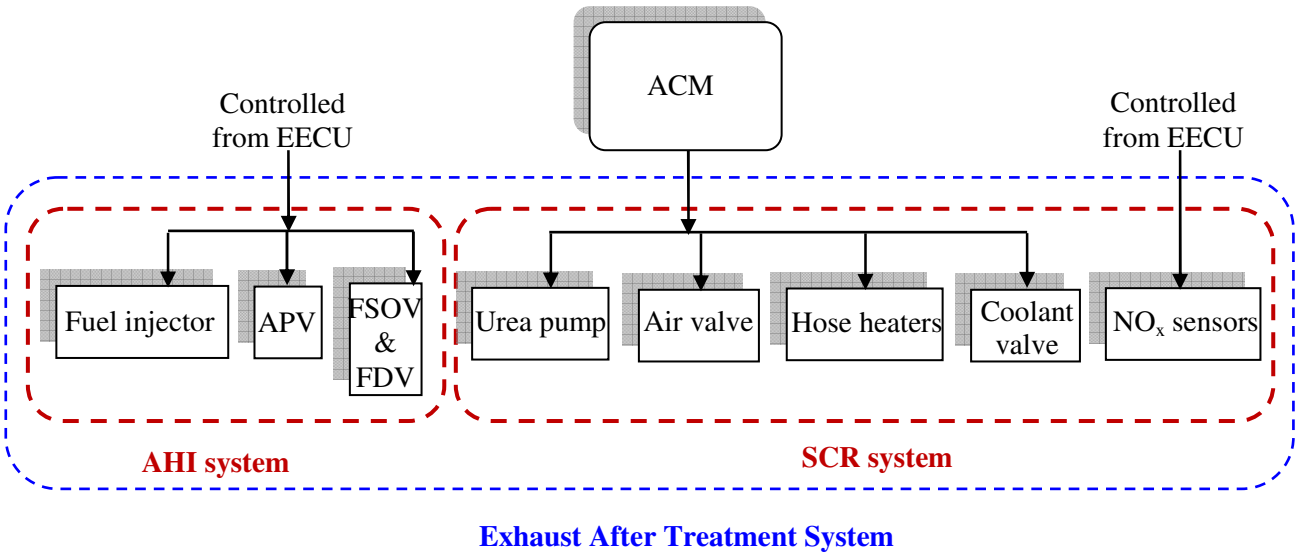

Figure 3.2 Electromechanical systems and components connected to the ACM

3.1 Exhaust After Treatment System (EATS)

The purpose of the exhaust after treatment system is to filter the exhaust gases from toxic substances with the help of a Urea solution[4] which is injected into the exhaust system between the turbocharger and the silencer with its built-in catalytic converter. The two main functions of the EATS are to reduce chemical pollutants (NOx, CO and HC) and the soot particles in the exhaust gas. The EATS is a needed work-around since the combustion process in the cylinders cannot reach the regulated emission levels on its own. The first subsystems in the EATS is the after treatment hydrocarbon injection system (AHI) passing by some thermal and chemical processes which are out of this thesis scope, and it ends by the selective catalyst reduction system (SCR) which shall be discussed later in this chapter.

3.1.1 After treatment Hydrocarbon Injection System (AHI)

The purpose of the AHI system is to inject fuel in the exhaust pipe in order to help burning soot, and to raise the temperature of the exhaust going through the SCR[5] system. All the AHI components are connected to the EECU. The AHI is shown in *Figure3.3* and it consists of two parallel supply lines for fuel and air connected with a fuel nozzle. The fuel line is connected to a fuel delivery valve which is used to control the amount of injected fuel, a non-return valve which prevents the fuel to flow in the reverse direction, a fuel pressure sensor used to measure the fuel pressure before and during injection, and a fuel shut off valve to control the fuel supply coming from the engine to the system. On the air supply line there is a purge valve which is used to purge the fuel line from fuel and also to cool down and clean the nozzle, also it is equipped with a non-return valve to make sure that the air flow is moving in one direction.

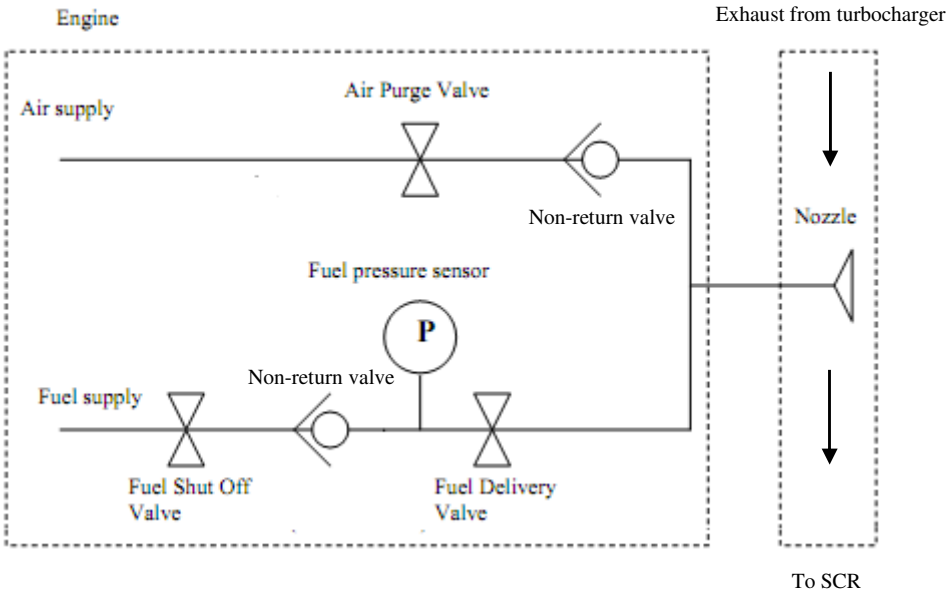

Figure 3.3 Overview of the AHI system

[4] ***Urea solution:*** is an organic compound handled in liquid form at the production plant and is then mixed with deionised water. The solution is injected in the exhaust system and when it is heated to about 200 cº it reacts with the nitrogen oxide emissions and converts into nitrogen and water within the SCR. The Urea solution normally freezes at -11ºc.

[5] ***SCR:*** is a means of converting nitrogen oxides with the aid of a catalyst into diatomic nitrogen, N2, and water, H2O.

3.1.2 Selective Catalyst Reduction (SCR)

The aim of the SCR system is to reduce the NOx emissions in the exhaust gas by injecting the Urea solution upstream the SCR catalyst converter. The urea is atomised through the Urea nozzle with the aid of pressurised air, controlled through an air valve. The Urea mist is sprayed ahead of the catalytic converter where it is quickly heated and forms ammonia. After the exhaust gases have been mixed with the ammonia, the exhaust gases are led further on into the SCR catalytic converter which reacts together with the ammonia and nitrogen oxides in the exhaust gases to form water vapour and harmless nitrogen gas.

The SCR system is shown in *Figure 3.4* and it comprises of the Urea tank, Urea dosing subsystem including Urea pump and air valve, two hose heaters, Urea air nozzle, Aftertreatment control module ACM, NOx sensors, tank level sensor, coolant valve, and the SCR catalyst converter. All valves, hose heaters and pump actuator are controlled by the ACM.

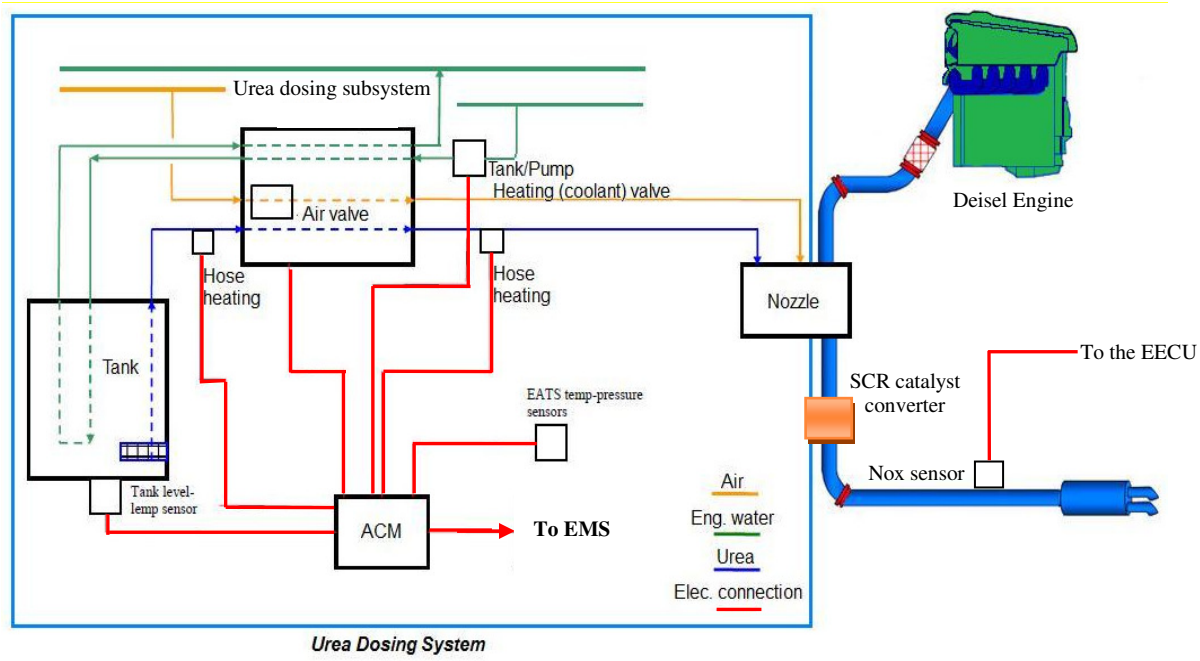

Figure 3.4 Overview of the SCR system with control signals from/to the ACM

Urea injection

The aim of the Urea injection is to distribute the Urea more evenly by injecting air together with the Urea. The system consists of the Urea air nozzle and the Urea dosing subsystem in *Figure 3.4* and in *Figure 3.5* it is shown in detail.

The Urea dosing subsystem comprises of an air valve, Urea pump, reed valve, air and Urea pressure sensors, and Urea temperature sensor.

When the solenoid of the urea pump is activated it makes one full stroke each time, delivering a defined amount of urea through the nozzle. The reed valve in *Figure 3.5* opens at approximately 4 bars which is required when the system shall be flushed before shut-down. The urea pump is a frequency controlled type with a maximum of 50 Hz, while the air valve is controlled by a PWM (duty cycle controlled) of around 800 Hz.

The ACM controls the air valve and the urea pump and measures the air pressure, the urea pressure and the urea temperature.

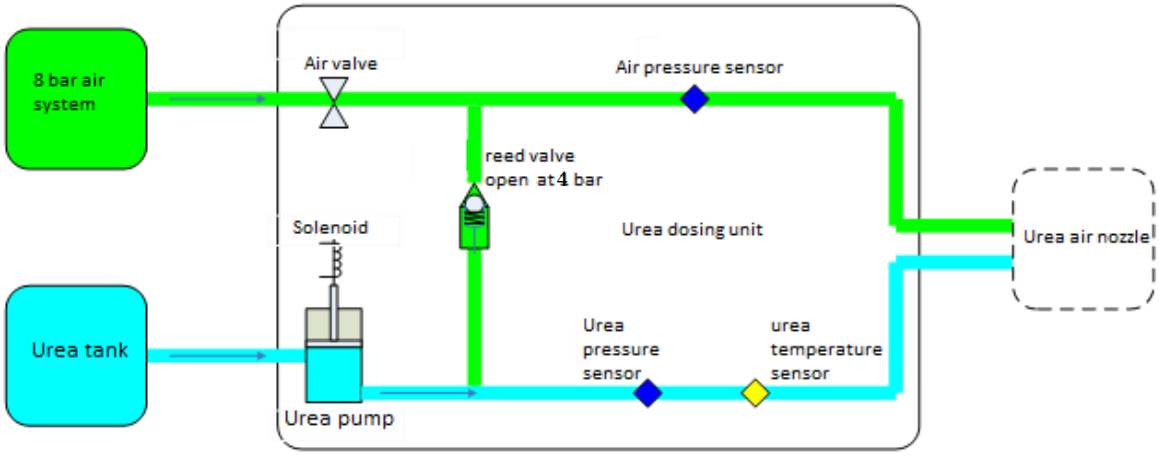

Figure 3.5 Urea dosing subsystem overview

Urea heating

The purpose of this function is to heat-up the urea hoses and tank when urea is frozen due to too cold temperature. In order to allow this operation the dosing system is equipped with 2 heating systems. An electrical heating for the urea hoses and a coolant valve is used to heat the urea pump and urea tank with the engine coolant liquid as shown in *Figure 3.4*.

The electrical heaters are connected with the ACM and they are controlled with PWM according to ambient air temperature threshold value, electric heating request from the heating mode control and battery voltage, while the coolant heating valve allows engine coolant liquid circulating in the urea tank (through the tank sensor). This heating valve is controlled through a coolant heating request from the ACM which depends on several inputs, and a urea tank and urea pump temperature threshold, i.e. these temperatures are above the respective temperature threshold.

NOx sensors

The NO_x sensors measure the amount of NO_x in the exhaust gases before and after the SCR. In *Figure 3.4* the placement of the NO_x sensors after the SCR catalyst converter can be seen. The sensors are connected with the EECU and the measured NOx value is comunicated over the bus to the ACM

3.2 Engine air management system

The engine air management system is mainly composed of a charge air cooler (CAC), an intake throttle valve (ITV), an electric preheater, and an exhaust gas recirculation system (EGR). *Figure 3.6* shows a simple diagram for the system layout. The electric loads in this system are mainly the electric preheater coil, the ITV and the EGR valve

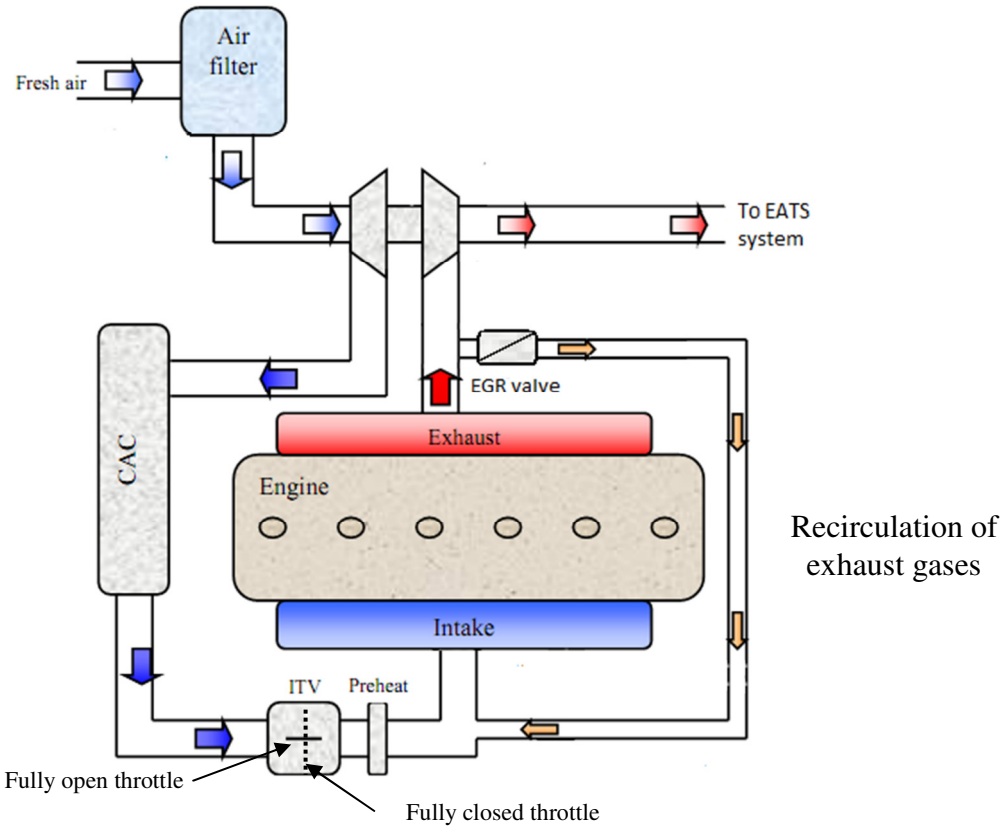

Figure 3.6 Overview of the air management system

3.2.1 Intake throttle valve (ITV)

The intake throttle is used for the heat regeneration purpose. It decreases the mass air flow and increase the exhaust temperature for the after treatment system. It consists of a throttle controlled by a dc electric motor mounted in the intake air system between the charger air cooler (CAC) and the intake of the engine as can be seen in *Figure 3.6*. The throttle controls the air flow to the engine basically by a disc that can be tilted. When the disc is parallel to the airflow it is easy for the air to pass, and when the disc is perpendicular to the air flow it is very hard for the air to pass. The "Diesel" throttle has a normal position which is fully open.
The ITV is connected to the EECU via the engine harness. In the EECU an H bridge drive is used for the electrical motor directional control by using a PWM duty cycle control. An analogue input is used for the throttle position sensor input.

3.2.2 Exhaust gas recirculation (EGR)

The EGR system is used to re-circulate a small amount of the exhaust gases through the intake manifold where it mixes with the intake air, as can be noticed in *Figure 3.6*. The EGR system of an engine has multiple purposes. The two main purposes are to increase the inlet manifold temperature for having better heat management control and to reduce the amount of NOx gases created by the engine during operation periods that usually results in high combustion temperatures. The EGR system consists of an EGR valve, two EGR coolers, and one venturi pipe with a differential pressure and temperature sensors for measuring the exhaust mass flow. The electric load in the EGR system is the EGR valve, the sensors electric consumption is considered to be negligible. The EGR valve assembly consists of a solenoid operated hydraulic servo actuator which operates a hot side poppet in a

proportional manner. A poppet is a normally closed 2 way valve which is designed to control the flow of exhaust gases in an exhaust recirculation system in the high temperature and high flow environment of diesel engines. The engine control module controls the EGR valve by a PWM voltage to the solenoid.

3.3 Fuel system

The Fuel system is divided into two main systems which are the low pressure, and the high pressure fuel systems. In *Figure 3.7* the fuel system is shown with the low pressure and the high pressure systems. The low pressure fuel system is responsible for supplying fuel to the engine with the right pressure, and to insure that there is no dirt or water in the fuel. The low pressure system doesn't contain any recognizable electric current consuming units, the low pressure fuel pump is mechanical and the temperature sensor doesn't consume any noticeable power. Therefore only the high pressure fuel system will be described more in details.

The high pressure fuel system is a distributed pump common rail system (DPCRS), where each cylinder has its own injector which contains a pumping element. The working principle of the high pressure fuel system is that a high pressure pump stores a reservoir of fuel at high pressure. The term "common rail" refers to the fact that all of the fuel injectors are supplied by a common fuel rail which is nothing more than a pressure accumulator where the fuel is stored at high pressure. This accumulator supplies multiple fuel injectors with high pressure fuel. When the fuel injectors are electrically activated, a hydraulic valve (consisting of a nozzle and plunger) is mechanically or hydraulically opened and fuel is sprayed into the cylinders at the desired pressure. Since the fuel pressure energy is stored remotely and the injectors are electrically actuated, the injection pressure at the start and end of injection is very near the pressure in the accumulator (rail).

The fuel injectors are solenoid valves which are controlled by a PWM converter through the EECU. The electric loads in the fuel system are the solenoid valves in the fuel injectors and the electric converter supplying the valves. The pressure electric sensor is not considered as an electric consuming load.

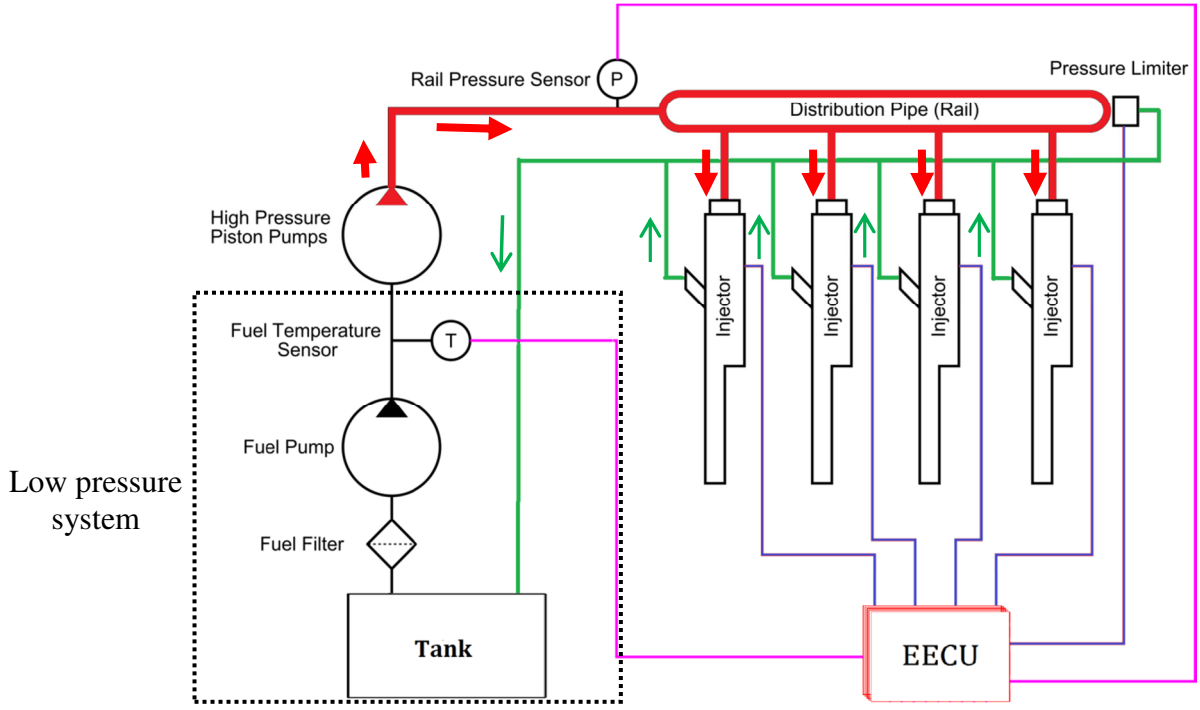

Figure 3.7 High pressure fuel system configuration

3.4 Cooling system

Different engine parts are cooled in different ways. Some of the heat is radiated from the sides of the engine itself, 10-15 % of the heat is dissipated by the lubricating oil and about 20-30 % is handled by the cooling system.

The latest heavy duty truck engines are equipped with a double circuit cooling system, as shown in *Figure 3.8.* The system basically consists of two cooling circuits that cool different subsystems and they are referred to as the High temperature (HT) and low temperature (LT) circuits. The HT circuit is the main cooling system of the engine block and therefore will have a higher temperature. The HT circuit includes a fully variable coolant pump, a radiator and a wax thermostat 3 way valve for bypassing the radiator when no further cooling is required. The LT cooling circuit is used to cool down the low temperature part of the Exhaust Gas Recirculation (EGR) and it includes a small fixed mechanical pump, a cooler known as the low temperature cooler (LTC) and a wax thermostat[6] valve is used in some designs. The main electrical loads used in the cooling system are three PWM controlled solenoid valves, whereas two are utilized in the pneumatic clutch, controlling the variable HT pump and one is used in the cooling fan.

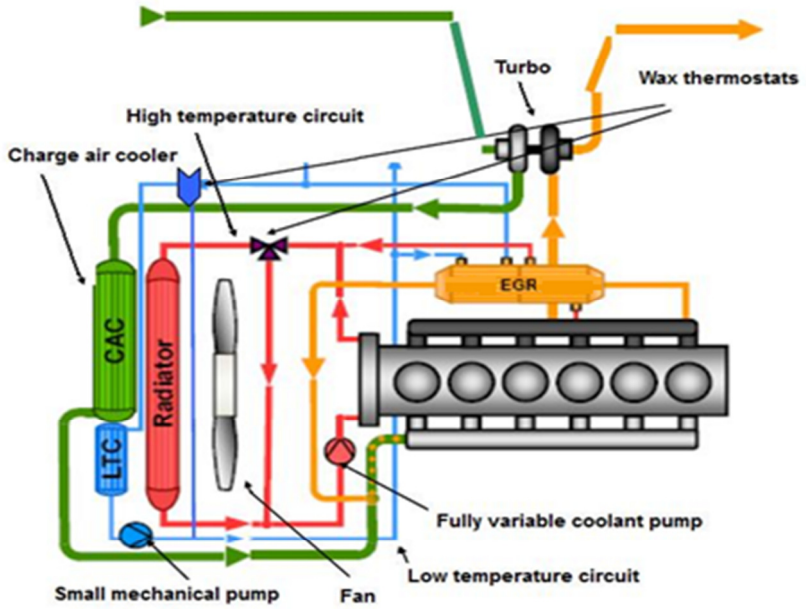

Figure 3.8 Double circuit cooling system, low and high temperature

The HT pump is driven by the drive pulley and the variable pump flow is controlled by a variable clutch which is actuated by a pneumatic cylinder, see *Figure 3.9*. The position of the cylinder is controlled by compressed air which is controlled by two solenoid valves. In addition there is a position sensor to indicate the position of the clutch and thereby the engagement ratio of the pump. The pneumatic cylinder has a single connection with the air valve unit containing the two valves. The piston in the cylinder has a spring counter force which will act to emptying the cylinder from air.

One valve is for filling the pneumatic cylinder with compressed air known as the fill valve. The type of the fill valve is N/C (Normally Closed) and the other valve is for

[6] ***Wax thermostat:*** "A thermostat in which the expansion of melting paraffin wax (in a rigid cylinder) deforms a moulded rubber membrane and displaces a piston/pin from the cylinder; this has the advantage of being insensitive to sudden temperature fluctuations or to the pressure in the system."

holding the compressed air so that the cylinder maintains its current position, the hold valve. The type of the hold valve is N/O (Normally Open). If the hold valve is not engaged the air in the cylinder will be drained and the pump will be fully engaged. The cylinder is connected to the exhaust and deflates under the action of its return spring. This is the default (failsafe) mode which occurs whenever there is no electrical supply to the valve unit. Both the fill and hold valves are controlled by PWM signals coming from the Engine ECU (EECU).

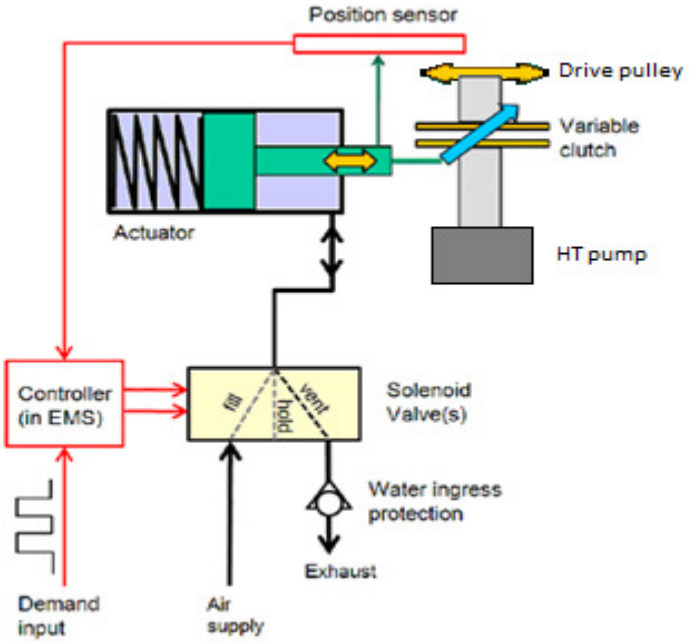

Figure 3.9 Schematic of the pneumatic clutch system for the HT pump

Another crucial component in the engine cooling system is the cooling fan. Cooling fans can be electrically driven or belt-driven by the engine. Truck engines are usually equipped with the belt-driven type since the engine is mounted vertically and the fan can be easily connected to the crank shaft of the engine. One of the well known belt driven fans which provides a controllable variable speed is the viscous type fans, which the fan speed is controlled by the amount of oil in the clutch housing.

The newer versions of clutches have an electrical controlled solenoid valve which controls the amount of oil admitted into the coupling. The solenoid valve operates with a pulse-width-modulated (PWM) signal coming from the EECU as can be seen in *Figure 3.10*, in addition the fan has a closed loop control and therefore uses a speed sensor for calculating the amount of error between requested speed and actual speed so the EECU can calculate the duty cycle of the PWM controlling the solenoid valve.

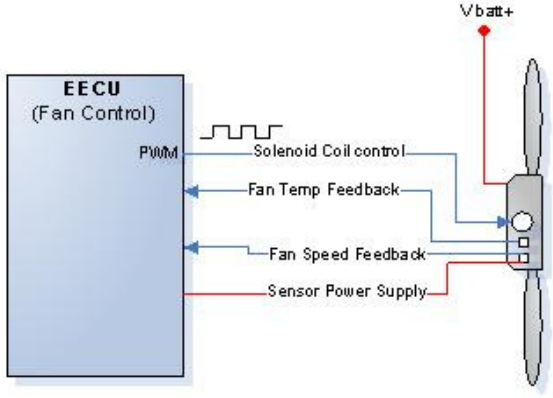

Figure 3.10 Cooling fan electrical control

3.5 Lubrication (oil) system

The main functions of the engine oil system is to reduce wear and friction, conduct heat, act as an sealing agent and keep the engine clean by preventing build-up of sludge and corrosion inside the engine. Today's heavy duty engines are equipped with a pressure lubrication system, whereby almost all the engine's components are lubricated by oil supplied under pressure via the oil pump. The oil pump is driven by the crankshaft through an idler gear. Hence only the cylinder walls and the timing gears are splashed-lubricated. A well designed oil system should be able to optimize the oil flow, temperature and pressure in different engine running conditions in order to decrease the average friction losses and decrease fuel consumption. This function is usually referred to as thermal management which is determined by two main concepts in the oil circuit, the oil thermostat control and piston cooling jet functions. In *Figure 3.11* the simplified lubrication system for a heavy duty engine is shown.

The two main electrical loads identified in the oil system are the 3-port thermostat valve (utilized in the oil thermostat control) and the piston cooling jet valve (has the main role in the piston cooling jet functions) which will be described in more details. To achieve the oil thermostat control, a closed loop control of the oil temperature is used, which includes a 3-port electrically controlled valve and an oil temperature sensor. The 3-port thermostat valve is controlled by a PWM signal (outgoing from the EECU) in such a way that when a 0 % duty cycle PWM is applied (no current) the valve is in "full cooling" position, i.e. all oil run through the oil cooler which is the fail-safe position. When 100 % duty cycle PWM is applied (max. current) the valve is in the "full by-pass" position, i.e. the valve closes the oil cooler branch and it opens the by-pass branch.

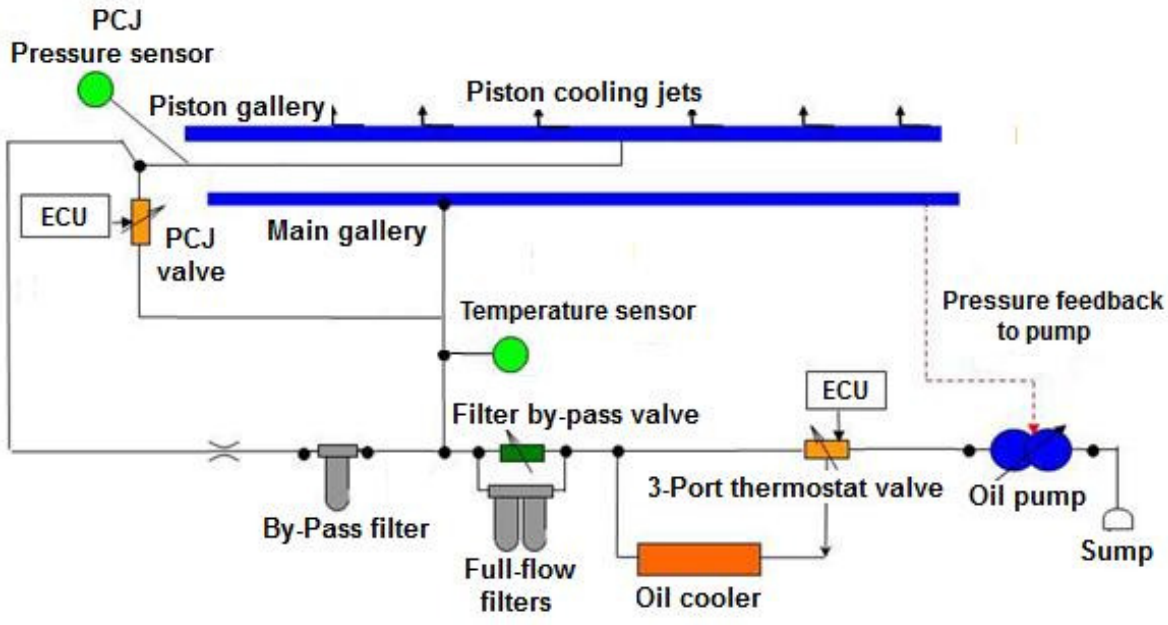

Figure 3.11 Simplified lubrication circuit in a heavy duty engines

The piston cooling jet (PCJ) valve is located at the inlet of the piston cooling jet gallery, as can be noticed in *Figure 3.11,* in order to manage the oil flow for the piston cooling jets. It spreads the oil under the pistons for the purpose of cooling. The aim is to reduce the fuel consumption, which is achieved by adjusting the piston cooling jet flow according to the need. The main risk, when controlling the piston cooling jet oil pressure, is piston seizing because of a too high piston temperature. An increased piston temperature can damage the piston structure and reduce the life expectancy of the piston. The control is

achieved by a PWM signal coming from the EECU to the solenoid in the valve, which works towards a spring. Furthermore an oil pressure sensor for the piston cooling jet function is positioned in the piston gallery. The sensor is used to provide a feedback signal to the control of the PCJ valve and to prevent a too low pressure.

Chapter 4
System modeling and simulations

In order to simulate the current consumption of the Urea dosing system, three major approaches of modeling were taken during the course of the project:

- Basic (block) model
- Detailed model
- General model

In this chapter three different models for the Urea dosage system shall be discussed (block model, detailed model, and general model), the general model is considered to be the final selected model in this project.

The basic (block) model is a simple and straight forward model, designed in Simulink® environment, with the general concept of calculating the current from the voltage and impedance. The basic model is a pure electrical model, having no mechanical perspective included. Moreover, the resistance and inductance were included as constant parameters. This model is reasonably sufficient for simulating the rather simple components such as the hose heaters and the coolant and air valves which are considered more as resistive loads. However, the results obtained from the basic model weren't realistic for the urea pump due to its complex electrical and mechanical structure.

The detailed model was designed only for the urea pump and it was implemented to describe the electrical and mechanical equations related to the theory of the system and to create a model quite similar to reality. Hence, the detailed model includes an extensive number of mechanical parameter, such as the dimensions of the Urea dosing pump and Urea mass to detailed electrical parameters such as variable inductance of the coil and the behaviour of the magnetic flux. With all this detailed information the model predicts the measurements well.

However the extensive level of details used, made it time consuming to build the model and to obtain the parameters needed. Therefore the general model was designed based on the two previous models (the basic and detailed models) as a compromise between the two. While designing the final general model the main focus was on two fundamental issues. First, the model should inherit the simplicity of the basic (block) model so the user does not require extensive information as input parameters to run the model and second, the accuracy of the model should be as close as possible to the detailed model and therefore to reality. This could be achieved by modeling the power flow and losses in the component.

4.1 Basic (block) modelling

In this section the model of the Urea dosage system implemented in Simulink® is explained. The idea of this type of modelling is to build separate blocks that can be detached when required or added if another component is added to the system. In this way the model can be modified easily when any change is applied in the future for the system. The current consumption for the Urea dosage system components, see *Figure 3.4* and *3.5* (Urea pump, coolant valve, air valve and the hose heaters), are modelled separately and the total current consumption for the system is modelled as the sum of the currents as shown in *Figure 4.1*. The current consumption is calculated by dividing the voltage to

each component with the transfer function of the components impedance. The impedance transfer function is based on the inductance and resistance of the solenoid components (pump and valves) and resistance for the heaters. The inductance of the Urea pump was estimated from values calculated for the detailed model that will be described later on in this chapter, while the inductance parameters for the air valve, and the coolant valve were given by the supplier.

To calculate the voltage to the components, the battery voltage, Urea dosage amount, pump temperature, tank temperature, air valve duty cycle, and ambient temperature are used and these signals are the input to the block model, as shown in *Figure 4.1*. There are no wiring connections between inputs and the electric components in *Figure 4.1,* instead blocks are used (blue blocks in *Figure 4.2*). The reason is to facilitate moving or changing any of these components separately and to reduce complexity of connected wires. In the following section the calculation of the voltage to each component will be described.

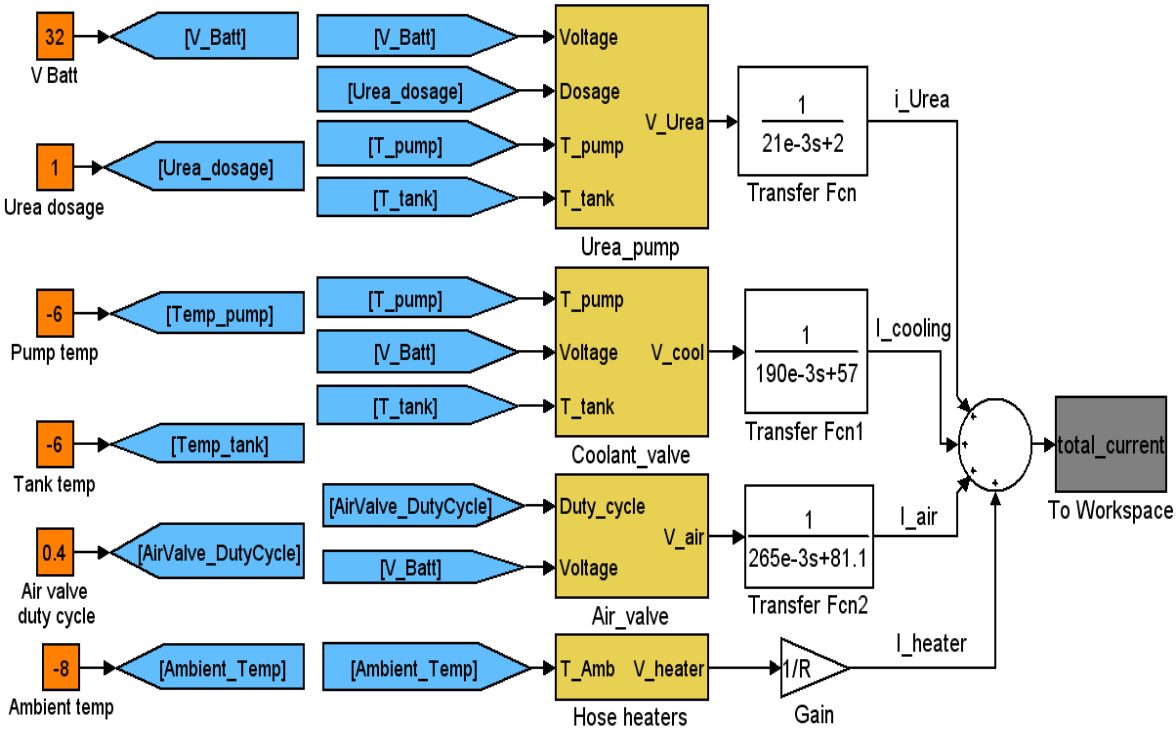

Figure 4.1 Block model for the current consumption of the Urea dosage system.

4.1.1 Urea pump model

The Urea pump is a solenoid pump, shown in *Figure 3.5*. When the voltage is applied to the coil, a current starts to flow in the coil which will pull the piston to the coil and fill the pump with Urea. When the voltage supply is removed, the current will reduce to zero and the spring in the pump will push the urea to the nozzle which sprays the urea into the exhaust pipe. Due to regular fluctuation of the battery voltage, the $\mathbf{t_{on}}$ has to be adjusted. *Table 4.1* shows the equivalent $\mathbf{t_{on}}$ time and the maximum frequency that can be reached with the pump for some voltage values. The table is given by the pump manufacturer and data can be updated to the model easily through the $\mathbf{t_{on}}$ and the maximum frequency maps found in the model as shown in *Figure 4.2,* where the internal structure of the Urea pump's block in Figure 4.1 is shown.

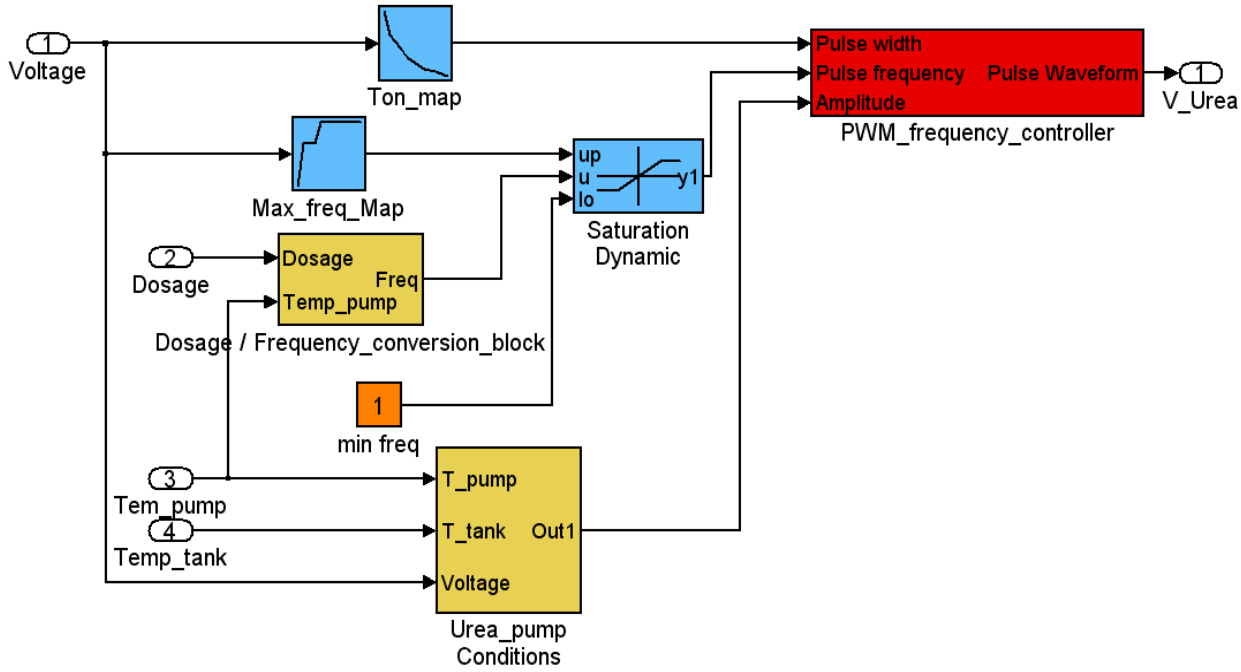

Figure 4.2 Overview of the internal structure of the Urea pump control system

Table 4.1 Voltage-t_{on} map supplied by the manufacturer

Voltage [V]	*Turn-on time [ms]*	*Max. frequency [Hz]*
10	17	35
12	14	45
14	13	45
16	12	45
18	11	50
24	9.5	50
28	9	50
32	8.5	50

By changing the frequency of the input voltage to the pump, the urea dosage can be controlled. The dosage /frequency conversion block shown in *Figure 4.2* is responsible for convert the Urea dosage signal to the corresponding frequency demand of the pump through the following equation

$$frequency = \frac{Pumping\ factor \times \text{Dosage}}{Density} \tag{4.1}$$

Where

$$Pumping\ factor = \frac{Max\ pump\ Frequency}{Max\ Urea\ flow} \tag{4.2}$$

From the data sheet of the pump, the maximum frequency is given to be 50 Hz and this corresponds to a maximum Urea flow of 2.15 cm^3/s, while the density of the Urea is calculated from the density map by using the corresponding pump temperature signal (T_pump). This mathematical equation is located inside the Dosage/frequency conversion block as shown in *Figure 4.3*.

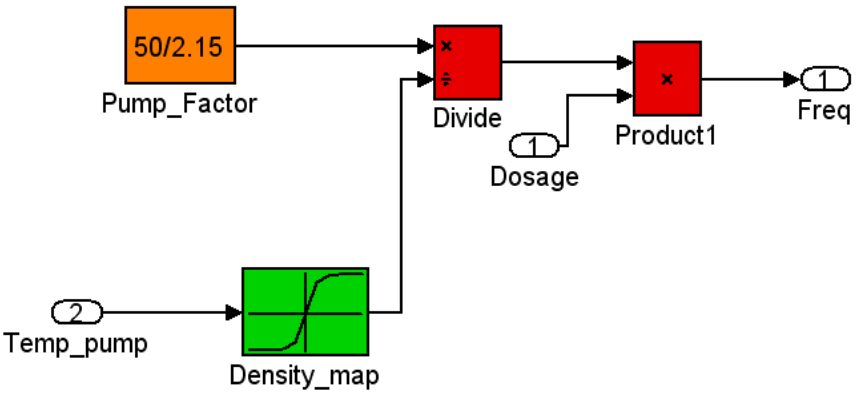

Figure 4.3 Dosage/frequency conversion block

The Urea pump conditions block shown in *Figure 4.2* is used to define conditions for activating the pump. The pump operation is mainly depending on temperature signals coming from the tank and pump temperature sensors. The pump works only when both temperatures are greater than -6 C˚ and in this case the battery voltage is provided as the amplitude output, otherwise zero is provided as an output to stop the operation of the pump. The PWM frequency controller shown in *Figure 4.2* has 3 inputs (pulse width, pulse frequency, and amplitude). The Pulse width gives the correct $\mathbf{t_{on}}$ from the map discussed before. The Pulse frequency input receives its signal from the dosage frequency conversion block and a saturation dynamic block which sets the maximum rated frequency that the pump could reach. The Amplitude signal gives out the dc voltage coming from the battery through the Urea pump conditions block.

4.1.2 Coolant valve model

Since the coolant valve is switched on or off only, it is considered to consume a fixed current during operation. The valve works under certain conditions which are defined in the internal structure of the Coolant_valve block in *Figure 4.4*. The operation of the coolant valve depends on the pump and tank temperature values coming from the temperature sensors. The valve should be activated only if both temperatures are less than 10 C˚ and the coolant voltage will be equal to the battery voltage in the vale, else the coolant voltage will be equal to zero.

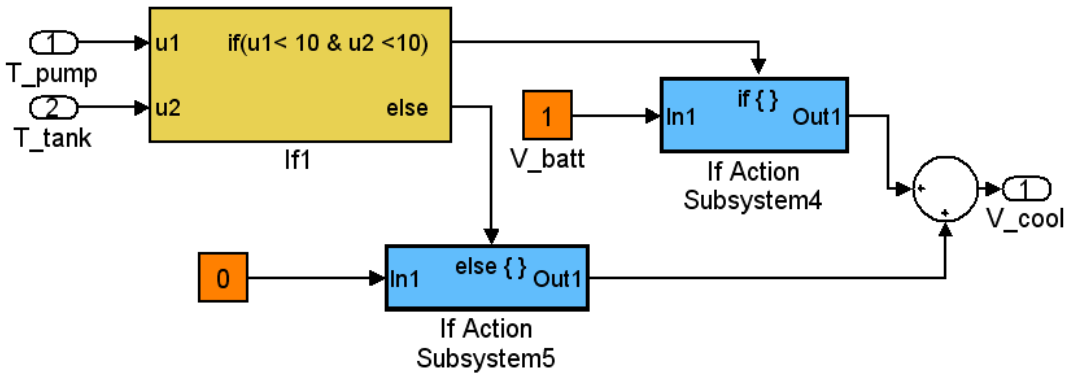

Figure 4.4 internal structure of the Coolant_valve

4.1.3 Air valve model

The air valve voltage is a PWM controlled voltage with a defined duty cycle. The duty cycle is used to control the air flow to the nozzle. For simplicity a fixed duty cycle of 0.4

was selected and this value is based on the normal operating range of the duty cycle. Thus since the control for the duty cycle is complicated and depends on many external parameters in the engine. The result will not show large error since the current consumption in the air valve is comparatively very small regarding to the other loads in the system.

4.1.4 Hose heaters model

The hose heaters operation can be divided into 3 different conditions. The first condition is when the ambient temperature is less than zero degrees. At this temperature the heaters will work with their full capacity (9 A) for each heater. The second condition is a linear relation between current consumption and ambient temperature rise. For the third condition the heaters will stop working when ambient temperature exceeds 4 degrees Celsius. In *Figure 4.5* the operation (current consumption) of one heater is shown for different ambient temperatures.

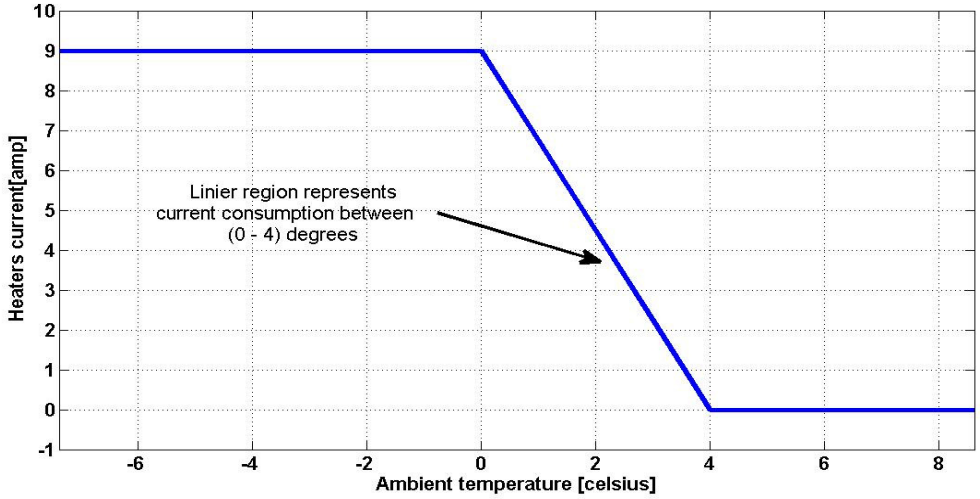

Figure 4.5 Current consumption in hose heaters during different ambient temperatures

All conditions where set in the heaters conditions block as shown in *Figure 4.6* which describes the internal structure of the Heaters_conditions shown in *Figure 4.1*.

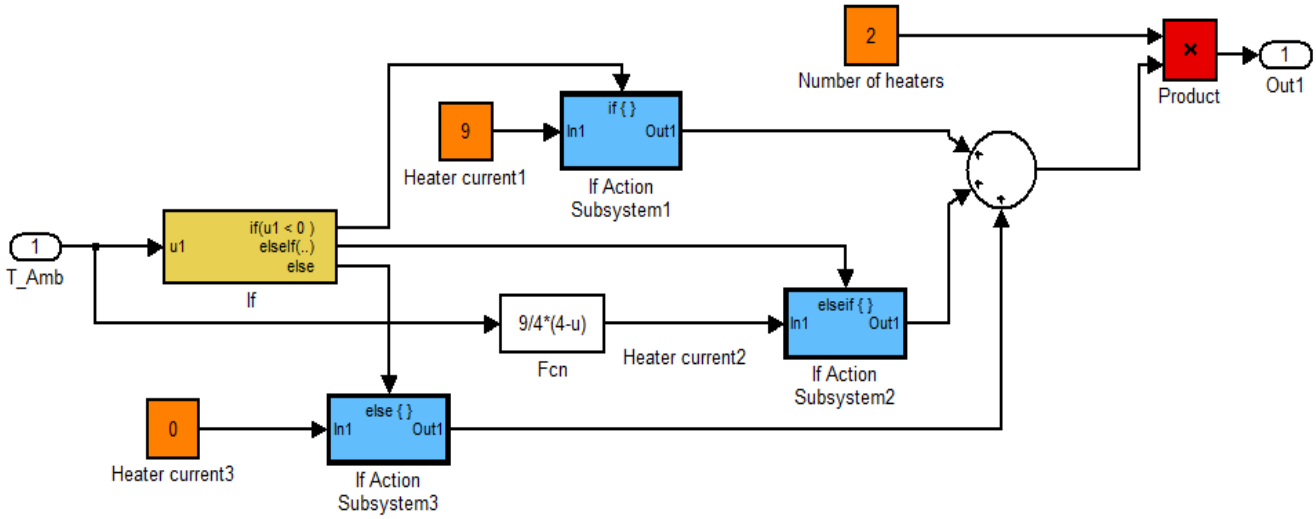

Figure 4.6 Operating conditions of the hose heaters

4.2 Detailed modelling of the urea pump

The detailed modelling is an extensive simulation for calculating the internal variable inductance of the Urea pump coil during the dynamic motion of the pump's solid core and under a variable magnetic flux. Also it was used to calculate the mechanical losses, which depends on several parameters like friction, spring, and damping forces during the movement of the pump core.

A simple drawing of the pump is shown in *Figure 4.7* and it gives an idea about the operation of the pump. The inner piston of the solenoid pump is normally relaxed back to the left side by the spring. When the electric power is applied to the coil denoted by the yellow colour, the piston is retracted to the right side (negative direction) by the act of the electric force $\mathbf{F_e}$ opposing the spring force and $\mathbf{F_s}$ the damping force $\mathbf{F_{damp}}$ occurring due to friction of the piston with the urea. At the end of the stroke a very high force is needed to simulate the stopping of the piston $\mathbf{F_{stop}}$, which shall be discussed later in the mechanical equation's part. During this operation the pump is filled with Urea. After the voltage pulse is removed, the piston will relax back fast (positive direction) by the act of the spring force and opposite to the damping force $\mathbf{F_{damp}}$ which will be created by the opposing Urea pressure this time, permitting the Urea to move through a small orifice and non-return valve to give the required pressure for the nozzle.

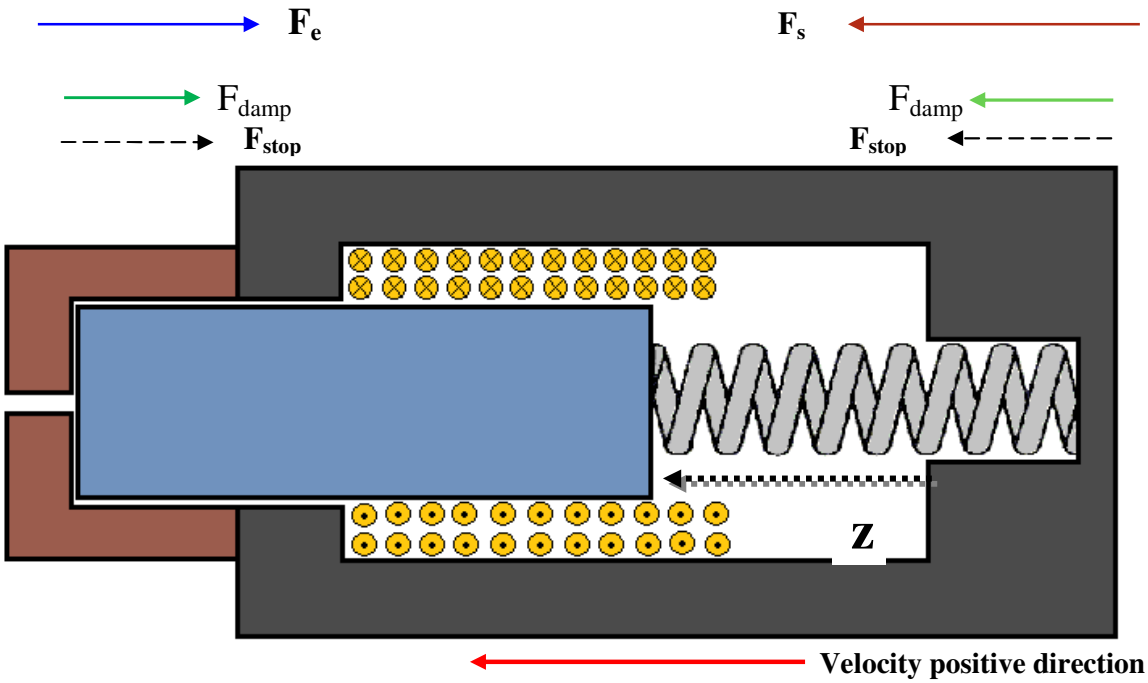

Figure 4.7 Simple construction of the Urea pump

4.2.1 Mechanical model

The mechanical equation of the pump according to Newton's second law of motion could be written as

$$ma = m\ddot{z} = m\dot{v} = F_e + F_s + F_{stop} - F_{damp} \tag{4.5}$$

The spring force $\mathbf{F_s}$ was assumed as a constant value (equals to 10 N.m) to match with the opposing electric force $\mathbf{F_e}$. The dosing process in this pump is done by the action of the spring force during the off period of the voltage pulse. When the coil is relaxed, the piston moves fast back to normal position and let the urea to be dosed. By trials, the damping force $\mathbf{F_{damp}}$ was derived as a function of the square of velocity and the direction of the piston.

$$F_{damp} = b_{Urea}\, v^2\, sign(v) \tag{4.6}$$

Where $\mathbf{b_{Urea}}$ is the damping coefficient of the Urea (with a value equals to 25) and **v** is the velocity of the piston.

The stopping force $\mathbf{F_{stop}}$ in *Figure 4.8* is a virtual representation for a strong opposing force against the piston at both ends of the stroke distance. This force must be huge enough to force the piston (only in simulation) to stop. The reason for using this force is to simulate the impact between the piston and the ending wall of the pump's chamber. Without using this force the piston will keep on moving in one direction without limits.

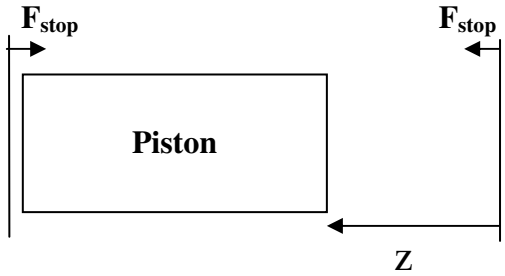

Figure 4.8 Stopping force from both sides on the piston

The stopping force is generated by a cascaded position and speed controller as shown in *Figure 4.9*. The mechanical system in *Figure 4.9* is modelled with (4.5). The closed loop speed and position controls were used to give an accurate value for the F_{stop} that is used to stop the piston at the ends of each stroke.

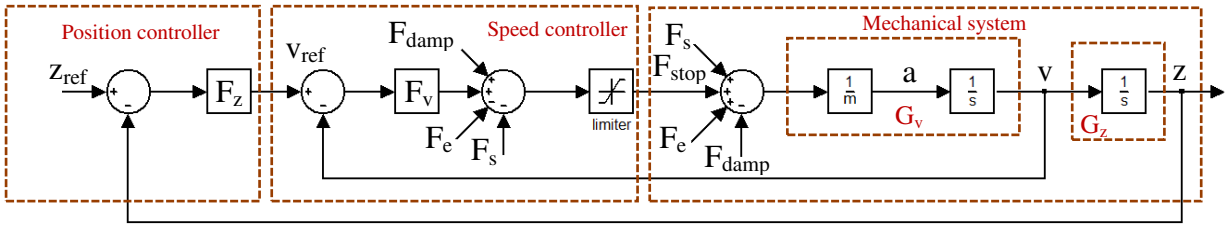

Figure 4.9 The speed and position control circuit of the stopping force F_{stop}

For the velocity controller in *Figure 4.9* feed forward terms for the spring, electric and damping forces are used to cancel the effect of these forces on the performance of the speed controller. With these terms added and by assuming that the limiter is not in operation the system that the speed controller, Fv, sees is

$$G_v = \frac{1}{m\, s} \tag{4.7}$$

By selecting that the closed loop system should be a first order system with bandwidth α_v the controller should be selected as

$$F_v = G_v^{-1} \frac{\alpha_v}{s} = \text{m s} \frac{\alpha_v}{s} = \alpha_v \, m \tag{4.8}$$

By assuming that the speed controller is much faster than the position controller it can be assumed that V_{ref} =V and with this assumption the system that the position controller sees becomes

$$G_z = \frac{1}{s} \tag{4.9}$$

In the same way as for the speed controller is assumed that the closed loop system should be a first order system with bandwidth α_z. With this selection the position controller should be selected as

$$F_z = \frac{\alpha_z}{s} \, s = \alpha_z \tag{4.10}$$

To have the speed controller faster than the position controller the bandwidth of the speed controller is selected as

$$\alpha_v = 10\alpha_z \tag{4.11}$$

4.2.2 Electric equations

The voltage and current wave forms given by the manufacturer are shown in *Figue 4.10*. The figure shows the voltage and current of the Urea pump coil ($\mathbf{V_c}$ and $\mathbf{I_c}$) when the input supply voltage for the system $\mathbf{V_d}$ is 32 volts, and the on time of the voltage is 8.5 ms. The inductance value of the coil is not constant during the whole period, it varies depending on the displacement of the piston inside the pump. When the electric force $\mathbf{F_e}$ exceeds the spring and the damping forces at the end of the linier region (approx. at 3 ms in *Figure 4.10*), the piston starts to move, the coil inductance **L** increases and the rate of change of coil current will decrease. The piston will reach the end of the stroke at 6 ms. This can be modelled as

$$V_c = \frac{dLi_c}{dt} + R \, i_c = L(Z) \frac{di_c}{dt} + i_c \frac{dL(Z)}{dt} + R \, i_c \tag{4.12}$$

Where $\mathbf{i_c}$ is the current in the coil, $\mathbf{V_c}$ is the coil voltage, and the coil inductance **L** is a function of the displacement **Z** taken by the piston.

After 6 ms and before the end of the $\mathbf{t_{on}}$ period (8.5 ms), the saturation limit for the magnetic flux linkage $\boldsymbol{\psi_{sat}}$ (flux linkage) will be reached leading to a fast increase of the current between (6-8.5 ms). In the off period, the current is decaying fast by the action of the coil voltage reversal as can be seen in *Figure 4.10*. This reversal is due to the discharge of the coil current via the power electronic supply connected to the coil.

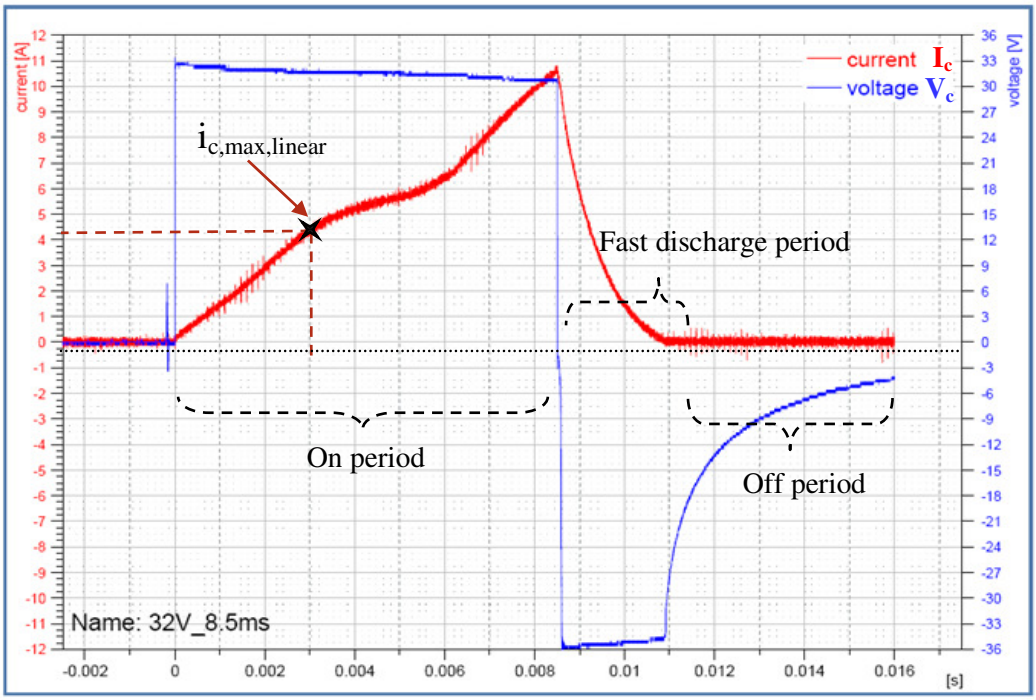

Figure 4.10 Manufacturer voltage-current wave form in the pump's coil

In *Figure 4.11* the power electronic supply for the pump is shown, with the two MOSFET switches drawn as ideal switches either closed or opened. *Figure 4.11a* shows two controlled MOSFET switches in their closing positions to allow the current to pass through the coil of the pump. The two diodes in the circuit will only work when the 2 MOSFET switches are off and then the coil voltage $\mathbf{V_c}$ is reversed to drain the stored current back to the batteries, as shown in *Figure 4.11b*.

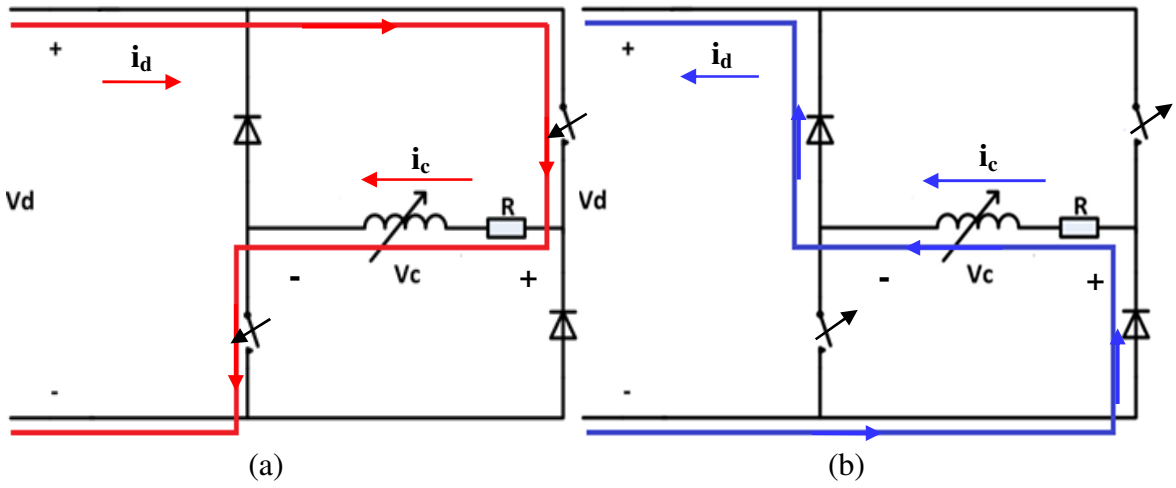

Figure 4.11 Power Electronic bridge power supply circuit of the Urea pump. Figure a) shows the on period and b) the discharge period for the current

From *Figure 4.10* the electric equations for the power electronic supply for the Urea pump were derived for the three different periods of operation. During the on period the two switches are on and the MOSFET can be modelled as a resistance. The coil voltage and the current from the battery can be expressed as

$$V_c = V_d - 2R_{dson}\, i_c \quad (4.13)$$

$$i_d = i_c \quad (4.14)$$

Where V_d is the battery voltage, V_c the voltage to the coil of the pump, i_c the coil current, i_d the battery current and R_{DSon} is the on resistance of the MOSFET. For the off period where there is a current through the coil, the diodes will conduct the current and the coil voltage will be negative. The coil voltage and the battery current can be expressed as

$$V_c = -V_d - 2V_{on} - 2R_{don}\, i_c \tag{4.15}$$

$$i_d = -i_c \tag{4.16}$$

Where V_{on} is the constant voltage drop of the diode when it is conducting and R_{don} is the resistance of the diode when it is conducting. This expression is only valid as long as there is a current through the coil. Since the voltage across the coil is negative, the current will decrease and when it reaches 0 A all switches will keep open until the MOSFET's are turned on again. In the off period the coil voltage and battery current can be expressed as

$$V_c = 0 \tag{4.17}$$

$$i_d = 0 \tag{4.18}$$

4.2.3 Magnetic calculations

The magnetic calculations are performed to calculate the variable inductance of the coil and to calculate the saturated magnetic flux linkage in the pump which helps for more accurate simulations for the consumed current in the coil. In these calculations the magnetic power losses were not taken into account because they were considered to be small. For a coil the relation between the applied voltage and the flux linkage can be expressed as

$$V_c = R_{ic}\frac{d\psi}{dt} \tag{4.19}$$

Where $\mathbf{V_c}$ is the applied voltage to the coil, $\mathbf{R}$ is the resistance of the coil, $\mathbf{i_c}$ the coil current and $\boldsymbol{\psi}$ is the flux linkage. For a linear magnetic circuit the relation between the flux linkage and the current can be calculated from

$$N\,I = R\,\varphi = R\,\frac{\psi}{N} \tag{4.20}$$

$$\mu = \frac{B}{H} \tag{4.21}$$

$$\Re = \frac{l}{A\mu_0\mu_r} \tag{4.22}$$

$$L = \frac{\psi}{I_o} \tag{4.23}$$

By formulating equation 4.20, 4.21, 4.22, and 4.23 general equations into the pump magnetic model

$$N\,I = \varphi\left(\frac{l_{core}}{A\,\mu_0\,\mu_r} + \frac{l_g + Z}{A\,\mu_0}\right) \tag{4.24}$$

Where

$$\varphi = B.A \tag{4.25}$$

Therefore,

$$N\,I = B\,A\left(\frac{l_{core}}{A\,\mu_0\,\mu_r} + \frac{l_g+Z}{A\,\mu_0}\right) \tag{4.26}$$

And the inductance of the coil in this case is equal to

$$L = \frac{\psi}{I} = \frac{N\,\varphi}{I} = \frac{N}{I}\,\frac{N\,I}{\frac{1}{A}\left(\frac{l_{core}}{\mu_0.\mu_r}+\frac{l_g+Z}{\mu_0}\right)} = \frac{N^2 A\,\mu_0}{\frac{l_{core}}{\mu_r}+(l_g+Z)} \tag{4.27}$$

And the coil voltage is

$$V_c = Ri_c + \frac{dL(z)i_c}{dt} \tag{4.28}$$

Where $\mathbf{l_{core}}$ is the core length, $\boldsymbol{\mu_r}$ is the relative permeability of iron, $\boldsymbol{\mu_0}$ is the absolute permeability, **φ** is the magnetic flux, **L** is the inductance of the coil, **N** is the number of coil turns, **A** is the cross sectional area of the piston, **B** is the magnetic flux density, **I** is the current passing in each wire of the coil, **ℜ** is the reluctance in the magnetic circuit, **Z** is the distance taken by the piston from the beginning of the stroke, and $\mathbf{l_g}$ is the air gap between the piston and the iron core which is not affected by **Z**, since it's fixed all the time.

Since the core (piston) of the pump is frequently moving, the value of the inductance of the coil differ between two ranges of inductance, the minimum and the maximum ($\mathbf{L_{min}}$, and $\mathbf{L_{max}}$) inductances of the coil, which represent the values of the internal inductance of the solenoid at the start of the piston's movement till the end of the stroke respectively.

By knowing the maximum coil current $\mathbf{i_{c,max,linear}}$ that can be reached before the piston starts to move as shown in *Figure 4.10*, the minimum inductance of the coil can be determined from

$$V_{c,meas} = i_{c,max,linear}.R + L_{min}.\frac{\Delta i_{linear}}{\Delta t_{linear}} \tag{4.29}$$

Therefore

$$L_{min} = \left(\frac{V_c - i_{max,linear}.R}{\frac{\Delta i_{linear}}{\Delta t_{linear}}}\right) \tag{4.30}$$

Where $\mathbf{\Delta i_{linear}}$ is the difference between any two current values in the linear region between (0-3 ms), and $\mathbf{\Delta t_{linear}}$ is the corresponding time values for these linear current values. The calculated value for the minimum inductance $\mathbf{L_{min}}$ was found equals to 18 mH.

It is more difficult to obtain the maximum inductance $\mathbf{L_{max}}$ in the same way as it was done for the minimum inductance $\mathbf{L_{min}}$. The reason for this is due to the nonlinearity of the current wave in the variable inductance area between (3 ms-6 ms), therefore $\mathbf{L_{max}}$ was estimated from the measured coil voltage and current shown in *Figure 4.12* as

$$\psi_{meas} = \int \left(V_{c,meas} - Ri_{c,meas}\right) dt \tag{4.31}$$

$$L_{meas} = \frac{\psi_{meas}}{i_{c,meas}} \tag{4.32}$$

Where $\mathbf{V_{c,meas}}$ is the measured voltage and $\mathbf{i_{c,meas}}$ is the measured current from *Figure 4.10*. ψ_{meas} is the estimated flux linkage and $\mathbf{L_{meas}}$ is the estimated coil inductance. In *Figure 4.12* the estimated coil inductance is shown. From *Figure 4.12* the increase of the inductance when the piston moves can be noticed between 3 and 6 ms. After 6ms the coil

saturates and the inductance value decreases. The value of the inductance before 3 ms should be around 18 mH but this is not what is seen in the figure. This might be due to offset in the measurements and uncertainties in the used resistance value. For the maximum inductance value 22.5 mH is used.

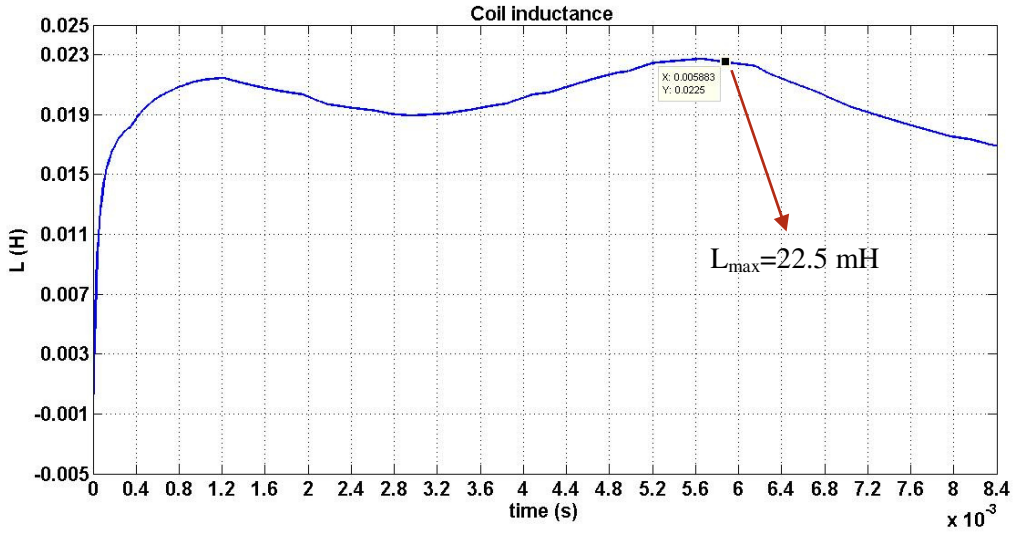

Figure 4.12 Shows the measured inductance values during 20 ms

From (4.27) the minimum and maximum inductance could be calculated as

$$L_{min} = \frac{N^2 A\,\mu_0}{\frac{l_{core}}{\mu_r} + l_g + Z_{max}} \tag{4.33}$$

and

$$L_{max} = \frac{N^2 A\,\mu_0}{\frac{l_{core}}{\mu_r} + l_g + Z_{min}} \tag{4.34}$$

By estimating the values of **A=** 19.6x10^{-4}, $\boldsymbol{\mu_r}$= 5500, $\mathbf{Z_{min}}$= 0, $\mathbf{Z_{max}}$= 2x10^{-3}, $\mathbf{l_{core}}$= 0.2 and substituting with (4.35) in (4.34)

$$l_g = \frac{L_{min}\left(\frac{l_{core}}{\mu_r} + Z_{max}\right) - L_{max}\left(\frac{l_{core}}{\mu_r} + Z_{min}\right)}{L_{max} - L_{min}} = 9.2x10^{-3} \tag{4.35}$$

and from (4.34)

$$N = \sqrt{\frac{L_{max}}{A.\mu_0}\left(\frac{l_c}{\mu_r} + l_g + Z_{min}\right)} = 290.43 \tag{4.36}$$

These equations can be used in the linear region of the coil, but they cannot be used in the saturated region. When the coil saturates it is the iron in the coil that saturates and the reluctance of the iron increases. The reluctance of the air gap is unaffected by the saturation, it is only affected by the position of the coil.

The relation between the current and the flux linkage can be expressed as

$$i_{c,meas} = (\mathfrak{R}_{iron} + \mathfrak{R}_{air})\frac{\psi}{N^2} \tag{4.37}$$

Where

$$\mathfrak{R}_{\text{air}} = \frac{l_g + Z}{A\mu_0} \tag{4.38}$$

and in the linear region

$$\Re_{iron} = \frac{l_{core}}{A\mu_0\mu_r}. \tag{4.39}$$

To model the saturation, the coil current is divided into two parts one from the air reluctance and one from the iron reluctance as

$$i_c = i_{iron} + i_{air} = \Re_{iron}\frac{\psi}{N^2} + \Re_{\boldsymbol{air}}\frac{\psi}{N^2} \tag{4.40}$$

The iron current contribution is estimated from the measured coil voltage and current wave forms in *Figure 4.10* and the estimated flux linkage as

$$i_{iron} = i_{c,meas} - \frac{\Re_{air}}{N^2}\psi_{meas} \tag{4.41}$$

In *Figure 4.13* the estimated flux linkage is plotted as function of the estimated iron current. From the figure, the knee when the iron saturates is clearly seen at

$$\psi = \psi_{sat} = 0.148\ wb \tag{4.42}$$

In the figure the modelled relation between the iron current contribution and the flux linkage is also shown. For the non-saturated region ($\psi \leq \psi_{sat}$) the relation is

$$i_{iron,unsat} = \frac{l_{core}}{N^2 A\,\mu_0\,\mu_r}\,\psi \tag{4.43}$$

Which is the vertical line in the figure and from the saturated region ($\psi > \psi_{sat}$) the relation is approximated as a linear relation as

$$i_{iron,sat} = I_{0,i} + K_\psi.\psi \tag{4.44}$$

Where $I_{0,i}$ = *-12.79*, and K_ψ = *86.4453*. The parameters of this linear relation are tuned to fit to the estimated curve in *Figure 4.13*. The saturation value for the flux linkage to be used in the model can be calculated as the value when the unsaturated and saturated model intersect, i.e $i_{iron,unsat} = i_{iron,sat}$ this gives

$$\frac{l_{core}}{N^2 A\,\mu_0\,\mu_r}\,\psi_{sat} = I_{0,i} + K_\psi\psi_{sat} \tag{4.45}$$

$$\psi_{sat} = \frac{I_{0,i}}{\left(\frac{l_{core}}{N^2\,A\,\mu_0\,\mu_r} - K_\psi\right)} = 0.148\ wb \tag{4.46}$$

To summarize, the electrical part of the Urea pump is modelled as

$$i_c = \begin{cases} \frac{l_{core}}{N^2\,A\,\mu_0\,\mu_r}\psi + \frac{l_g+z}{N^2\,A\,\mu_0}\psi & if\ \psi \leq \psi_{sat} \\ I_{0,i} + K_\psi\psi + \frac{l_g+Z}{N^2 A\,\mu_0}\psi & if\ (\psi > \psi_{sat}) \end{cases} \tag{4.47}$$

and the flux linkage is calculated with (4.31), but using the inputs to the model instead of the measured values.

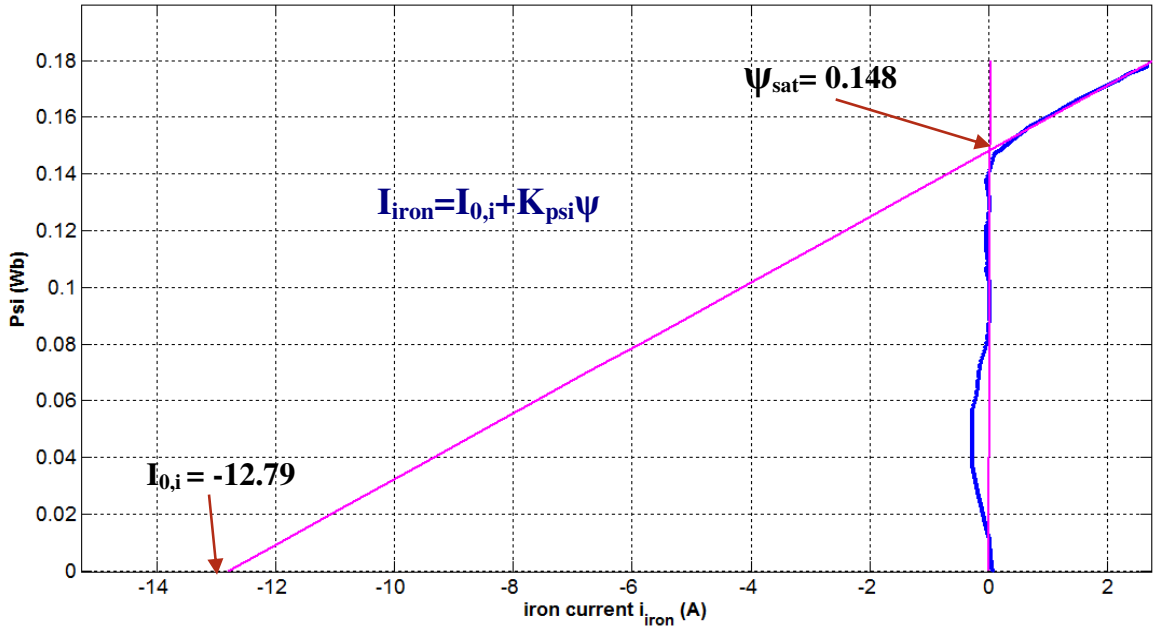

Figure 4.13 Relation between magnetic flux & iron current

The force from the current in the coil can be calculated from the energy stored in the magnetic field. The energy stored in the field can be defined as [9]

$$W_\psi = \int_0^\psi i_c \, d\psi = \int_0^\psi P_{siosat} + K_{psi}\,\psi + \frac{l_g+Z}{A\,N^2\,\mu_0}\,\psi \, d\psi \tag{4.48}$$

$$W_\psi = P_{siosat}\,\psi + \frac{K_{psi}\,\psi^2}{2} + \frac{(l_g+Z)\,\psi^2}{2\,A\,N^2\,\mu_0} \tag{4.49}$$

The force can be calculated as

$$F_e = -\frac{dW_\psi}{dZ} = -\frac{\psi^2}{2.N^2.A.\mu_0} \tag{4.50}$$

Where $\mathbf{W_\psi}$ is the energy stored in the field, and the electric force $\mathbf{F_e}$ is not depending on whether the iron is saturated or not, since the mmf of the iron is independent from the position of the piston **Z**.

4.2.4 System model

The Urea dosage system is implemented in Matlab by using the state space form as

$$\dot{X}(t) = A(t)x(t) + B(t)u(t) \tag{4.51}$$

$$Y(t) = C(t)x(t) + D(t)u(t) \tag{4.52}$$

Where **X** are the states, **U** are the inputs, and **Y** are the outputs. The model is implemented in simulation by using the S-function structure as shown in *Figure 4.14*. The inputs to the model are the voltage coming from the battery $\mathbf{V_d}$ and the pulse signal which represents the electronic switching periods that is responsible for setting the $\mathbf{t_{on}}$ and

the frequency of that voltage pulse. The coil voltage is calculated from the voltage and the control signal by using (4.13), (4.15), or (4.17) depending on the control signal and the coil current. The state-space equations are implemented as

$$\frac{d\psi}{dt} = V_c - R\, i_c \tag{4.53}$$

$$\frac{dv}{dt} = \frac{1}{m}\left(F_e + F_s + F_{damp} + F_{stop}\right) \tag{4.54}$$

$$\frac{dZ}{dt} = v \tag{4.55}$$

The selected outputs are the states and the signals needed for the figures. The selected outputs in this model were; the flux linkage **ψ,** coil current $\mathbf{i_c}$, pistion velocity **v,** distance taken by the piston **Z**, electric force $\mathbf{F_e}$, the spring force minus damping force ($\mathbf{F_s - F_{damp}}$), stopping force $\mathbf{F_{stop}}$.

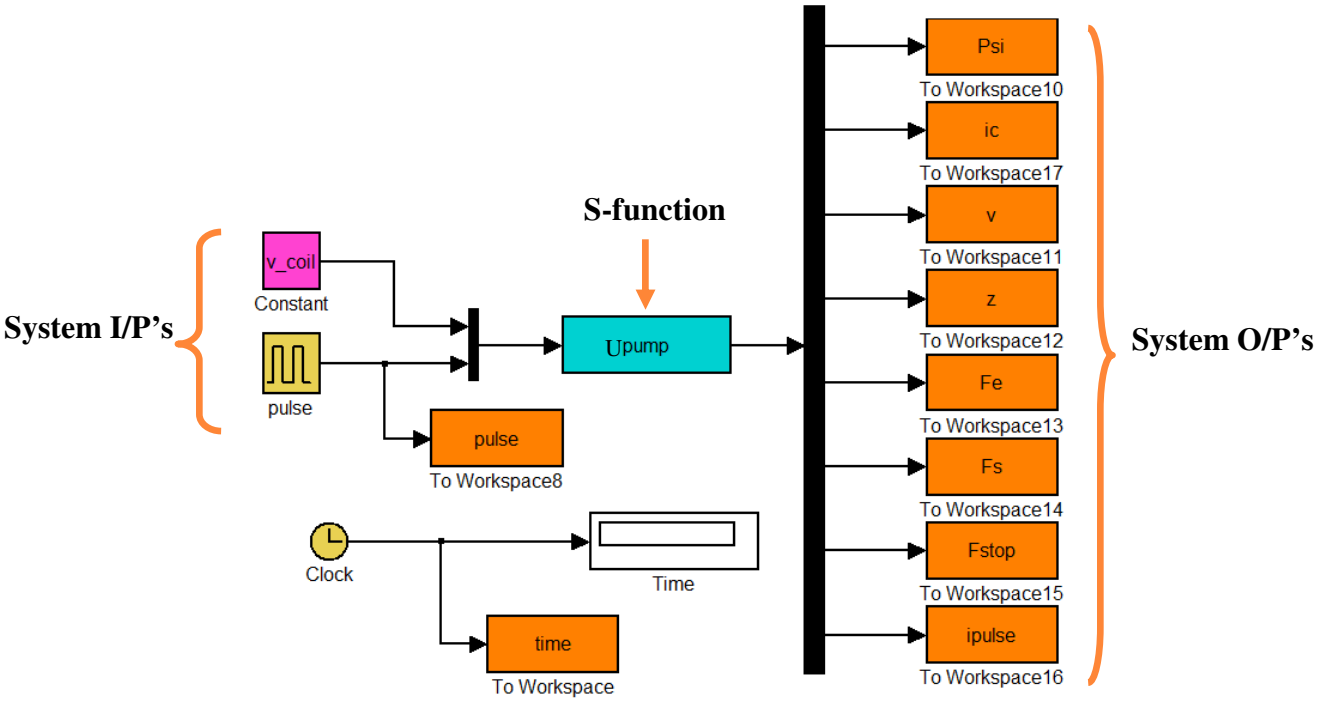

Figure 4.14 Urea pump simulation in Simulink®

4.3 General current consumption model

The general model is the goal for this project. It relates the current consumption of the system to the inputs and output without explicitly taking into account the internal workings of the system. It is designed in a way that makes it possible to be used for electric components with different internal parameters.

4.3.1 Description of the general model

The target of this final model is to calculate the average current consumption by describing the losses and the output power as a function of the inputs and outputs of the

component/system. From this, the average current consumption of the component/system is calculated as

$$i_{d,ave} = \frac{P_{in}}{V_{batt}} = \frac{P_{out} + P_{load} + P_{no\ load} + P_{mec}}{V_{batt}} \tag{4.56}$$

The average current is obtained by studying the power flow to the component. To calculate the power losses in the pump, the power flow technique was used as shown in the diagram of *Figure 4.15*. However the output mechanical power is not equal to the input electric power until all the losses are subtracted from the input [10].

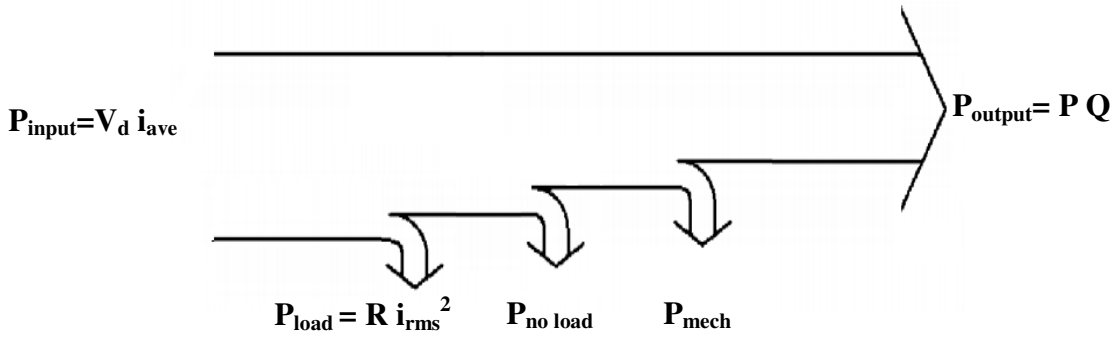

Figure 4.15 Power flow diagram

Before deriving the final expression for the power flow equation, a single simplification can be done by omitting the core losses $P_{no\ load}$ since the pump is either on or off. Therefore the output power will be assumed to be the Urea flow and the Urea pressure as shown

$$V_d . i_{d,ave} = R . i_{c,rms}^2 + P . Q + P_{mech} \tag{4.57}$$

Where **P** is the Urea system pressure equals to 3 bar ($3x10^5$ Pascal), and **Q** is the flow of the Urea in (m^3/s). From the detailed model a substitution in (4.57) with different values of input voltage $\mathbf{V_d}$, average input current $\mathbf{i_{d,ave}}$, flow of urea **Q** by changing the PWM frequency, and the rms coil current $\mathbf{i_{c,rms}}$ were done to calculate the mechanical losses $\mathbf{P_{mech}}$ as a percentage of $\mathbf{P_{load}}$.

For estimating the RMS value of the coil current**,** $\mathbf{i_{c,rms}}$, the coil is assumed to be a pure R-L circuit with a fixed **L**. The inductance is selected to be within $\mathbf{L_{min}}$ and $\mathbf{L_{max}}$ (of the pump's coil inductance in the detailed model). Selecting this value shall be discussed later in Chapter 5. Another approximation that was made in the general model was to assume an ideal power electronic supply, this means that the electronic switches are lossless ($\mathbf{v_d}$, $\mathbf{v_{on}}$, $\mathbf{R_{on}}$, $\mathbf{R_{Dson}}$ are equal to zero). From *Figure 4.11* it is assumed that the coil current starts from 0 at t=0 and then it increases due to that the battery voltage is applied across the R-L circuit. During this time the coil current can be described as

$$i_c(t) = \frac{V_{batt}}{R}\left(1 - e^{\frac{-R}{L}t}\right) \qquad 0 \le t \le T_{on} \tag{4.58}$$

where $\mathbf{T_{on}}$ is the total on time, **L** is the inductance of the coil, **R** is the resistance of the coil and $\mathbf{V_{batt}}$ is the battery voltage. The peak current that is reached during the on period is

$$i_c(T_{on}) = \frac{V}{R}.\left(1 - e^{-\left[\frac{R}{L}.T_{on}\right]}\right) \tag{4.59}$$

For the off time the negative battery voltage is applied across the R-L circuit until the coil current has reduced to zero. During the off time the coil current can be described as

$$i_c(t) = \left(I_{on,max} + \frac{V}{R}\right) e^{-\left[\frac{R}{L}(t-T_{on})\right]} - \frac{V}{R} \qquad T_{on} < t \leq T_{off} \tag{4.60}$$

$$i_c(t) = \frac{V}{R}\left(2\, e^{\frac{-R}{L}(t-T_{on})} - e^{\frac{-R}{L}t} - 1\right) \qquad T_{on} < t \leq T_{off} \tag{4.61}$$

Where T_{off} can be calculated as ($i_c(T_{off})=0$)

$$T_{off} = \frac{-L}{R}\, ln\left(\frac{1}{2e^{\frac{-R}{L}T_{on}}}\right) - 1 \tag{4.62}$$

The coil current for the period can be summarized as

$$i_c \begin{cases} \frac{V}{R}.\left(1 - e^{-\left[\frac{R}{L}T_{on}\right]}\right) & for\ 0 \leq t \leq T_{on} \\ \frac{V_{batt}}{R}\left(2\, e^{\frac{-R}{L}(t-T_{on})} - e^{\frac{-R}{L}t} - 1\right) & for\ T_{on} < t \leq T_{off} \\ 0 & for\ t < T_s \end{cases} \tag{4.63}$$

Where T_s is the period time. The RMS values of the coil current can be calculated as

$$i_{c,rms} = \sqrt{\frac{1}{T}\left(\int_0^{t_{on}} i_c(t)^2_{rise} + \int_{t_{on}}^{t_{off}} i_c(t)^2_{decay}\right)} = \sqrt{\frac{1}{T}\left(\int_0^{T_{on}} \left(\frac{V}{R}\left(1 - e^{-\left[\frac{R}{L}T_{on}\right]}\right)\right)^2 dt + \int_{T_{on}}^{T_{off}} \left(2\, e^{\frac{-R}{L}(t-T_{on})} - e^{\frac{-R}{L}t} - 1\right)^2 dt\right)} \tag{4.64}$$

By using the analytical equations for plotting the coil current wave and match it with the detailed model as shown in *Figure 4.16*. The new inductance value for the general model could be estimated by tuning the inductance value in the analytical equations untill the RMS values for both the analytical and the detailed currents overlapped together.

Note: that the inductance value should be within the maximum and minimum inductance values $\boldsymbol{L_{max}}$ *and* $\boldsymbol{L_{min}}$ *for the pump coil in the detailed model.*

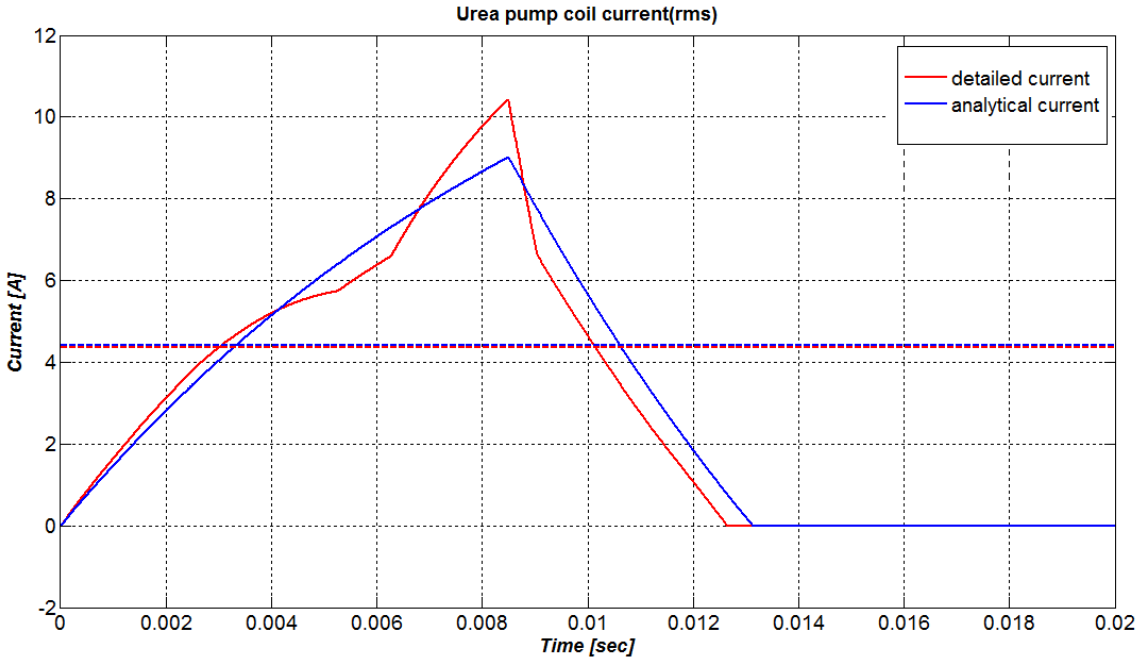

Figure 4.16 Shows the analytical and the detailed coil currents I_c, and $I_{c,rms}$

The mechanical losses can be difficult to estimate without performing measurements. In this model the mechanical losses are used to tune the current consumption of the general model to the average current consumption of the detailed model. The tuning is performed in Chapter 5 (*Table 6.8*) and it showed that a good fit could be obtained if the mechanical losses where modelled as

$$\boldsymbol{P_{mech} = K_{loss}(V_{batt})P_{load}} \tag{4.65}$$

Where $K_{loss}(V_{batt})$ is a factor depending on the battery voltage and $\mathbf{P_{load}}$ is the load losses of the pump, the losses in the coil resistance. The average supply current for the Urea is calculated with the general model as

$$\boldsymbol{i_{d,ave} = \frac{P_{cu}+P.Q+P_{cu}K_{loss}}{V_{batt}} = \frac{R(1+K(V_{batt}))i_{c,rms}{}^2+PQ}{V_{batt}}} \tag{4.66}$$

4.3.2 Program implementation

The program for the general model simply consists of two main parts. The first part is an M-file containing the analytical equations for calculating the rms current, and all the input parameters such as; coil resistance, coil inductance, input voltage, urea density, tank temperature, required dosage amount, ... etc. The second part is the *Simulink*® file that contains the working conditions for the pump, frequency limitations, and the maps needed such as: T_{on} map, maximum frequency map, and $\mathbf{P_{mech.loss}}$ table. See *Figure 4.17*. These maps and conditions are the same as was used in the basic (block) model of the system.

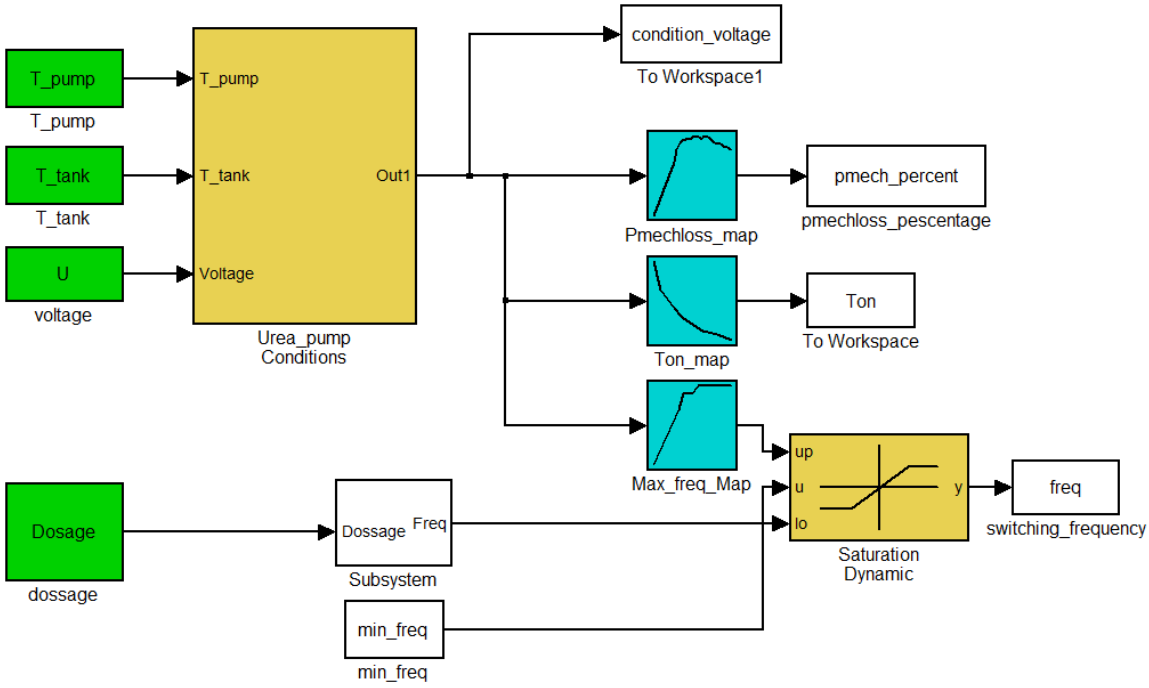

Figure 4.17 Simulink® circuit for the general model

Figure 4.18 describes how the program works in general. First the user inserts the input data to the GUI display which by turn will forward the data to the Simulink® file and run it, then after the Simulink® check all the temperature conditions and the lookup tables located in the model in *Figure 4.17*, and then the Simulink® handles its outputs to the M-file to calculate the current consumption by using the analytical equations in the M-file. Finally the output results of the M-file program are displayed on the graphical user interface (GUI) as shown in the following figure 4.18.

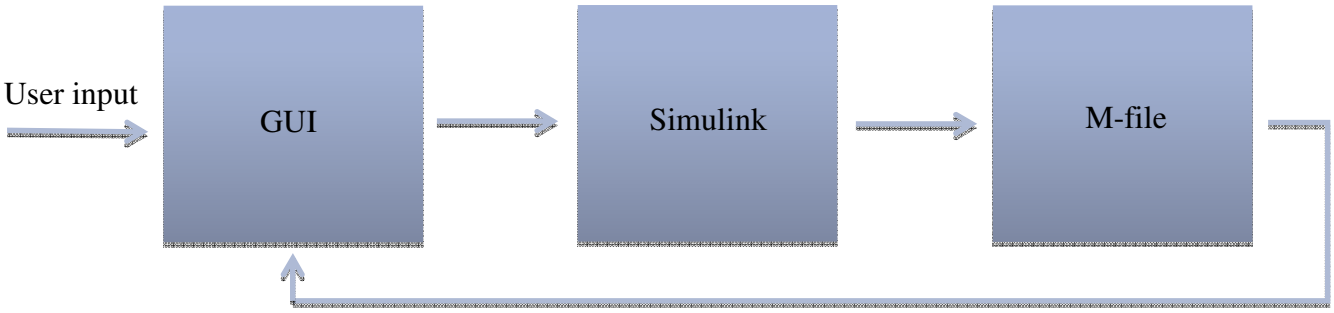

Figure 4.18 General model layouts

Chapter 5
Analysis and results

This chapter will discuss about the results obtained from the different models and provide a good understanding regarding the comparison between these results and real measured values. Finally the total current consumption of the urea dosing system will be presented in different modes of operation (Cold start, normal start, idle and steady-state operation) and temperature conditions. For the basic (block) model, current consumption of all components, including the urea pump, coolant valve, air valve and electric hose heater will be discussed. Moreover, in the detailed and general model the focus will be on the improved current results of the urea pump which will be analysed thoroughly through figures and tables.

5.1 Basic (block) model results

Urea Pump

As mentioned earlier in the basic model the urea pump current consumption was simply calculated according to the input voltage waveform with a fixed value of resistance and inductance. *Figure 5.1* illustrates the urea pump current waveform and its average value with an input voltage of 32 V, frequency of 50 Hz (equal to 2.41 gr/s urea dosage), resistance of 2 Ω and inductance of 21 mH. The inductance value was determined from the detailed model since it was not presented in the data sheet.

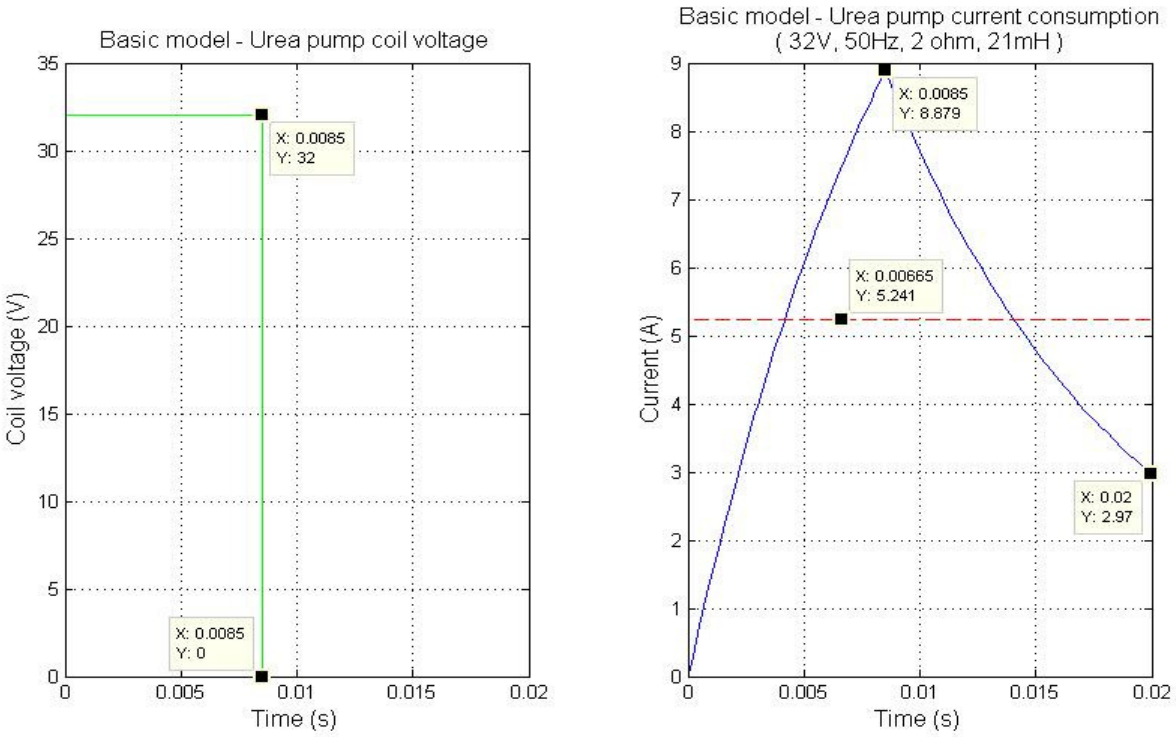

Figure 5.1 Basic model- Urea pump coil voltage and current consumption (i_c)

According to the manufacturer's data sheet the t_{on} time for 32 V is 8.5 ms therefore the current reaches to 8.87 A and after 8.5 ms the voltage becomes zero as can be noticed in *Figure 5.1*. Since in the basic model there is no forced decaying of current (no voltage

reversal) and considering the amount of inductance (21 mH), the current decreases quite slowly whereas in 20 ms the current reaches to 2.97 A and needs longer time to reach zero. As a result, making too many general assumptions to simplify the model led to lowering the accuracy of the model, which was verified by comparing the current waveform obtained by the basic model and the measurements carried out on the pump. Moreover, as mentioned earlier the basic model is a pure electrical model meaning that no mechanical issues such as the mechanical forces, friction and losses are taken into consideration which leads to getting far from the reality and hence from realistic results. Therefore, a detailed study of the system including the mechanical perspective was required to make it possible to simplify the system for developing the final general model by taking accurate assumptions.

Coolant valve

According to the data sheet specifications, the cooling valve has a fully open or fully closed (on/off) mechanism, which operates depending on the pump and tank temperatures as explained in section 4.1.2. The valve has a resistance of 57 Ω and a variable inductance of 188.8 -194.7 mH. *Figure 5.2* shows the coolant valve current waveforms corresponding to 28 V constant battery voltage. The blue curve represents the current waveform resulted with resistance of 57 Ω and fixed minimum inductance of 188.8mH (for simplicity only the minimum inductance has been considered). The red dashed line is the current waveform obtained solely from a fixed 57 Ω resistance without considering any inductance.

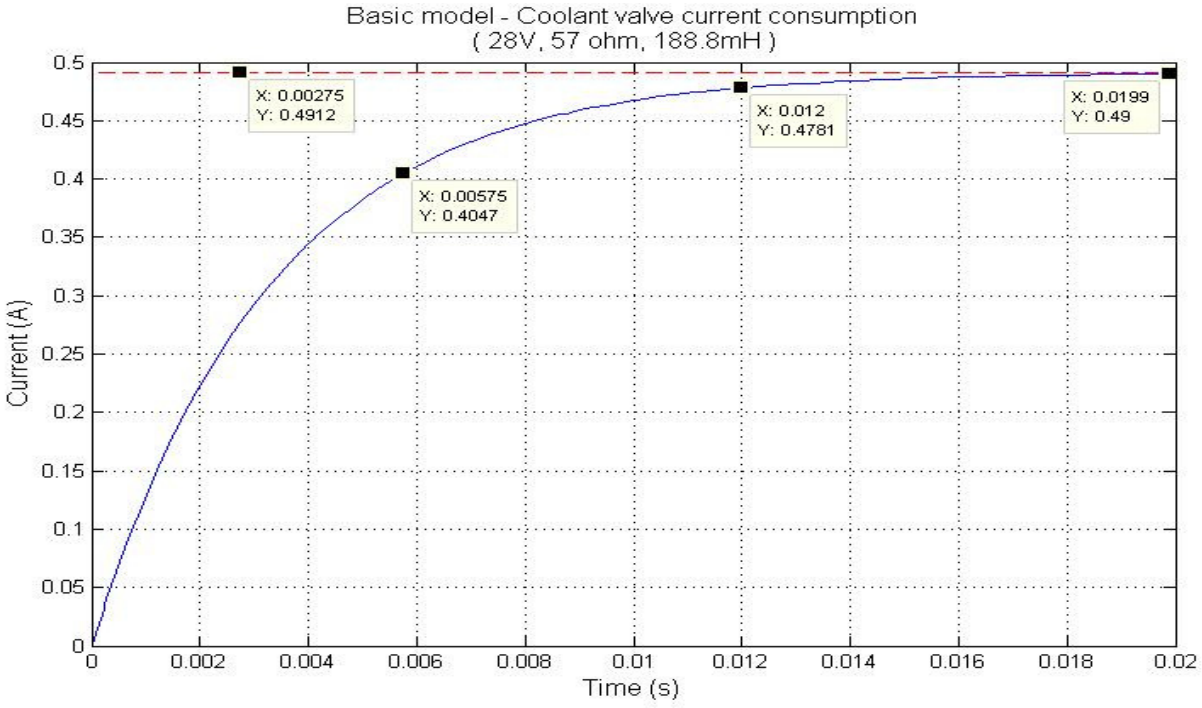

Figure 5.2 Basic model- Coolant valve current consumption

As can be noticed in *Figure 5.2* the coolant valve is a fast acting valve, the current (blue curve) reaches its steady state value in 20 ms. Moreover, due to the large resistance value the steady state current value is quite low, 0.49 A. Due to the fact that the on time of the coolant valve is much longer than the current rise time the dynamics of the valve have been neglected in the model of the valve. Therefore, the valve is modelled as a resistance of 57 Ω only and this results in a constant current consumption when the valve is on, red dashed line in *Figure 5.2*.

Air valve

The air valve is a PWM controlled solenoid valve with a supply of 28 V and constant switching frequency of 800 Hz. Moreover, the valve has a resistance of 81.1 Ω, variable inductance of 260 – 290 mH and is duty cycle controlled which works with 3 main duty cycles of 20, 40 and 60 %. 20 % duty cycle is used to provide 2 bar air pressure in the priming (Start up) of the urea dosing system, while 40 % is in normal operation of the system to provide 3 bar air pressure and finally 60 % duty cycle is used in the after run that provides 4 bar air pressure to flush out the remaining urea in the pipe lines before the system is turned off. *Figures 5.3, 5.4 and 5.5* present the current waveforms of the air valve in 20, 40 and 60 % duty cycle (for simplicity the minimum inductance value of 260 mH is considered). As seen in the figures the current wave form (blue curves) reach their steady state point in around 15 ms and keeps on fluctuating between two constant current values due to the 800 Hz supply frequency. Therefore, since the inductance doesn't play an effective role after the steady state has been reached and the current rapidly reaches its steady state values, the air valve model uses the resistivity only, neglecting the inductance which results in constant current values of 0.07, 0.14 and 0.21 A depending on the corresponding duty cycle (This is shown as the red dashed line in the Figures).

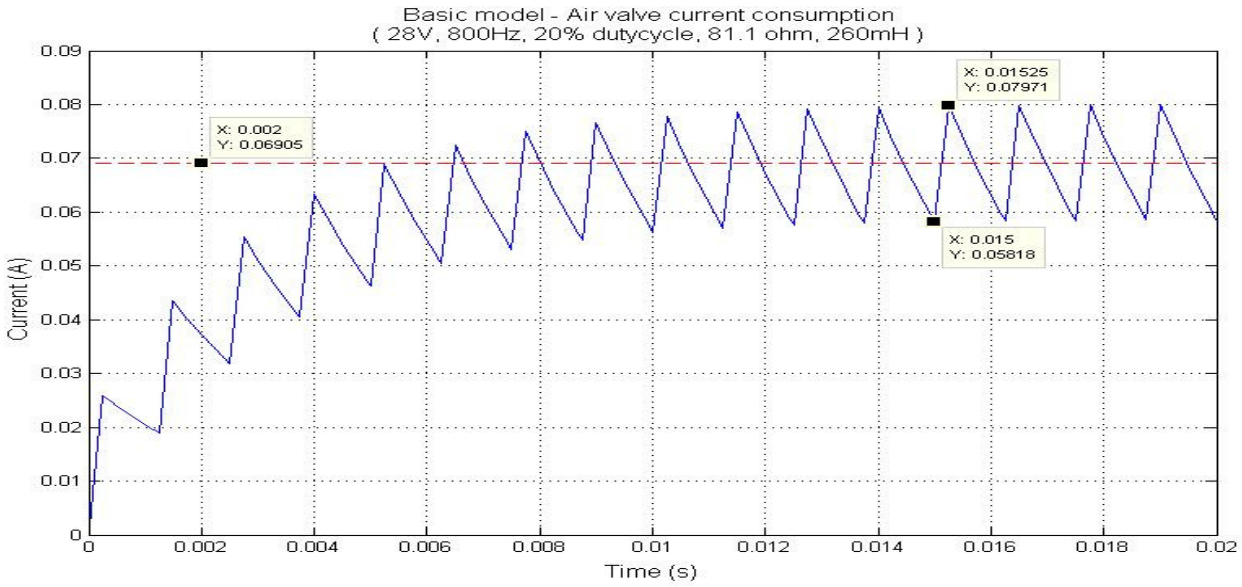

Figure 5.3 Basic model- Air valve current consumption (20 % duty cycle)

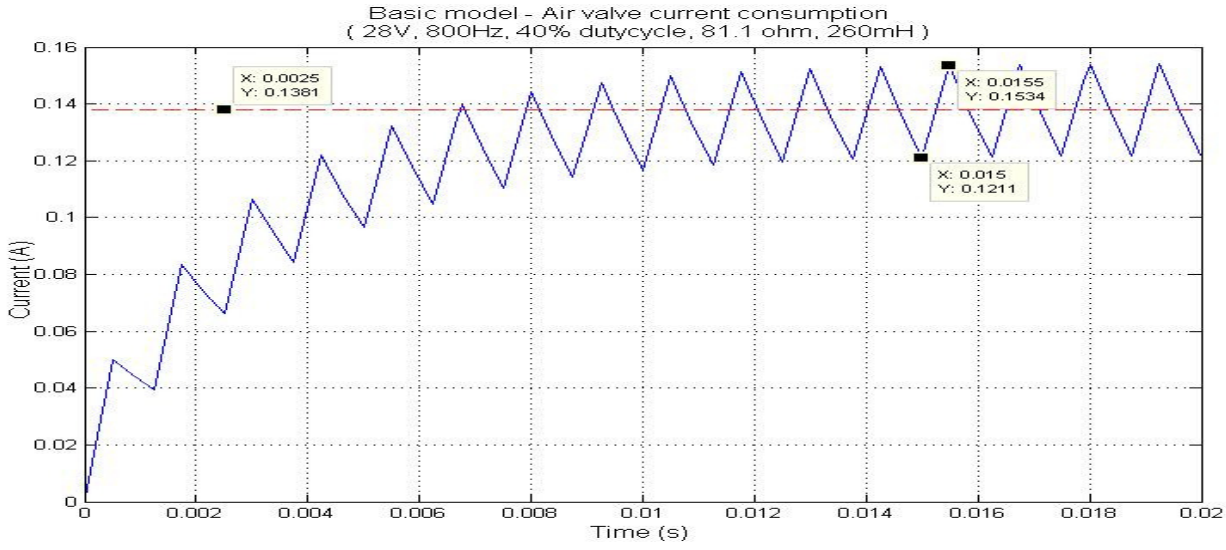

Figure 5.4 Basic model- Air valve current consumption (40 % duty cycle)

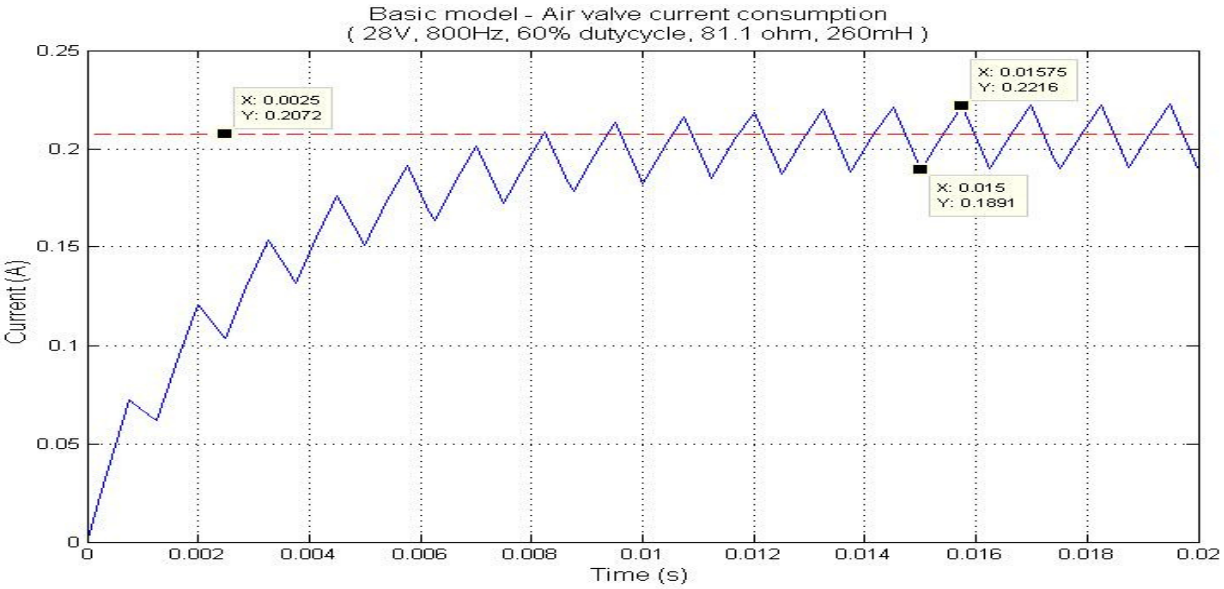

Figure 5.5 Basic model- Air valve current consumption (60 % duty cycle)

Hose heaters

As discussed in section 4.1.4 the electric hose heaters work in full heating mode when the temperature is below 0 °C which consumes 9 A according to the manufacturer's data sheet and in temperature above 4 °C the heaters turn off. At temperatures between zero and 4 °C the current consumption is linear to the temperature as is shown in *Figure 4.5*.

Since there was no information regarding the type of heater and its specification and the heater wasn't available for measurements, the heater was assumed to be a resistive electric heater and the current consumption was modeled by dividing the supply voltage (28 V) with its resistance (3.11 Ω considering 9 A maximum current). Moreover, the 0-4 °C linear current consumption was modeled as a duty cycle controlled supply voltage varying from 100 to 0 % between these temperatures according to *Table 5.1*.

Table 5.1 Electric hose heater current consumption chart

Temp. [°C]	*Current[A]*	*Duty cycle [%]*
0	9	100
0.5	7.875	87.5
1	6.75	75
1.5	5.625	62.5
2	4.5	50
2.5	3.375	37.5
3	2.25	25
3.5	1.125	12.5
4	0	0

5.2 Detailed model results

The detailed model of urea pump is the closest model to the reality since it is designed according to the measurements, including the electronic control circuit and the magnetic calculations on one hand and the mechanical displacement and forces on the other (as explained thoroughly in previous chapter). Moreover, in this model a reversed voltage has been implemented and the coil inductance is a variable inductance that changes according to the displacement of the plunger.

Figure 5.6 illustrates the urea pump current waveform and its average value with the corresponding coil voltage starting at 32 V, frequency of 50 Hz (equal to 2.41 gr/s urea dosage), resistance of 2 Ω and variable inductance of 18.5 - 22.5 mH.

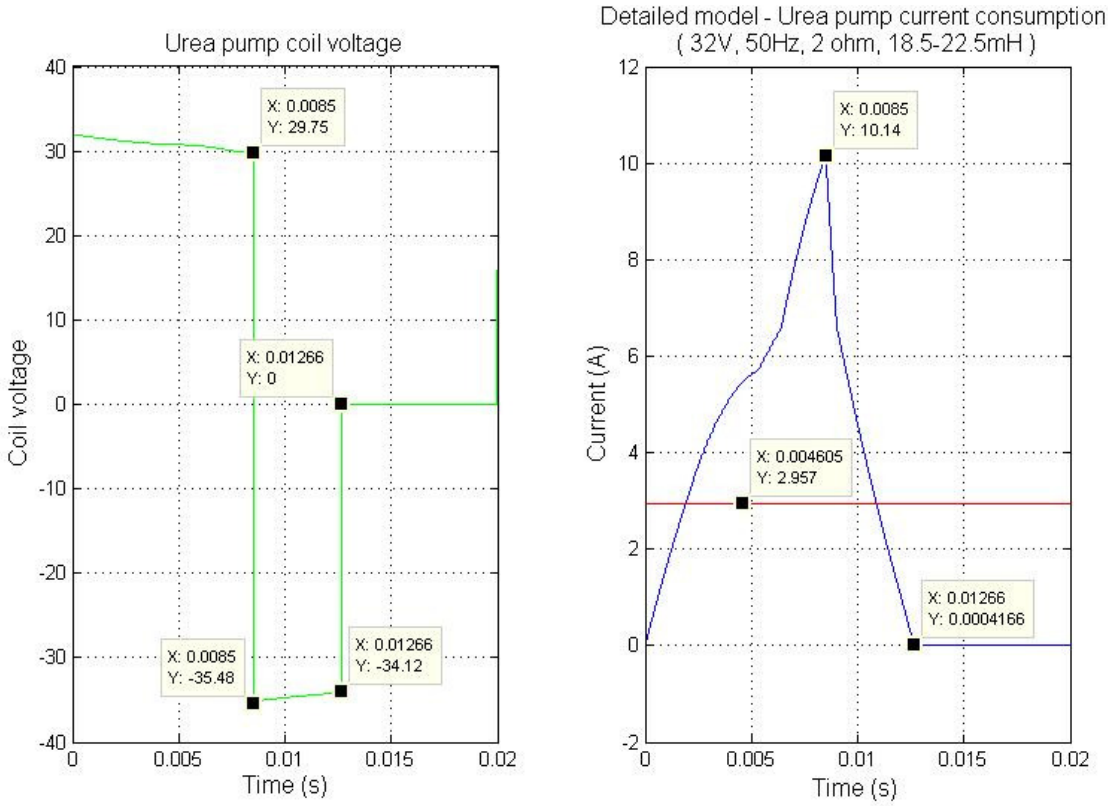

Figure 5.6 Detailed model-Urea pump coil voltage and current consumption (i_c)

As seen in *Figure 5.6*, the voltage profile starts at 32 V and during the on period of 8.5 ms it decreases to 29.75 V due to the switch resistances (R_{dson}) in the electronic control circuit. After 8.5 ms there is a negative voltage of -35.48 V due to the voltage drop over the diodes (V_{on}) and the diode resistance (R_{on}) and finally in 12.66 ms the voltage reaches zero. It should be mentioned that the voltage reversal appears on the coil due to the stored energy inside the coil whereas during discharging of this energy the negative voltage will appear since now the supply is receiving power instead of producing.

As for the current waveform, at the beginning, before the plunger starts to move the coil inductance is 18.5 mH. The current starts to increase to around 5 A and after the electrical force becomes greater than its opposing forces the plunger starts to move inside the coil causing the coil inductance to increase to 22.5 mH (this is the saddle point of the current waveform where the current increase slows down). Eventually, after the plunger reaches its end point the current keeps on increasing until it reaches 10.14 A at 8.5 ms. This current increase is due to the saturation of the iron core, where the flux is reaching its maximum value and the current keeps on rising. After 8.5 ms voltage reversal takes place and since there is a negative voltage (Due to current discharge in the coil), the current has a fast decrease until it reaches zero (when voltage becomes zero) at 12.66 ms.

The detailed model was tested and used several times for simulating the urea pump current consumption for different voltages (and the corresponding t_{on} time) and different frequencies. Furthermore, calculations of the electrical and mechanical forces were done based on the results obtained from the detailed model in order to calculate the mechanical losses and to utilize these losses and generalize it for the final general model.

Tables 5.2, 5.3 and *5.4* show the average (AVG) and RMS urea pump current consumption results obtained from the detailed model for different voltages and frequencies. It should be noted that $\mathbf{i_c}$ is the current in the coil and $\mathbf{i_d}$ is the current from the battery, see *Figure 4.11*.

Table 5.2 Detailed model – Average and RMS current values, (32 V, t_{on}: 8.5 ms)

Freq. [Hz]	i_d AVG [A]	i_c AVG [A]	i_d RMS [A]	i_c RMS [A]
50	1.3859	2.9574	4.2661	4.2661
45	1.2427	2.6616	4.0471	4.0471
40	1.1087	2.3659	3.8157	3.8157
35	0.9666	2.0701	3.5691	3.5691
30	0.8285	1.7744	3.3045	3.3045
25	0.6929	1.4787	3.0166	3.0166
20	0.5544	1.1829	2.6981	2.6981
15	0.4142	0.8872	2.3366	2.3366
10	0.2772	0.5915	1.9079	1.9079
5	0.1386	0.2957	1.3491	1.3491

Table 5.3 Detailed model – Average and RMS current values, (28 V, t_{on}: 9 ms)

Freq. [Hz]	i_d AVG [A]	i_c AVG [A]	i_d RMS [A]	i_c RMS [A]
50	1.2803	2.7611	3.8145	3.8145
45	1.1523	2.4849	3.6187	3.6187
40	1.0242	2.2089	3.4118	3.4118
35	0.8963	1.9327	3.1913	3.1913
30	0.7682	1.6566	2.9547	2.9547
25	0.6401	1.3805	2.6973	2.6973
20	0.5121	1.1044	2.4125	2.4125
15	0.3841	0.8283	2.0893	2.0893
10	0.2561	0.5522	1.7059	1.7059
5	0.128	0.2761	1.2063	1.2063

Table 5.4 Detailed model – Average and RMS current values, (24 V, t_{on}: 9.5 ms)

Freq. [Hz]	i_d AVG [A]	i_c AVG [A]	i_d RMS [A]	i_c RMS [A]
50	1.2147	2.5483	3.4116	3.4116
45	1.0904	2.2935	3.2365	3.2365
40	0.9718	2.0387	3.0514	3.0514
35	0.8481	1.7838	2.8543	2.8543
30	0.7269	1.529	2.6426	2.6426
25	0.6073	1.2742	2.4124	2.4124
20	0.4859	1.0193	2.1577	2.1577
15	0.3635	0.7645	1.8686	1.8686
10	0.2429	0.5097	1.5257	1.5257
5	0.1215	0.2548	1.0788	1.0788

As shown in *Tables 5.2, 5.3* and *5.4* the current consumption is increasing as the frequency is getting higher which is natural since for higher frequency the urea dosing amount is higher, hence the pump consumes more current. In addition there is not a big difference in the current profile in different voltages (slightly higher in higher voltage) since as the voltage is decreasing the t_{on} time is increasing.

Tables 5.5, 5.6 and *5.7* show the urea pump electrical and mechanical powers and their corresponding losses, described in section 4.3 for different voltages and frequencies.

The power can be calculated from the $\mathbf{i_{d,AVG}}$ and $\mathbf{i_{c,RMS}}$ values in *Tables 5.2, 5.3 and 5.4* according to (4.57) which can be also written as

$$\boldsymbol{P_{electric} = P_{copper} + P_{mech}} \tag{5.1}$$

Where $P_{electric}$ is the electrical power, P_{copper} is the copper losses and

$$\boldsymbol{P_{mech} = PQ + P_{mech.loss}} \tag{5.2}$$

In (5.2), **P** is the pump urea pressure in Pascal, **Q** is the urea flow in m^3/s and $P_{mech.loss}$ is the mechanical losses in Watts.

Table 5.5 Detailed model – Power and loss values, (32 V, t_{on}: 8.5 ms)

Freq. [Hz]	$P_{electric}$ *[w]*	P_{copper} *[w]*	$P_{mechanic}$ *[w]*	*PQ [w]*	$P_{mech.loss}$ *[w]*	$P_{mech.loss}/P_{copper}*100$
50	44.3488	36.3992	7.9495	0.645	7.3045	20.06%
45	39.7664	32.758	7.0083	0.580	6.4283	19.62%
40	35.4784	29.1191	6.3592	0.516	5.8432	20.06%
35	30.9312	25.4769	5.4542	0.4515	5.0027	19.63%
30	26.512	21.8394	4.6725	0.387	4.2855	19.62%
25	22.1728	18.1997	3.973	0.3225	3.6505	20.05%
20	17.7408	14.5594	3.1813	0.258	2.9233	20.07%
15	13.2544	10.9193	2.335	0.1935	2.1415	19.62%
10	8.8704	7.2801	1.5902	0.129	1.4612	20.07%
5	4.4352	3.6401	0.795	0.0645	0.7305	20.06%
						19.88% (Avg)

Table 5.6 Detailed model – Power and loss values, (28 V, t_{on}: 9 ms)

Freq. [Hz]	$P_{electric}$ *[w]*	P_{copper} *[w]*	$P_{mechanic}$ *[w]*	*PQ [w]*	$P_{mech.loss}$ *[w]*	$P_{mech.loss}/P_{copper}*100$
50	35.8484	29.1	6.7475	0.645	6.102	20.97%
45	32.2644	26.1899	6.0744	0.580	5.494	20.97%
40	28.6776	23.2807	5.3968	0.516	4.88	20.96%
35	25.0964	20.368	4.727	0.4515	4.276	20.99%
30	21.5096	17.46	4.049	0.387	3.662	20.97%
25	17.9228	14.5508	3.3719	0.3225	3.049	20.95%
20	14.3388	11.6403	2.6984	0.258	2.44	20.96%
15	10.7548	8.7303	2.0244	0.1935	1.83	20.96%
10	7.1708	5.8201	1.3506	0.129	1.221	20.98%
5	3.584	2.9103	0.6736	0.0645	0.609	20.93%
						20.96% (Avg)

Table 5.7 Detailed model – Power and loss values, (24 V, t_{on}: 9.5 ms)

Freq. [Hz]	$P_{electric}$ [w]	P_{copper} [w]	$P_{mechanic}$ [w]	PQ [w]	$P_{mech.loss}$ [w]	$P_{mech.loss}$ /P_{copper}*100
50	29.1528	23.278	5.8747	0.645	5.229	22.46%
45	26.1696	20.9498	5.2197	0.580	4.639	22.14%
40	23.3232	18.622	4.7011	0.516	4.185	22.47%
35	20.3544	16.294	4.0603	0.4515	3.608	22.14%
30	17.4456	13.9666	3.4789	0.387	3.091	22.13%
25	14.5752	11.6393	2.9358	0.3225	2.613	22.45%
20	11.6616	9.3113	2.3502	0.258	2.092	22.47%
15	8.724	6.9833	1.7406	0.1935	1.5471	22.15%
10	5.8296	4.6555	1.174	0.129	1.045	22.45%
5	2.916	2.3276	0.5883	0.0645	0.523	22.47%
						22.33% (Avg)

As can be seen in *Tables 5.5, 5.6* and *5.7* almost all the electric power is turned into copper and mechanical losses and a very small portion actually does the mechanical work (**PQ**). The main reason of implementing these power calculations is to calculate the mechanical loss ($P_{mech.loss}$) and to find a method to generalize it in order to utilize it in the final general model as a constant loss factor. As a result, the mechanical losses are calculated as a percentage of the copper losses (P_{copper}) as shown in the tables. This was done since for each voltage with its corresponding t_{on} time, the mechanical losses are quite the same percentage of the copper losses for different frequencies. *Table 5.8* illustrates the corresponding $P_{mech.loss}/P_{copper}$ values in percentage for different voltages and their related t_{on} times obtained from the detailed model at 25 Hz. In the general model the mechanical losses will be modelled as a constant percentage of the copper losses for each voltage according to *Table 5.8*.

Table 5.8 Detailed model – $P_{mech.loss}/P_{copper}$ percentages and their corresponding voltage values

Voltage [V]	T_{on} [ms]	$P_{mech.loss}$ / P_{copper}*100	Voltage [V]	T_{on} [ms]	$P_{mech.loss}$ / P_{copper}*100
10	17	15.089%	24	9.5	22.452%
11	15.5	18.779%	25	9.375	22.221%
12	14	20.817%	26	9.25	21.930%
13	13.5	21.384%	27	9.125	21.472%
14	13	21.495%	28	9	20.956%
15	12.5	21.733%	29	8.875	20.968%
16	12	22.033%	30	8.75	20.656%
17	11.5	22.139%	31	8.625	20.214%
18	11	22.321%	32	8.5	20.058%
19	10.75	22.403%	33	8.375	19.556%
20	10.5	22.426%	34	8.25	19.391%
21	10.25	22.407%	35	8.125	19.054%
22	10	22.186%	36	8	18.988%
23	9.75	22.347%			

5.3 General model results

The general model is the final model for simulating the current consumption of the urea pump. It is a simplified version of the detailed model and it includes the condition settings of the basic model. As discussed in section 4.3 for the general model the urea pump current wave form, $\mathbf{i_c}$, is simulated with a fixed value of the inductance and a constant supply voltage (not considering the voltage drops over the electronic control circuit's switches and diodes) according to (4.63). Moreover, the RMS value of the current ($\mathbf{i_{c,rms}}$ that is equal to $\mathbf{i_{d,rms}}$) is calculated through (4.64) which is used in (4.66) to calculate the final consumed average current value ($\mathbf{i_{d,avg}}$) of the urea pump.

Figure 5.7 shows the coil current, i_c, for the general model of the urea pump and its average value, $\mathbf{i_{c,avg}}$, with the corresponding coil voltage starting at 32 V, frequency of 50 Hz (equal to 2.41 gr/s urea dosage), resistance of 2 Ω and fixed inductance of 21 mH. The inductance value is selected to be between the minimum and maximum inductance value of the detailed model and the value was selected to give a reasonable RMS current value, $\mathbf{i_{c,rms}}$, in comparison to the RMS current value of the detailed model.

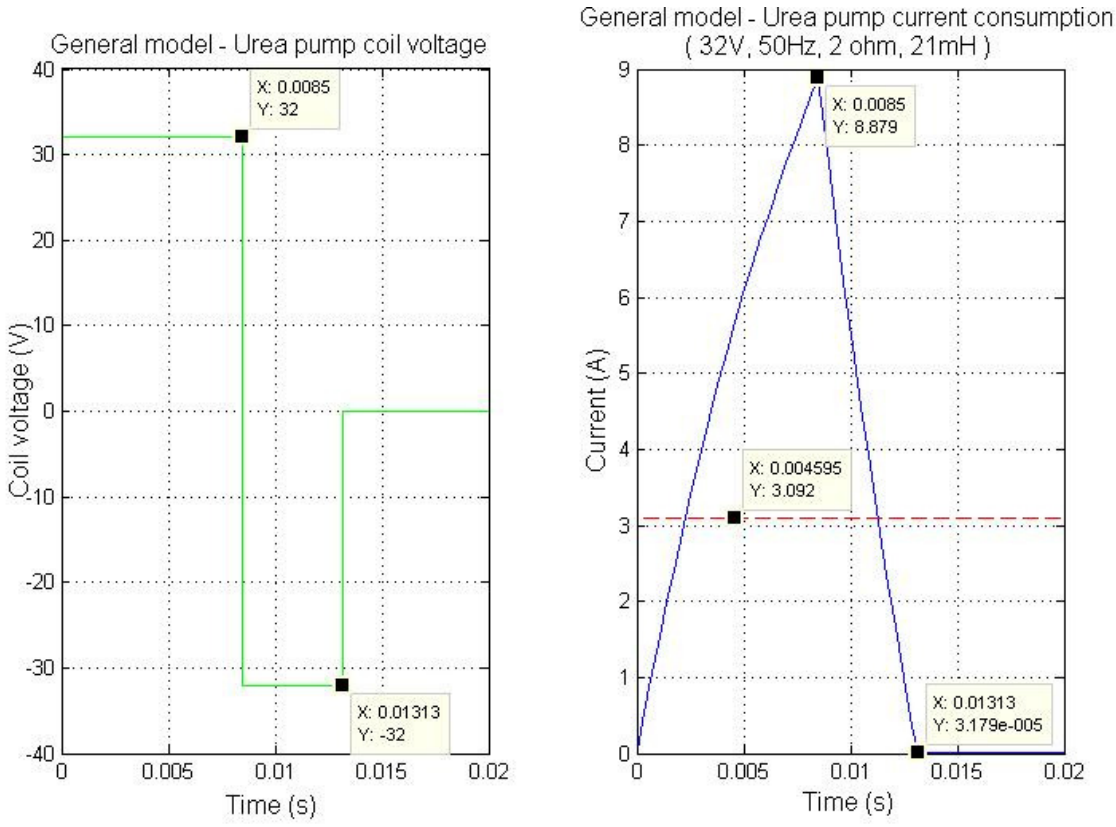

Figure 5.7 General model-Urea pump coil voltage and current consumption ($\mathbf{i_c}$)

As seen in *Figure 5.7*, the coil voltage waveform has simply two constant voltages of 32 and -32 volts and the t_{off} time is calculated according to (4.62). Since a fixed inductance is used the current rise waveform is similar to the basic model. However due to the implemented negative voltage the current decreases rapidly (simulating the fast discharge), whereas in 13.13 ms it reaches to zero, which makes it quite similar to the detailed model current waveform shown in *Figure 5.6*. Moreover, the average current value ($\mathbf{i_{c,avg}}$) has decreased from 5.24 A to 3.09 A in comparison with the basic model and its quite close to the average current value of the detailed model which was 2.95 A for this operation conditions.

In order to understand better the effect of the power flow equation (4.57) on the average current value of the urea pump from the battery perspective ($\mathbf{i_{d,avg}}$) and compare it to average current value obtained directly from the i_d waveform, *Figure 5.8* can be studied. There are two average current values resulted from the general model, the red line is the analytical average current value that has been obtained directly from the analytical equations used in the general model by simply converting the $\mathbf{i_c}$ current curve obtained from (4.63) to the corresponding $\mathbf{i_d}$ curve and calculating its average value which is only used in this figure and is not been considered anywhere since is not the final result. The green line is shown as the average current value from the general model ($\mathbf{i_{d,avg}}$) which is obtained by (4.66) after considering the copper and mechanical losses as discussed at the beginning of this section. The general model gives an average current value of 1.44 A whereas the average current value obtained directly from the i_d waveform is 1.18 A. The model comparison in section 5.5 further discusses that, results obtained from the general model (considering the power flow equation) gives more precise results, which is closer to the detailed model and the real measured average current values on the pump. Similar to the detailed model, the general model has been used and tested several times to compare the resulted values with the detailed model. *Tables 5.9, 5.10* and *5.11* show the average and RMS urea pump current consumption results ($\mathbf{i_c}$ and $\mathbf{i_d}$) obtained from the general model in different voltages and frequencies.

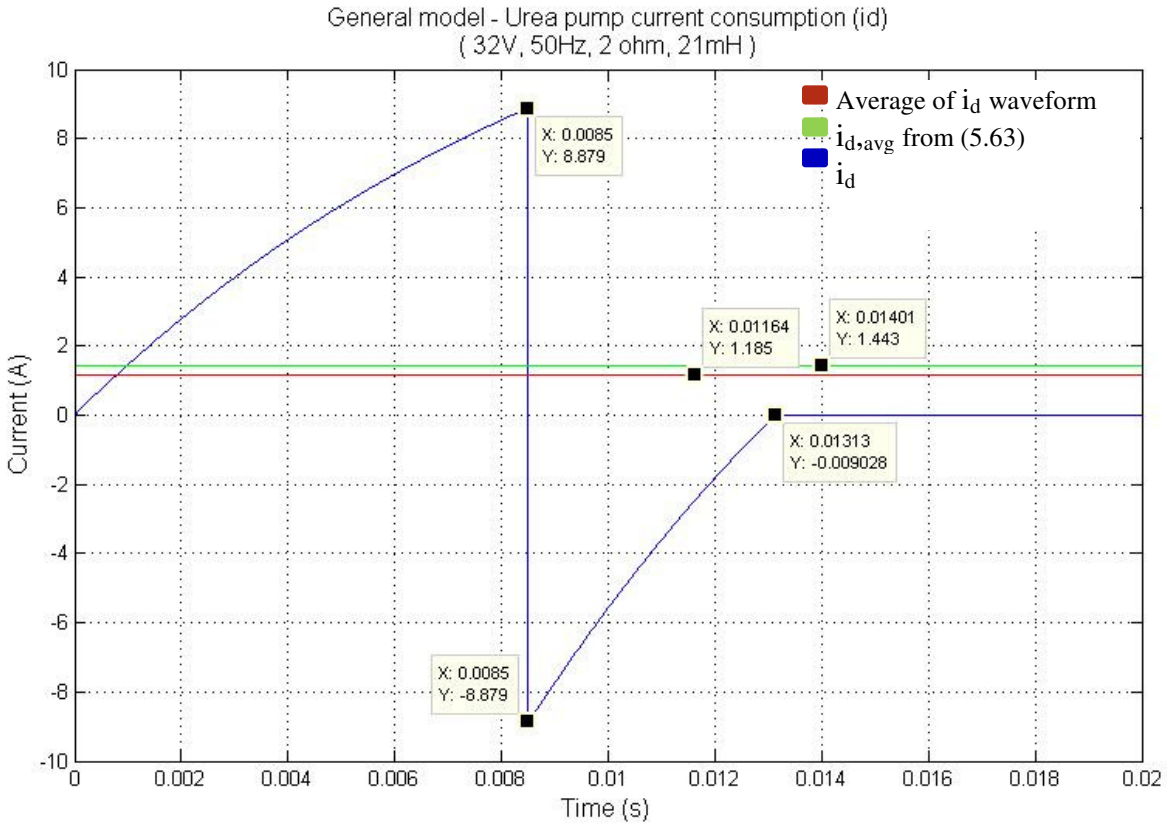

Figure 5.8 General model - Urea pump battery current consumption

Table 5.9 General model – Average and RMS current values, (32 V, t_{on}: 8.5 ms)

Freq. [Hz]	i_d AVG [A]	i_c AVG [A]	i_d RMS [A]	i_c RMS [A]
50	1.4431	3.092	4.3547	4.3547
45	1.2988	2.7828	4.1312	4.1312
40	1.1545	2.4736	3.8949	3.8949
35	1.0102	2..1644	3.6434	3.6434
30	0.8658	1.8552	3.3731	3.3731
25	0.7215	1.546	3.0792	3.0792
20	0.5772	1.2368	2.7541	2.7541
15	0.4329	0.9276	2.3851	2.3851
10	0.2886	0.6184	1.9475	1.9475
5	0.1443	0.3092	1.3771	1.3771

Table 5.10 General model – Average and RMS current values, (28 V, t_{on}: 9 ms)

Freq. [Hz]	i_d AVG [A]	i_c AVG [A]	i_d RMS [A]	i_c RMS [A]
50	1.4503	2.9583	4.0645	4.0645
45	1.3053	2.6625	3.8559	3.8559
40	1.1602	2.3666	3.6354	3.6354
35	1.0152	2.0708	3.4006	3.4006
30	0.8702	1.775	3.1483	3.1483
25	0.7251	1.4791	2.874	2.874
20	0.5801	1.1833	2.5706	2.5706
15	0.4351	0.8875	2.2262	2.2262
10	0.2901	0.5917	1.8177	1.8177
5	0.145	0.2958	1.2853	1.2853

Table 5.11 General model – Average and RMS current values, (24 V, t_{on}: 9.5 ms)

Freq. [Hz]	i_d AVG [A]	i_c AVG [A]	i_d RMS [A]	i_c RMS [A]
50	1.4243	2.7573	3.7006	3.7006
45	1.2818	2.4815	3.5107	3.5107
40	1.1394	2.2058	3.3099	3.3099
35	0.997	1.9301	3.0961	3.0961
30	0.8546	1.6544	2.8664	2.8664
25	0.7121	1.3786	2.6167	2.6167
20	0.5697	1.1029	2.3404	2.3404
15	0.4273	0.8272	2.0269	2.0269
10	0.2849	0.5515	1.6549	1.6549
5	0.1424	0.2757	1.1702	1.1702

Tables 5.9, 5.10 and 5.11 clearly illustrate the change of the average and RMS current values according to the frequency for each supply voltage level and its corresponding t_{on} time. The main values in these tables are the $\mathbf{i_{d,avg}}$ values representing the average current consumption of the urea pump from the battery, which is calculated according to the method described in section 4.3. To compare the $\mathbf{i_{d,avg}}$ values obtained from the general model and detailed model it can be seen that the general model has slightly (in worst case in 24 volts around 0.2 A) higher values which is reasonably good since it's a much simpler model compared to the detailed model.

5.4 Comparison between the models and measurements

Urea pump

Regarding the urea pump, few measurements were performed in the test lab during primary stages of the project. Unfortunately, due to change in the configuration of the pump, measured results could not be confirmed and documented. Therefore the manufacturer's measurements of coil voltage and current shown in *Figure 4.10* were taken as reference.

In the following all the results obtained by the basic, detailed and general models will be compared and analysed with the manufacturer's measurements on the pump. First there will be a comparison between the urea pump coil current waveforms ($\mathbf{i_c}$) and their average values ($\mathbf{i_{c,avg}}$) and then a comparison regarding the urea pump current consumption from the battery ($\mathbf{i_d}$) and their corresponding average values ($\mathbf{i_{d,avg}}$) which is the final target.

Figure 5.9 gives a clear comparison of the urea pump coil current consumption ($\mathbf{i_c}$) wave forms that were presented in the previous sections of this chapter. The red curve represents the resulted current from the data sheet, green is the general model, blue presents the detailed model and finally the magenta curve is the resulted current from the basic model. It should be noted that all these results are obtained with 32 V, 50 Hz, and resistance of 2 Ω according to the conditions of the pump during measurements. Moreover, as mentioned before the data sheet and detailed model have a variable inductance of 18.5 – 22.5 mH and the general and basic model use a fixed inductance of 21 mH. For easy comparison, few data points showing the maximum current values (at 8.5 ms), average values and the time that the current reaches zero have been presented in the figure.

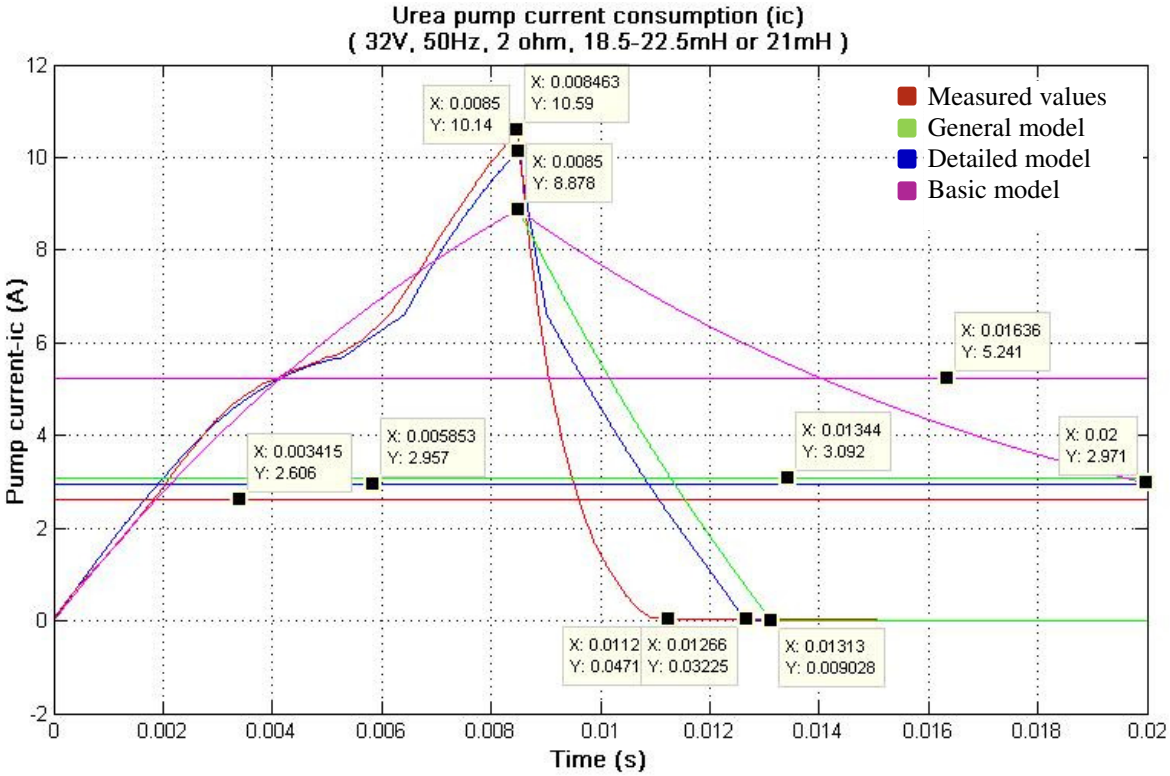

Figure 5.9 Urea pump current consumption – coil perspective ($\mathbf{i_c}$) and ($\mathbf{i_{c,avg}}$)

According to *Figure 5.9* it is clearly evident that the average coil current for the detailed model (2.9 A) is the closest model to the measured value of 2.6 A. This since it includes the variable inductance and the negative voltage (voltage reversal) similar to the real system. The main issue causing the difference of results between these two wave forms

(detailed and measurements) is the time that the current reaches zero. For the detailed model this time (12.6 ms) is a bit greater than the zero reaching time of the measurements (11.2 ms), which may be due to the elements inside the electronic control circuit that affects the negative voltage waveform, see *Figure 4.11*. Furthermore, the average coil current for the general model (3.09 A) is quite close to the measurements, since it uses a reasonable value of inductance (between the maximum and minimum inductance value) and has the voltage reversal characteristic. However, since the negative voltage doesn't reach -35 V (see *Figure 5.7*) as the voltage for the measurements and the detailed model does, the time of current reaching zero is a bit longer (13.1 ms).

Finally the basic model has the worst average current (5.2 A) compared to the measurements and this is due to that the model does not include the electronic control circuit. Therefore the model does not include the voltage reversal characteristic causing the fast current discharge. The large time for the current discharge brings up the average current value.

It should be mentioned that all the currents discussed in *Figure 5.9* are from the pump coil perspective ($\mathbf{i_c}$). However, in general when discussing the current consumption of a component within the powertrain, the current consumption from the battery side (battery perspective) or the supply is more relevant. Therefore, in *Figure 5.10* the urea pump battery current ($\mathbf{i_d}$) is shown for the different models, together with the average values of the currents. For the detailed and basic models the average is calculated as the average of the current waveform and for the general model it is calculated with (4.66).

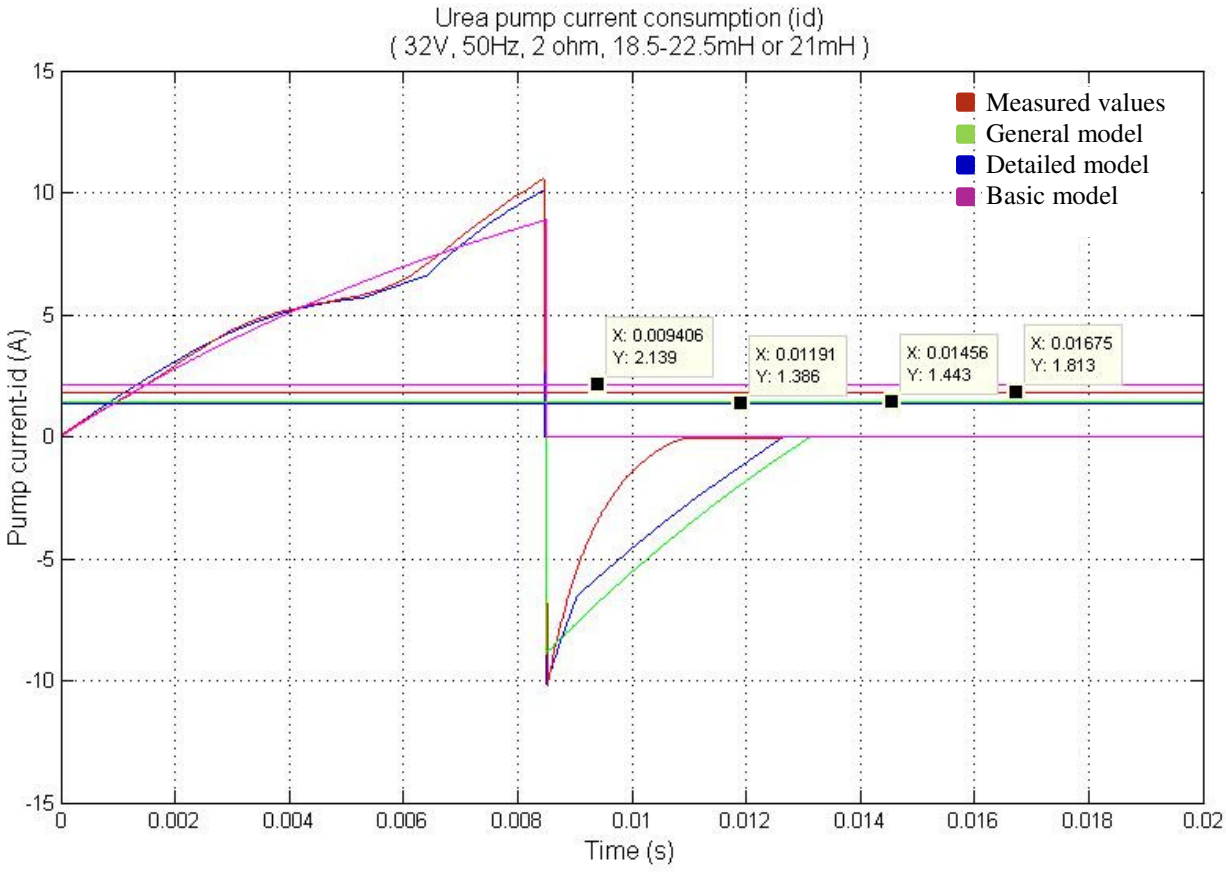

Figure 5.10 Urea pump current consumption – battery perspective ($\mathbf{i_d}$) and ($\mathbf{i_{d,avg}}$)

As can be seen by comparing *Figure 5.9* and *Figure 5.10*, the pump battery current consumption waveform ($\mathbf{i_d}$) is quite similar to the coil current waveform ($\mathbf{i_c}$). The main

difference between these two current waveforms is that after the t_{on} time when the voltage reversal takes place the battery current changes its direction flowing from the coil towards the battery. Therefore after the t_{on} time there is a negative current until the voltage reaches zero as well as the current. It should be noted that while the current is negative (after the t_{on} time), the energy stored in the magnetic field is transferred back to the supply, hence lowering the average current value ($\mathbf{i_{d,avg}}$) in comparison to ($\mathbf{i_{c,avg}}$). However, in the basic model since there is no electronic control circuit causing the voltage reversal, the current becomes zero after the t_{on} time (there is no current flowing back to the battery). In this case the coil is short circuited through a freewheeling diode and the magnetic energy is dissipated in the coil resistance.

In *Figure 5.10*, there are also 4 data points showing the average battery current consumption ($\mathbf{i_{d,avg}}$) obtained from the models and the measured values. According to the measured value on the pump, the average current is 1.81 A, whereas the detailed model gives an average current of 1.38 A, and the average current resulted by the basic model is 2.14 A. The average current value obtained from the general model is 1.44 A which is reasonably close to the detailed model (1.38 A). This shows that with the help of the analytical equations and loss calculations (that were based on the detailed model) the general model is tracking the detailed model with a good accuracy of 95.65 %. Furthermore, the above comparison proves that the Average current obtained from the general model (1.44 A) is also the reasonably close to the measured average current value (1.81 A).

It should be mentioned that the difference between the general model and the measurements (0.37 A) could be due to the unknown parameters of the details in the electronic control circuit of the pump, which causes a rapid current decrease for the measured current when the voltage reversal takes place. These unknown parameters in the control circuit could cause the gap between the results obtained from the detailed model and real measurements and since the general model is designed according to the detailed model it will keep about the same amount of difference in comparison to the real measured values. *Table 5.12* illustrates accuracy of the average current ($\mathbf{i_{d,avg}}$) resulting from the general model in comparison to the detailed model and measured average current value of the urea pump for 32 V and 50 Hz . As can be seen in *Table 5.12* the general model has an accuracy of 104.30 % in comparison to the detailed model and an accuracy of 79.60 % in comparison to the measurements.

Table 5.12 Accuracy of obtained average current values for the general model compared with the detailed model and with the measured average values. (32 V, 50 Hz)

		Detailed model	*Measured value*
General model	1.44 A	1.38 A	1.81 A
		104.30%	79.60%

Air valve

The average current of the air valve was measured in the test lab under 28 V supply voltage and with the valve specifications explained in section 6.1. The measurements were carried out with the three main working duty cycles (20, 40 and 60 %) of the air valve, and the average current values were measured to 0.084 A, 0.155 A and 0.218 A respectively. It should be mentioned that these values are actually quite similar to the current values obtained from the basic model (0.069 A, 0.138 A and 0.207 A) which simply uses only the

resistance value of the valve neglecting its inductance, which produces accuracy values of 82.1 %, 89 % and 94.4 % respectively.

5.5 Total urea dosing system current consumption

In this section the total average current consumption of the urea dosing system, comprising of one urea pump, a coolant valve, an air valve and two electric hose heaters will be calculated according to the results obtained from the general model (for the urea pump) and the basic model (for air valve, coolant valve and hose heaters) in different modes of operation and temperature condition scenarios.

All the calculations and results presented in this section are based on a fixed 28 V supply voltage representing the vehicle battery voltage (neglecting the voltage fluctuations in the battery). Moreover, the electrical parameters of the components are as following:

- Urea pump: R=2 Ω, L=21 mH
- Coolant valve: R=57 Ω, L=188.8 mH
- Air valve: R=81.1 Ω, L=260 mH
- Hose heaters: R=3.11 Ω

As mentioned in Chapter 4, the hose heaters work depending on the ambient temperature, and the coolant valve and urea pump work depending on the urea tank and pump temperatures. *Table 5.13* illustrates the temperature dependent working conditions of the urea dosing system's components.

Table 5.13 Temperature dependent working conditions of the urea dosing system

		Working condition			
	Temperature [°C]	Hose heaters	Urea pump	Coolant valve	Air valve
Ambient	T ≤ 0	Full On	-	-	Not temperature dependent
	0 < T < 4	linear	-	-	
	T ≥ 4	Off	-	-	
Pump & Tank	T ≤ −6	-	Off	On	
	−6 < T < 10	-	On	On	
	T ≥ 10	-	On	Off	

The average current consumption of each component in addition to the total current consumption of the urea dosing system, according to different modes of operation and various temperature conditions are presented in *Table 5.14*. The operation modes includes the cold start, Normal start, idle and steady-state running. Moreover, three different temperature scenarios have been considered for each mode in order to illustrate different working conditions for components and to calculate and analyse the effect of these conditions on the total average current consumption of the urea dosing system. As shown in *Table 5.14*, to make it simple the pump and tank temperatures are assumed the same and various combinations of ambient and pump/tank temperatures have been taken into account in order to consider all the possible working scenarios of the components.

Table 5.14 Average current consumption of the urea dosing system in different modes and temperature conditions

		Temperature [°C]		Average current consumption [A]				
		Ambient	Pump & Tank	Hose heaters	Urea pump	Coolant valve	Air valve	Total
Vehicle modes of operation	Cold start	-20	-18	9 x 2	Off	0.49	0.07	**18.56**
		-5	-5	9 x 2	0.29	0.49	0.07	**18.85**
	Normal start	23	25	Off	0.14	Off	0.07	**0.21**
		3	5	2.25 x 2	0.14	0.49	0.07	**5.2**
		8	9	Off	0.14	0.49	0.07	**0.7**
	Idle	-4	-2	9 x 2	0.72	0.49	0.14	**19.35**
		2	3	4.5 x 2	0.72	0.49	0.14	**10.35**
		9	11	Off	0.72	Off	0.14	**0.86**
	Steady State	-4	-2	9 x 2	1.45	0.49	0.14	**20.08**
		1	3	6.75 x 2	1.45	0.49	0.14	**15.58**
		12	14	Off	1.45	Off	0.14	**1.59**

It should be noted that in the starting modes the air valve is in its priming condition (20 % duty cycle) and in the Idle and steady-state modes in normal operation (40 % duty cycle). Furthermore, the frequency of the urea pump in cold start is 10 Hz and in normal starting mode is 5 Hz. In the idle mode the frequency of the urea pump has been considered to be 25 Hz, whereas in steady mode (to obtain the maximum average current consumption of the pump) the maximum frequency of 50 Hz has been taken into account.

As seen in *Table 5.14*, the maximum average current consumption of the urea dosing system (20.08 A) occur for cold condition in the steady-state mode. This is due to the fact that in this condition the heaters are fully on, the coolant valve is on too and the urea pump is dosing it's maximum value of urea (2.4 gr/s) at 50 Hz frequency. This means steady state operation at high speed, since the amount of urea dosage increases by vehicle speed due to increasing exhaust pollutants with speed. However the system consumes the minimum (0.21 A) in the normal starting mode in warm conditions, while the heaters and coolant valve are off and the pump is dosing low amount of urea (0.48 gr/s) at 10 Hz frequency and the air valve is in its priming condition. *Table 5.15* summarizes the average current consumption for each component in the urea dosing system.

Table 5.15 Average current consumption for each component in the urea dosing system

Average current consumption [A]			
Hose heaters	Urea pump	Coolant valve	Air valve
0 – 18	0 - 1.45	0 - 0.49	0 - 0.21

As shown in *Table 5.15*, the two hose heaters are the highest current consumers in the urea dosing system. However, since they are only used when the ambient temperature is bellow 4 °C, the most of the time the truck is operating without them. This totals the average current consumption of the urea dosing system up to 2.15 A with turned off hose heaters.

Chapter 6
Graphical User Interface (GUI)

6.0 Introduction

This chapter introduces the basic elements of the MATLAB® Graphical User Interface, and shows an overview on the designed GUI for this project. The chapter does not contain a complete description of components or GUI features, but it does provide the basics required to create functional GUIs for simulating the current consumption for components and systems based on the model described in Chapter 4.

A graphical user interface (GUI) is a graphical interface to a program. The main reason GUI is used is because it makes things simple for the end-users of the program. Without using the GUI, people would have to work from the command line interface, which can be extremely difficult and frustrating. A good GUI can make programs easier to be used, provided with a consistent appearance and with intuitive controls like pushbuttons, list boxes, sliders, menus, etc. The GUI should behave in an understandable and predictable manner, so that users know what to expect when performing an action. For example, when clicking a pushbutton, the GUI should initiate the action described on the label of the button [11]. The typical stages that are used for creating a GUI can be stated as:

1. Designing the GUI

2. Laying out the GUI using the Layout Editor

3. Programming the GUI by writing callbacks in the M-file Editor

4. Saving and Running the GUI

6.1 Graphical user interface development environment (GUIDE)

GUIDE is MATLAB®'s graphical user interface design environment which provides a set of tools for creating graphical user interfaces (GUIs). These tools could be used to perform the following tasks:

1. **Layout the GUI**
   Using the GUIDE Layout Editor, see *Figure 6.1*, helps for layout a GUI easily by clicking and dragging GUI components such as panels, buttons, text fields, sliders, menus, etc into the layout area. GUIDE stores the GUI layout in a FIG-file.

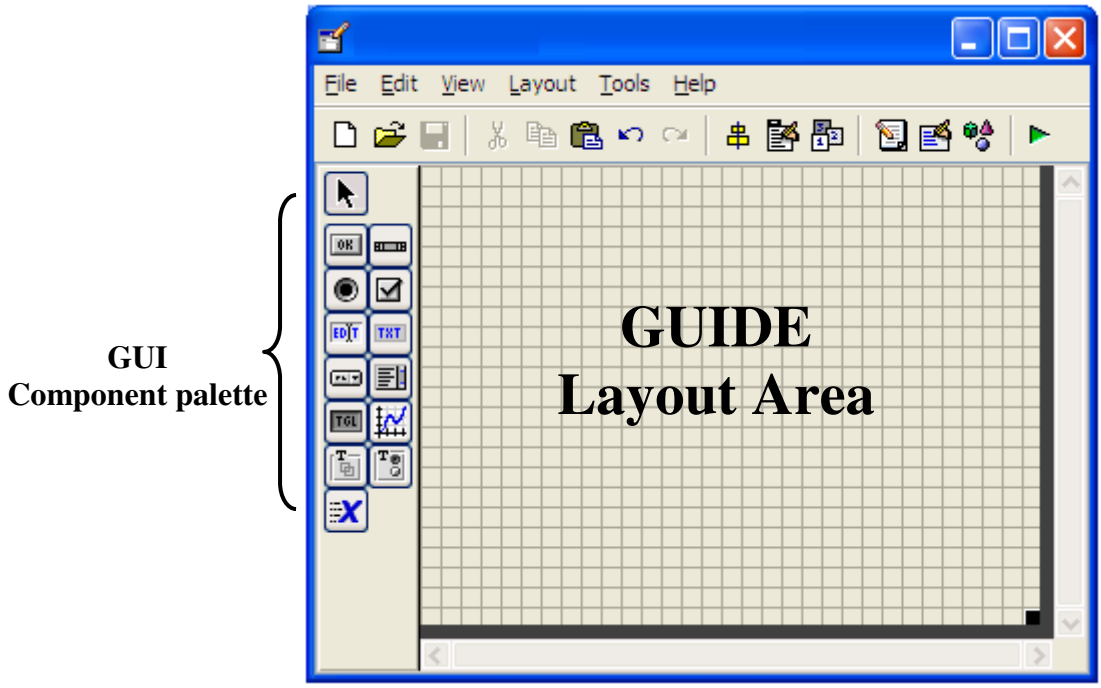

Figure 6.1 GUIDE layout editor

2. **Programming the GUI.**
   GUIDE automatically generates a MATLAB® M-file that controls how the GUI operates. The code in that file initializes the GUI and includes function templates for the most commonly used callbacks for each component and the commands that execute when a user clicks a GUI component. Using the MATLAB® editor helps the user for adding code to the callbacks to perform the needed functions [12].

   A callback is a function that contains a sequence of commands that is associated with a specific GUI component (such as panels, buttons, text fields, sliders, menus, etc) or with the GUI figures itself. The callbacks control GUI or component behavior by performing some action in response to an event for its component. The event can be a mouse click on a push button, menu selection, key press, etc. This kind of programming is often called event-driven programming, where a callback is usually made of the following stages:

1. Getting the handle of the object initiating the action (the object provides event / information / values)

2. Getting the handles of the objects being affected (the object that whose properties are to be changed) [13]

3. Getting necessary information / values

4. Doing some calculations and processing

5. Setting relevant object properties to effect action

Each kind of callback has a triggering mechanism or event that causes it to be called. The following table shows two callback properties that are used in this project's GUI, their triggering events, and the components to which they apply.

Table 6.1 Callback properties used in this project

Callback property	Triggering event	components
Callback	Control action. Executes for example, when a user clicks push button or selects a menu item.	Context menu, menu user interface controls
CreateFcn	Initializes the component when it is created, it executes after the component or figure is created, but before it is displayed.	Axes, button group, context menu, figure, menu, panel, push tool, toggle tool, toolbar, user interface control

6.2 Designed GUI for the general model

Designing a GUI was a part of this project, since it would be difficult to work with the MATLAB® M-files directly every time the used want to change any of the parameters in the program. The first step in designing the GUI is to identify the inputs and the outputs that need to be displayed on the display screen of the user interface as following:

Selected inputs for the GUI: Supply input voltage, Urea dosage amount, air valve duty cycle, Urea pump and tank temperatures, ambient temperature, Urea pump inductance, resistance, maximum frequency, and maximum dosage amount, air valve and coolant valve resistances, and heater current.

Selected outputs for the GUI: Average battery current consumption with the four different loads (Urea pump, air valve, coolant valve, and hose heaters) beside the total battery average current consumption for the summation of all loads.

6.3 GUI layout for the general model

GUI layout is divided into 4 different panels and one graphical plot axes as shown in *Figure 6.2.*

Urea dosage system (UDS) input parameters panel:
This panel contains the edit buttons for the input supply voltage, the Urea dosage required for the EATS system, and the air valve duty cycle as a percentage from (0-1).

Temperature panel:
Contains all the temperature values for the pump, tank, or the ambient used in the simulations to determine which component that is operated and which is not, according to their designed threshold value.

Components parameters panel:
It contains the fixed internal parameters for each component in the system as shown in *Figure 6.2.* These parameters could be changed only when a component (pump, air valve, coolant valve, or hose heater) is going to be replaced by a new one. When the user click the" change parameters" button located at the bottom of the panel, a separate SUB-GUI as shown in *Figure 6.3* will show up where all the values can be modified.

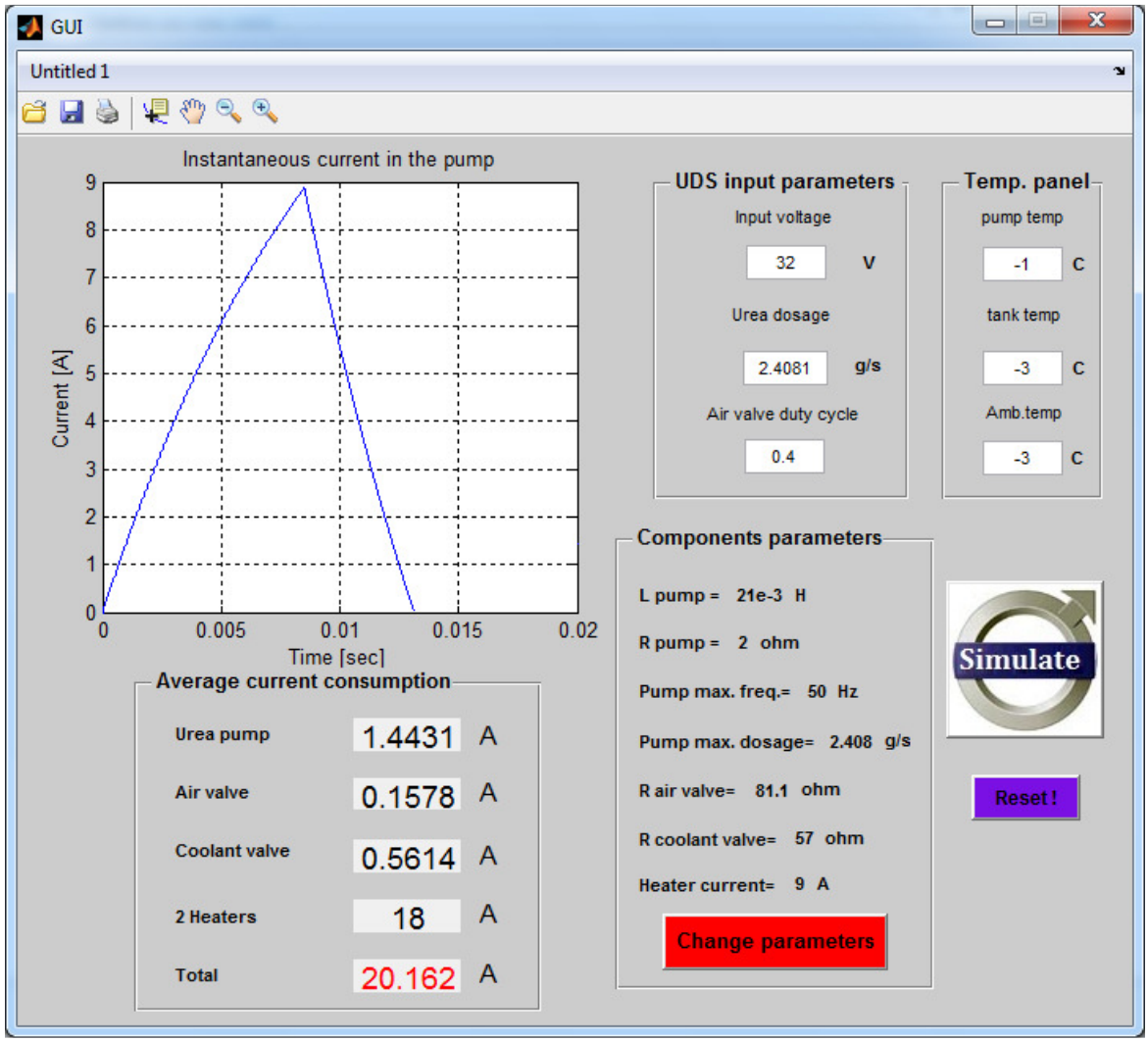

Figure 6.2 GUI layout for the general model

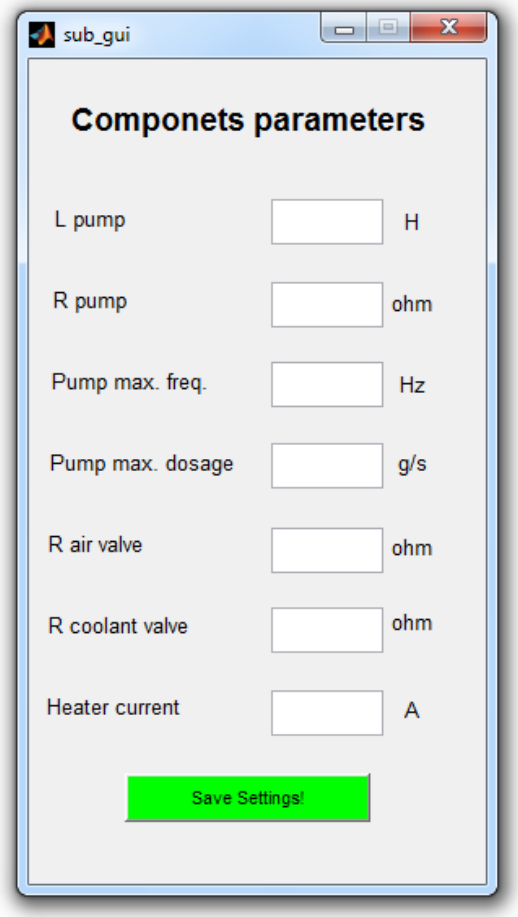

Figure 6.3 Overview of the SUB-GUI display panel

Average current consumption panel:
This panel is responsible for displaying the outputs for the average current consumption of the battery power supply according to different connected loads. Also it displays the total current consumption for the battery with all the loads connected.

Graphical plot axes:
It displays the instantaneous current in the Urea pump only, since the other loads could be represented as resistive loads only.

6.4 programming the GUI for the general model

As mentioned before in section 6.1, the GUIDE creates two MATLAB® files. The first one is a *.fig* file for the GUI display, and the second file is a *.m file* which contains the functions and callbacks for the GUI program as described in the following.

Simulate push callback:
This function executes simulations and results when pressing the *Simulate push button.* The input parameters of the general model shown in *Figure 4.17* are located in this function. The function is also responsible for calling the Simulink® file of the general model and executing all the equations for the current calculations [14].

Change pump callback:
When pressing the change parameters button, the function calls the SUB-GUI file responsible for changing the component parameter values.

Reset callback:
This function is activated when pressing the reset button, it calls back for another .mfile called *reset_gui* which delete and clear all the edit values and results in the GUI display. The rest of the functions are edit callbacks for the input values for the GUI, and *CreateFcn* functions for every button which are left without any change.

Chapter 7
Conclusion and future work

7.1 Discussion around the electric current calculations purpose & difficulties

The frequent need for calculating the electric current consumption for electric loads inside Diesel trucks is increasing every day, since the truck systems are getting more complex and many of the mechanical systems are now being replaced by electro-mechanical and electronic units. Furthermore, new systems, like the Engine After Treatment System (EATS) which is required by the European commission according to the European emission standard has increased the electric loads in the truck.

In order to install a new component in the system, there must be an extensive study for the influence of the installed component on the total load sharing, and the state of charge (SOC) for the truck's battery. Whereas the difficulties facing engineers working in calculating and estimating the increase of the electric current consumption in the powertrain systems lies in several reasons as concluded below:

1. Obtaining the continuous average current consumption of a component (from data sheets by the manufacturer) is not enough to estimate the current consumption since the whole systems have to work simultaneously to observe the real current consumption for each unit by taking in account the conditions for each unit to turn on or off.

2. The internal parameters (inductance and resistance), frequency, duty cycle, and input voltage could be a good start for calculating the current consumption for a new component, but the electronic control circuit responsible for controlling the component is still playing the main role for determining the exact consumed current. Thus, a corporation with the programming engineers is essential to understand the control circuits for each unit.

3. Building a general model simulating real systems in the powertrain is not an easy task, since each type for electric component (heaters, pumps, motors, etc...) will have its different model construction.

4. Estimating the current consumption in an early stage of a project will not be accurate, since in most of the cases the programming engineers will work on reducing the consumption in later stage of the project, but it will give some useful data about current limitations. An example in this case is the Urea pump current consumption which was reduced in a smart way without changing the voltage amplitude **V** or playing with the $\mathbf{t_{on}}$ duration of the main voltage wave pulse as shown in *Figure 7.1a*. Current reduction was based on chopping the voltage pulse with very high frequency (8 kHz-10 kHz) as shown in *Figure 7.1b* in this way the current consumption was reduced significantly.

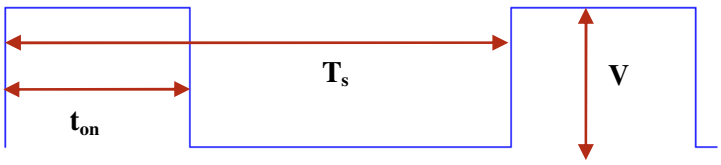

(Figure 7.1a)

(Figure 7.1b)

Figure 7.1a and b Shows the PWM pump voltage before and after treatment

7.2 Comparison

In this report 3 models for the UDS has been implemented for calculating the average electric current consumption of the system.

- Basic model
- Detailed model
- General model

Heaters and solenoid valves were implemented by using the basic model structure and they were simply represented as resistances without taking into account the inductance values or the internal coils. The accuracy of the implemented model was found to be 98 % of the real measured values which is an accurate value to take into account.

The Urea pump was modelled in three steps. The basic model was just to give some sensing values for the current consumption without taking magnetic or mechanical losses in consideration and by using only a fixed inductance value for the pump's coil. It gave a rough current consumption value of 50% error compared with the measured current in the actual pump, but as a start it was a good guide.

The detailed model is considered to be the reference model in this project and it is used for comparison with the other models. Due to lack of information from the pump supplier, a lot of assumptions have been made to this model to obtain some unknown data of the pump, for example: variable inductance of the pump's coil when the pump's piston is fully retracted and extended, and the internal mechanical losses. An error of 23.8 % in the current consumption for the detailed model to the measured value was found and that was because of the several assumptions that were taken when building the detailed model.

Finally the general model which is the goal for this project, it is considered as a simplified detailed model by making some approximations. At different voltages and frequencies, the general model average electric current consumption in the Urea pump $\mathbf{I_{d,ave}}$ was found with an accuracy between 95.5 - 96 % of the detailed model values with the same voltage-frequency conditions.

As a final conclusion of the models done, the general model could be used for calculating the electric current consumption in new added units to the electric system in the powertrain only if a detailed data could be handled by the supplier or by having the right measuring equipment to measure these values in the lab.

Advanced simulation software like SABER SKETCH could be used in some cases, when it is quite difficult to obtain the data required for simulations by measurements or by obtaining private data from the supplier. SABER software has a large number of library components which are already designed and include complex electro-mechanical units like electric motors, valves, battery models, etc…, these units could be directly used with only few required data inputs that could be easily obtained or estimated.

7.3 Future work

The next step for this study will be the expansion of the model to cover the rest of the Powertrain systems. The different types of components that could exist in any Powertrain systems can be classified as following:

- heaters
- Solenoid valves
- Linear (solenoid) pumps
- Electric motors (stepper, dc)
- Fuel Injectors

Fuel injectors and electric motors still need to be modelled and also more measurements need to be done in the labs. In the end it's clear that the electric component in the Powertrain of an engine truck will not only depend on the data sheet values coming from the manufacturer. It will also need practical experiments on new components to avoid occurring errors in calculations and to reduce assumptions like what has been done in the detailed model.

References

[01] Anu, M., 1997. Introduction to modeling and simulation. In simulation conference proceedings. Winter, 1997. Binghamton, USA.

[02] Magdi, K.K., 2000. The Case for the Diesel Engine. [Online]. DieselNet Technology Guide. Available at: http://www.dieselnet.com/tech/diesel_case.html [Accessed 19 March 2011]

[03] U.S. Department of Energy. Office of Energy Efficiency and Renewable Energy. 2003. [Online]. Just the Basics: Diesel Engine. Available at: http://www1.eere.energy.gov/vehiclesandfuels/pdfs/basics/jtb_diesel_engine.pdf [Accessed 21 March 2011]

[04] Blair, G.P., 1996. Design and Simulation of Two-Stroke Engine. The Society of Automotive Engineers, Warrendale, PA

[05] Magdi K.K., 2008. What Are Diesel Emissions. [Online]. DieselNet Technology Guide. Available at: http://www.dieselnet.com/tech/emi_intro.html [Accessed 19 March 2011]

[06] European commission environment. 2011. [Online]. Transport and environment. Road vehicles. Available at: http://ec.europa.eu/environment/air/transport/road.htm [Accessed 23 March 2011]

[07] Emission standards, European Union. 2009. [Online]. Heavy-Duty Diesel Truck and Bus Engines. Available at: http://www.dieselnet.com/standards/eu/hd.php [Accessed 23 March 2011]

[08] The wikibook of automatic Control Systems and Control Systems Engineering with classical and modern techniques and advanced concepts. 2011. [Online]. Available at: http://en.wikibooks.org/wiki/Control_Systems/Modern_Controls/Print_version [Accessed 14 June 2011]

[09] Hamdi, Essam. 2003. Permanent magnet and variable reluctance drive systems. Gothenburg, Sweden: Chalmers Reproservice

[10] Chapman, Stephen J., (1991). Electric Machinery fundamentals, 2nd rev. ed. USA: McGraw-Hill College

[11] MATLAB GUI Tutorial - For Beginners blinkdagger, n.d., [Online]. Available at: http://blinkdagger.com/matlab/matlab-gui-graphical-user-interface-tutorial-for-beginners/ [Accessed 20 July 2011]

[12] "What Is GUIDE? Creating Graphical User Interfaces (MATLAB®)", n.d., [Online]. Available at: http://www.mathworks.com/help/techdoc/learn_matlab/f5-999209.html [Accessed 20 July 2011]

[13] "Writing Code for Callbacks; Coding a Programmatic GUI (MATLAB®)", n.d., [Online]. Available at: http://www.mathworks.com/help/techdoc/creating_guis/f16-999606.html [Accessed 22 July 2011]

[14] “MATLAB GUI Tutorial - Buttons and Button Group Panel blinkdagger”, n.d., [Online]. Available at: http://blinkdagger.com/matlab/matlab-gui-tutorial-buttons-button-group/ [Accessed 22 July 2011]

Appendix

1. ***Hesselman engine:*** "The Hesselman engine is a hybrid between a petrol engine and a Diesel engine introduced by Swedish engineer Jonas Hesselman in 1925. It represented the first use of direct gasoline injection on a spark-ignition engine."

    - Lindh, Björn-Eric (1992) (in Swedish). Scania fordonshistoria 1891-1991. ISBN 91-7886-074-1. (Translated title: Vehicle history of Scania 1891-1991)
    - Olsson, Christer (1987) (in Swedish). Volvo – Lastbilarna igår och idag. ISBN 91-86442-76-7. (Translated title: Volvo trucks yesterday and today)

2. ***Vehicle bus:*** "A vehicle bus is a specialized internal communications network that interconnects components inside a vehicle. Protocols include Controller Area Network (CAN), Local Interconnect Network (LIN) and others."

    - Ronald W. Cox, Local Area Network Technology Applied to Automotive Electronics Communications, IEEE Transactions on Industrial Electronics, VOL. IE-32, No. 4, November 1985, Page 327-333

3. ***NO_x:*** is a generic term for the mono-nitrogen oxides NO and NO_2

4. ***Urea solution:*** is an organic compound handled in liquid form at the production plant and is then mixed with deionised water. The solution is injected in the exhaust system and when it is heated to about 200 cº it reacts with the nitrogen oxide emissions and converts into nitrogen and water within the SCR. The Urea solution normally freezes at -11ºc.

5. ***SCR:*** is a means of converting nitrogen oxides with the aid of a catalyst into diatomic nitrogen, N2, and water, H2O.

6. ***Wax thermostat:*** "A thermostat in which the expansion of melting paraffin wax (in a rigid cylinder) deforms a moulded rubber membrane and displaces a piston/pin from the cylinder; this has the advantage of being insensitive to sudden temperature fluctuations or to the pressure in the system."

    - Wax-type thermostat. 2011. [Online]. Definition. Available at: http://www.cardictionary.com/definition/wax-type-thermostat.html [Accessed 09 Sep. 2011]